Modulation of Insulin/IGF Signalling to Improve Mammalian Healthspan

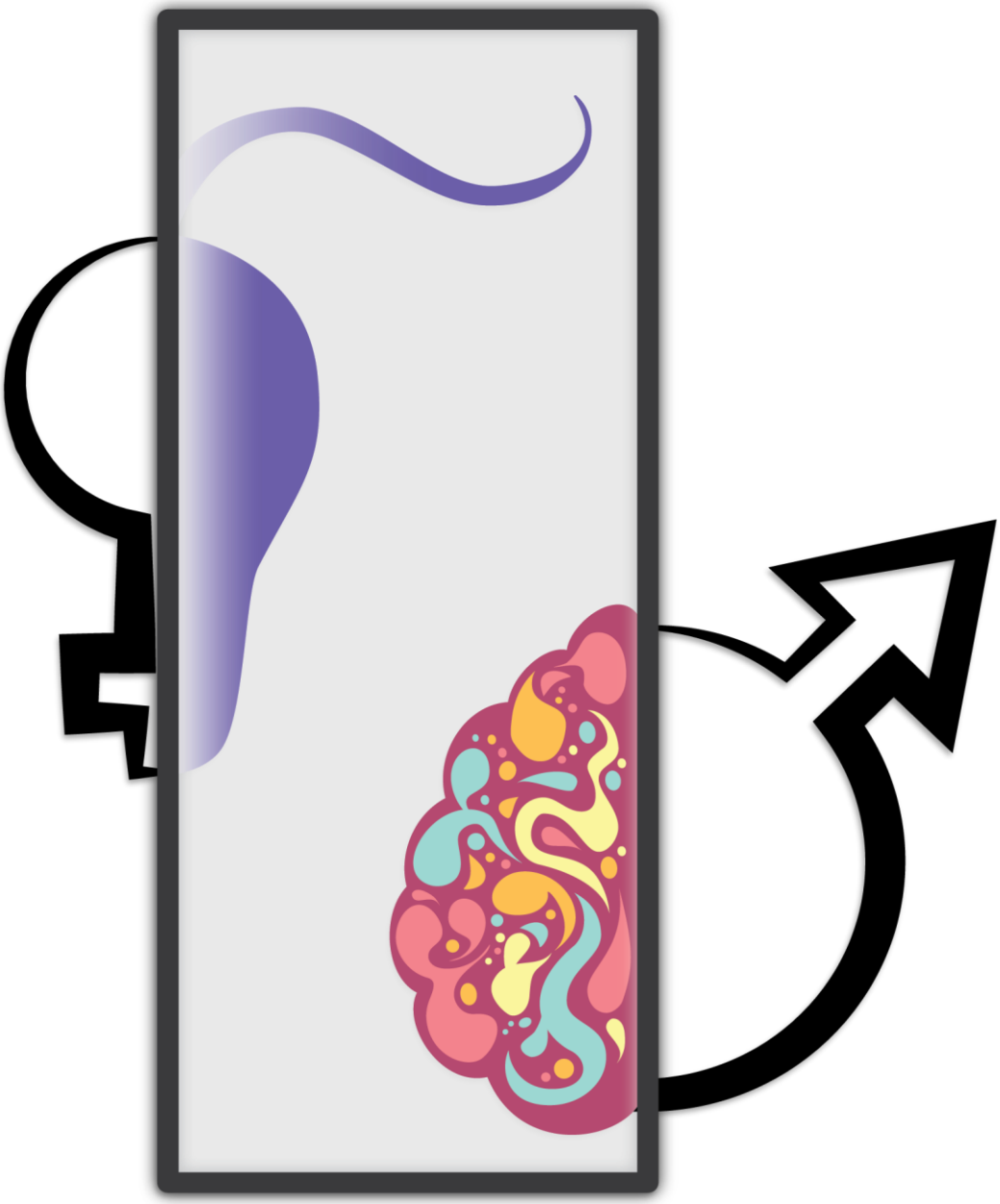

Maarouf Baghdadi

2022

Modulation of Insulin/IGF Signalling to Improve Mammalian Healthspan

Inaugural-Dissertation zur

Erlangung des Doktorgrades

der Mathematisch-Naturwissenschaftlichen Fakultät

der Universität zu Köln

vorgelegt von

Maarouf Baghdadi

aus Beirut, Libanon

Köln, 2022

Gutachter: **Prof. Dr. Linda Partridge**

Prof. Dr. Aleksandra Trifunovic

Tag der mündlichen Prüfung: 10 August 2022

The dissertation has been accepted by the Faculty of Mathematics and Natural Sciences of the University of Cologne.

I. Table of contents

I. Table of contents 4

II. Acknowledgments 6

III. Abbreviations 8

1. Aim of the thesis 9

1.1 Summary 9

1.2 Zusammenfassung 10

2. Methods 13

2.1 Mouse work 13

2.1.1 Mouse Generation 13

2.1.2 Mouse Husbandry 14

2.1.3 Mouse Metabolic Phenotyping 14

2.1.4 Mouse Cognitive Phenotyping 15

2.2. Molecular biology 17

2.3. Mitochondrial respirometry 18

2.4 Metabolomics 19

2.5 Statistics 21

3. Reduced insulin signalling in neurons induces sex-specific health benefits 22

3.1 Introduction 23

3.2 Results 24

3.2.1 Increased lifespan and health parameters in Irs1KO mice 24

3.2.2. Tissue-specific Irs1 knockout mice 29

3.2.2.1 Generation and validation of tissue-specific Irs1 knockout mice 29

3.2.2.2 Tissue-specific knockout of Irs1 in liver, muscle, fat or neurons does not extend lifespan in mice 32

3.2.2.3 IRS1 deletion in liver, muscle or fat does not improve health 33

3.2.2.4 Neuron-specific Irs1 knockout mice show male-specific improvement in metabolic health 42

3.2.3. Characterisation of mitochondrial function in Irs1KO and nKO brains 47

3.2.3.1 Irs1KO and nKO brains exhibit sex-specific, age-dependent mitochondrial dysfunction 47

3.2.3.2 Irs1KO and nKO brains have sex-specific and age-dependent ISR up-regulation 48

3.2.3.3 Sex-specific ISR up-regulation leads to neuronal metabolic adaptation 48

3.2.3.4 IRS1 deletion in peripheral tissues did not activate an ISR signature 52

3.2.4 Neuronal ISR in response to IRS1 deletion induces systemic benefits through an FGF21-independent mechanism 53

3.3 Discussion 56

4. Cognitive effects of whole body Irs1 knockout 59

4.1 Introduction 60

4.2 Results 61

4.2.1 Locomotor learning, neuromuscular strength, and non-aversive exploratory behaviour of Irs1KO mice 61

4.2.2 Irs1KO mice have reduced exploration and anxiety-like behaviour 64

4.2.3 Elimination of age-dependent anxiety-like behaviour in old Irs1KO mice by low-light conditions 64

4.2.4 Intact long-term reference memory in Irs1KO mice 67

4.2.5 Improved short-term contextual memory in Irs1KO mice 70

4.3 Discussion 72

5. Sex-specific effects of Cre expression in Syn1Cre mouse model 75

5.1 Introduction 76

5.2 Results 77

5.2.1 No deficit in motor learning, neuromuscular strength and non-aversive exploratory behaviour in Syn1Cre mice 77

5.2.2 Reduced exploration and sex-specific increase in anxiety-like beheaviour in Syn1Cre mice 79

5.2.3 Impairment in learning and long-term spatial reference memory in Syn1Cre mice 81

5.2.4 Increased hypothalamic hGH expression leads to sex-specific decrease in Syn1Cre growth 85

5.2.5 Intact systemic metabolic parameters in Syn1Cre mice 88

5.3 Discussion 91

6. List of figures 93

7. List of tables 95

8. Bibliography 96

9. Signed thesis declaration 109

10. Publications 110

II. Acknowledgments

First and foremost, I would like to express my gratitude to Prof. Dr. Linda Partridge for her trust in me and giving me the freedom to design and carry out my own projects. Your support has taught me to look for truth and knowledge myself, and not resign to what is available at hand. I appreciate your efforts that empowered me to take decisions and make things happen. You have been given me a lot of freedom, responsibility and independence, as well as supported me in getting immersed in the ageing field through many international conferences. I feel that my time in your group has prepared me for the next step, in whatever form that takes.

A special thanks to my two mentors, Prof. Dr. Steven Kushner and Dr. Joris Deelen, who saw the potential in me even when I did not. Their compassion, kindness and support were critical for me to continue on the path and reach my goals even when my will wavered.

My thanks to my thesis committee members for their support and guidance, namely Prof. Dr. Steven Kushner and Prof. Dr. Manolis Pasparakis. I am extremely grateful for the thesis defence committee members, Prof. Dr. Steven Kushner and Prof. Dr. Aleksandra Trifunovic for evaluating my work and being part of this exciting rite of passage. A special thanks to Dr. Joris Deelen for agreeing to write my thesis protocol and being part of the defence.

A special thanks to Dr. Sebastian Grönke for critical feedback throughout the years that have undoubtedly helped me improve as a scientist, a presenter and a writer. Your feedback was critical when big decisions needed to be made during my project. I would also like to thank Dr. Tobias Nespital's efforts in setting up the lifespans and organising the peripheral tissue knockout mice and his feedback on my ethics permission applications. Your help was critical to the timely completion of the project.

A big and immeasurable gratitude for my good friend Sandra Buschbaum. You were a monumental support system during the long hours in the mouse house and a great friend outside the lab, especially when we were the only lab members during lockdown that were still working every day to collect my old age tissues. It has been truly a pleasure getting to know you during our daily interactions.

I would also like to acknowledge the great support of the CGA program coordinators and directors for their tireless effort in preparing us for the next step of our scientific journey. A special thank you to Dr. Daniela Morrick and Jenny Ostermann for their great help in making sure my PhD went steadily.

One of the highlights of my time in the MPI-AGE has been our tremendous facilities that give scientists the opportunity to get the input of experts in their respective fields which was an indispensable pillar of my projects. The members of the Proteomics, Metabolomics and Bioinformatics facilities were great collaborators in this effort. A big thank you goes to facility that I made use of almost daily, the Comparative Biology facility, where fantastic care takers in Jerome Henn, Silvia Teckenburg and Iwetta Gniadek took care of all my animals. A special thank you to Andrea Mesaros and Martin Purrio in the Phenotyping facility, who were great collaborators and friends, and were instrumental in getting all the various phenotyping done in high quality and a timely manner.

I want to thank all the former and current lab members in the department for making this an unforgettable and intellectually stimulating experience, I have been extremely lucky to share the department with such a group of great scientists and friends. A special thanks to Dr. Victor Bustos, Dr. Oliver Hahn and Dr. Javier Morón Oset for very interesting discussions during lunch breaks about the ageing field and the newest exciting science, as well as the random “Victor” questions. I also want to acknowledge a great friend and companion on my PhD journey, Dr. Javier Morón Oset. Our common passion for neuroscience meant we directly hit it off. Sharing the office with you has been a treat and your work ethic has been an inspiration. From the late-night scientific discussions about our data to the many laughs we had, it was truly a pleasure. Further, I would like to thank everyone in the F1 group for great companionship and for making re-entering society after the long pandemic break such a pleasure. A special thanks to Carolina and Lisonia for being great, thoughtful office neighbours, I truly appreciate our many fun and interesting discussions. I would also like to thank Christine and Oliver, who helped with organisation and administrational issues so that I can focus on the science. Your support is truly invaluable in keeping everything in the lab running smoothly.

Of course, my most heartfelt appreciation and thanks to the never-ending support and love I have received from my family back home in Lebanon. Thank you for giving me the opportunity to spend many long days and nights in the lab to chase my dreams. It is truly a privilege I do not take lightly. A special thanks to my brother Jihad and my sister Dalia for designing such a wonderful piece of art for my thesis cover.

III. Abbreviations

2PG	2-Phosphoglyceric acid
ANCOVA	Analysis of covariance
ANOVA	Analysis of variance
ATF4	Activating Transcription Factor 4
ATF5	Activating Transcription Factor 5
AUC	Area under the curve
B2M	Beta-2-microglobulin
BAT	Brown adipose tissue
CHOP	DNA Damage Inducible Transcript 3
Cish	Cytokine inducible SH2-containing protein
CNS	Central nervous system
Cre	Cre recombinase
EE	Energy expenditure
ELISA	Enzyme-linked immunosorbent assay
F1P	Fructose-1-phosphate
FBP	Fructose-1,6-bisphosphate
FCCP	Trifluoromethoxy carbonylcyanide phenylhydrazone, Carbonyl cyanide 4-(trifluoromethoxy)phenylhydrazone
FGF21	Fibroblast growth factor 21
fKO	Fat-specific Irs1 knockout
G1P	Glucose-1-phosphate
G1P	Glucose-1-phosphate
G6P	Glucose-6-phosphate
GH	Growth hormone
Ghrh	GH releasing hormone
gKO	Gut-specific Irs1 knockout
GTT	Glucose tolerance test
hGH	Human growth hormone
IGF1	Insulin-like growth factor 1
IIS	Insulin/insulin-like growth factor 1 signalling
IRS1	Insulin substrate receptor 1
Irs1KO	Irs1 knockout mice
ISR	Integrated stress response
ITT	Insulin tolerance test
lKO	Liver-specific Irs1 knockout
mKO	Muscle-specific Irs1 knockout
NAA	Non-aversive arena
nKO	Neuron-specific Irs1 knockout
NOR	Novel object recognition
OF	Open field
OXPHOS	Oxidative phosphorylation
Q-RT-PCR	Quantitative real-time polymerase chain reaction
RER	Respiratory exchange ratio
Syn1Cre	Cre under rat-Synapsin I promoter
WAT	White adipose tissue

1. Aim of the thesis

1.1 Summary

Research into ageing has revealed the malleability of the process and the importance of sex differences in modulating the response to longevity interventions. The importance of sex in mediating healthy ageing is evident in the brain, where sex is a major risk factor for some disorders. For example, women are twice as likely as men to suffer from Alzheimer's Disease and men twice as likely as women to incur Parkinson's Disease, two common and debilitating age-associated neurological disorders. My thesis underscores the importance of including both sexes when performing exploratory scientific studies where the effect of sex on a variable is unknown.

Suppressed activity of the insulin/insulin-like growth factor signalling (IIS) pathway is a highly conserved and robust intervention that ameliorates the effects of ageing. While many invertebrate studies have dissected the role of IIS in ageing and have found tissue- and sex-specific effects, the role of different tissues and impact of sex in the longevity benefits of IIS reduction in mammals remain elusive. To address this gap, I first fully characterised male and female insulin receptor substrate 1 (Irs1) knockout (Irs1KO) mice. Then, I generated tissue-specific Irs1KO models targeting the major insulin-sensitive metabolic organs (liver, muscle, fat and brain) in male and female mice, and assessed the effects on body composition, energy expenditure and peripheral metabolism I found neuronal IRS1 deletion to be unique in triggering sex-specific health benefits in male mice. In the first section of the Thesis, I shed light on a mechanism by which reduced neuronal insulin signalling mediates mitochondrial phenotypes in Irs1KO mice, and I highlight the sex-specific nature of the neuronal mitochondrial stress response.

IRS1 deletion is a robust method for lifespan extension and induction of metabolic health benefits. However, the effect of IRS1 deletion on cognitive function has not been assessed. Therefore, I asked whether IRS1 deletion reduced age-associated cognitive decline in young and old female and male mice. First, I found that IRS1 deletion did not lead to deficits in locomotor or exploratory behaviour, but it did lead to an age-associated reduction in anxiety. Next, I found no significant difference in the capacity of Irs1KO mice to perform a hippocampus-dependent spatial learning task and form long-term memory. Finally, I assessed short-term memory and found a significant enhancement in old Irs1KO mice, suggesting a reduction in age-associated cognitive decline. In the second section, I present data indicating the lack of sex-specific deficits in Irs1KO cognitive and motor function as well as a mitigation of age-dependent cognitive decline.

Cognitive decline, a risk factor for dementia, is a major source of dependence in the elderly population, leading to increased societal and economic burden. I tested whether neuronal IRS1 deletion would be sufficient to delay or prevent cognitive decline in an ageing mouse model. I used a genetic tool to target IRS1 deletion to a widespread neuronal population. I therefore assessed whether the genetic tool itself induced phenotypes that could confound the effects of Irs1 deletion before moving on to study nKO mice. First, I characterised behavioural and metabolic parameters in male and female mice that expressed Cre under the rat-Synapsin I promoter (Syn1Cre). I found that Syn1Cre expression alone led to a sex-specific increase in anxiety and an inability to perform a spatial learning task in male Syn1Cre mice. Moreover, I found evidence of increased human growth hormone (*hGH*) expression in the brain due to the expression of a Cre-hGH transcript, leading to a negative feedback loop in the growth pathway resulting in a sex-specific reduction of

body size in male Syn1Cre mice. Finally, I tested peripheral metabolism and found no significant difference in glucose tolerance, insulin sensitivity, energy expenditure or locomotor activity in male or female Syn1Cre mice. In the third section, I report that the Syn1Cre genetic model may be an appropriate tool for the study of neuronal control of peripheral metabolism, but not for behavioural studies. Therefore, I was unable to move forward with the characterisation of the neuron-specific IRS1 mutant.

1.2 Zusammenfassung

Die Alternsforschung hat die Formbarkeit dieses Prozesses und die Bedeutung der Geschlechtsunterschiede im Bezug auf Maßnahmen zur Verlängerung der Lebenserwartung aufgezeigt. Die Bedeutung des Geschlechts bei der Vermittlung des gesunden Alterns zeigt sich im Gehirn, wo das Geschlecht ein wichtiger Risikofaktor für einige Erkrankungen ist. So erkranken Frauen doppelt so häufig wie Männer an der Alzheimer-Krankheit und Männer doppelt so häufig wie Frauen an der Parkinson-Krankheit, zwei der altersbedingten und einschränkendsten neurologischen Störungen. Meine Dissertation unterstreicht, wie wichtig es ist, beide Geschlechter einzubeziehen, wenn wissenschaftliche Studien durchgeführt werden, bei denen der Einfluss des Geschlechts auf eine Variable unbekannt ist.

Die Unterdrückung der Aktivität des Insulin-/Insulin-ähnlichen Wachstumsfaktorsignalwegs (IIS) ist eine hochkonservierte und robuste Intervention, die die Auswirkungen des Alterns abschwächt. Während viele Studien an Wirbellosen die Rolle von IIS bei der Alterung untersuchten und Geschlechtsunterschiede feststellten, sind die Gewebe und Mechanismen, die die Vorteile einer IIS-Reduktion bei Säugetieren für die Langlebigkeit vermitteln, nach wie vor nicht bekannt. Um diese Lücke zu schließen, habe ich zunächst männliche und weibliche Insulinrezeptor-Substrat 1 (Irs1)-Knockout-Mäuse (Irs1KO) vollständig charakterisiert. Daraufhin erstellte ich gewebespezifische Irs1KO-Modelle, die auf die wichtigsten insulinempfindlichen Stoffwechselorgane (Leber, Muskel, Fett und Gehirn) bei männlichen und weiblichen Mäusen abzielten, und bewertete die Auswirkungen auf die Körperzusammensetzung, den Energieverbrauch und den peripheren Stoffwechsel. Im ersten Abschnitt der Dissertation beleuchte ich einen Mechanismus, durch den eine reduzierte neuronale Insulinsignalisierung mitochondriale Phänotypen in Irs1KO-Mäusen vermittelt, und ich hebe die geschlechtsspezifische Natur der neuronalen mitochondrialen Stressreaktion hervor.

Die Deletion von IRS1 ist eine robuste Methode zur Verlängerung der Lebensspanne und kann die metabolische Gesundheit fördern. Die Auswirkungen der IRS1-Deletion auf die kognitiven Funktionen wurden jedoch noch nicht erforscht. Daher bin ich der Frage nachgegangen, ob die Deletion von IRS1 den altersbedingten kognitiven Abbau bei jungen und alten weiblichen und männlichen Mäusen verringert. Zunächst stellte ich fest, dass die Deletion von IRS1 nicht zu Defiziten in der Fortbewegung oder im Erkundungsverhalten führte, wohl aber zu einer altersbedingten Verringerung der Ängstlichkeit. Ich fand keinen signifikanten Unterschied in der Fähigkeit von Irs1KO-Mäusen, eine vom Hippocampus abhängige räumliche Lernaufgabe zu lösen und ein Langzeitgedächtnis zu bilden. Schließlich untersuchte ich das Kurzzeitgedächtnis und fand eine signifikante Verbesserung bei alten Irs1KO-Mäusen, was auf eine Verringerung des altersbedingten kognitiven Verfalls hindeutet. Im zweiten Abschnitt stelle ich Daten vor, die auf das Fehlen geschlechtsspezifischer Defizite in der kognitiven und motorischen Funktion von Irs1KO-Mäusen sowie auf eine Abschwächung des altersbedingten kognitiven Abbaus hinweisen.

Kognitiver Abbau, ein Risikofaktor für Demenz, ist eine Hauptursache der Pflegebedürftigkeit in der älteren Bevölkerung und führt zu einer erhöhten gesellschaftlichen und wirtschaftlichen Belastung. Vor diesem Hintergrund wollte ich testen, ob die Deletion von neuronalem IRS1 ausreicht, um den kognitiven Verfall in einem alternden Mausmodell zu verzögern oder zu verhindern. Ich verwendete ein genetisches Instrument, um die Deletion von IRS1 in einer weit verbreiteten neuronalen Population zu erreichen. Ich untersuchte daher, ob das genetische Werkzeug selbst Phänotypen hervorruft, die die Auswirkungen der IRS1-Deletion beeinträchtigen könnten. Zunächst

charakterisierte ich Verhaltens- und Stoffwechselparameter bei männlichen und weiblichen Mäusen, die Cre unter dem Ratten-Synapsin I-Promotor (Syn1Cre) exprimierten. Ich stellte fest, dass die Expression von Syn1Cre allein bei männlichen Syn1Cre-Mäusen zu einer geschlechtsspezifischen Zunahme von Angstzuständen und der Unfähigkeit, eine räumliche Lernaufgabe zu lösen, führte. Darüber hinaus fand ich Hinweise auf eine erhöhte Expression des menschlichen Wachstumshormons (hGH) im Gehirn aufgrund der Expression eines Cre-hGH-Transkripts, was zu einer negativen Rückkopplungsschleife im Wachstumsweg führte, die eine geschlechtsspezifische Verringerung der Körpergröße bei männlichen Syn1Cre-Mäusen zur Folge hatte. Schließlich habe ich den peripheren Stoffwechsel getestet und keinen signifikanten Unterschied in der Glukosetoleranz, der Insulinsensitivität, dem Energieverbrauch oder der Bewegungsaktivität bei männlichen oder weiblichen Syn1Cre-Mäusen festgestellt. Im dritten Abschnitt berichte ich, dass das Syn1Cre-Genmodell ein geeignetes Instrument für die Untersuchung der neuronalen Kontrolle des peripheren Stoffwechsels sein könnte, nicht aber für Verhaltensstudien. Daher konnte ich die Charakterisierung dieser neuronenspezifischen IRS1-Deletion nicht weiterverfolgen.

2. Methods

2.1 Mouse work

2.1.1 Mouse Generation

Whole body *Irs1* knockout (Irs1KO) mice were generated previously[1], and kindly provided by Dr. Dominic Withers. Previous data from Irs1KO mice were generated in the C57BL/6J background[1]. However, due to genetic mutations in the C57BL/6J line that may confound metabolic traits, we chose to generate the Irs1KO mice in the C57BL/6N background[2]. After embryo transfer of Irs1KO embryos from C57BL/6J into C57BL/6N mice, we observed Irs1KO progeny to drop dramatically in the third generation to approximately 3% Irs1KO mice born from breeding of heterozygous parents. Following attempts to optimise diet and housing conditions, Irs1KO progeny continued to stay far below the expected ratio in subsequent generations (~7% Irs1KO mice with normal levels of heterozygous and wild type mice observed in litters). Additionally, we tried to generate a Cre-specific whole body Irs1KO in the C57BL/6N background via the ActinCre driver line. However, attempts to generate ActinCre +/T::Irs1 fl/fl led to similarly low rates of Irs1KO mice (~2%). The lack of Irs1KO progeny in the C57BL/6N background could be due to general incompatibility of insulin pathway mutations in this background. Therefore, we generated the Irs1KO mouse in a more robust C3B6 hybrid mouse background. Irs1KO mice were backcrossed for 4 generations from C57BL/6J to a C57BL/6N and into a C3H/HeOuJ background. Heterozygous female C3H/HeOuJ *Irs1* -/+ mice were mated with male heterozygous male C57BL/6N *Irs1* -/+ mice to generate hybrid C3B6F1 whole body Irs1 knockout (Irs1KO) mice used throughout this study.

Irs1 tissue-specific KO mice were generated in the C57BL/6N background using BAC clones from the Taconic Artemis C57BL/6J RPCIB-731 BAC library as previously described[3]. The strategy resulted in the generation of *Irs1loxP/loxP* mice for further use in tissue-specific knockout generation by crossing with tissue-specific *Cre* mice.

For tissue-specific knockout of *Irs1*, *Irs1loxP/loxP* mice were crossed with mice expressing Cre-recombinase under the control of the mouse albumin enhancer and promoter, or the alpha-fetoprotein enhancers (*AlfpCre* mice[4]), or the creatine kinase promoter (CkmmCre mice[5]), or the adiponectin promoter (AdipoqCre[6]), or the villin promoter (Villin1Cre mice[7]) or the rat-Synapsin 1 promoter (*Syn1Cre* mice [8]). Breeding *Irs1loxP/loxP* AlfpCre mice with *Irs1loxP/loxP* mice resulted in hepatocyte specific *Irs1* deletion (AlfpCre +/T::Irs1fl/fl denoted as lKO), *Irs1loxP/loxP* CkmmCre with *Irs1loxP/loxP* mice resulted in skeletal muscle specific *Irs1* deletion with partial deletion in cardiac muscle (CkmmCre +/T::Irs1fl/fl denoted as mKO), *Irs1loxP/loxP* AdipoqCre mice with *Irs1loxP/loxP* mice resulted in *Irs1* deletion in both white and brown adipose tissue (AdipoqCre +/T::Irs1fl/fl denoted as fKO). Finally, due to a recommendation of reports of germline deletion in Syn1Cre in mice[9], only female *Irs1loxP/loxP* Syn1Cre mice were bred with male *Irs1loxP/loxP* mice to produce neuron specific *Irs1* deletion (Syn1Cre +/T::Irsfl/fl denoted as nKO). All crosses generated littermate controls (Irsfl/fl) mice.

2.1.2 Mouse Husbandry

All mice were randomly allocated to groups of four to five same-sex individuals under specific pathogen-free conditions in individually ventilated cages (Techniplast UK Ltd, Kettering, Northamptonshire, UK) in a controlled temperature and humidity environment with 12-h light/dark cycle (lights on from 06:00 - 18:00) and provided ad libitum access to food [ssniff® R/M-H phytoestrogen-poor (9% fat, 34% protein, 57% carbohydrate) ssniff Spezialdiäten GmbH, Soest, Germany] and water. Sentinel mice in the animal room were regularly checked for mouse pathogens according to FELASA recommendations [10].

Mouse ethics

Ethical permission requests were filed under 84-02.04.2014.A424 and 81-02.04.2019.A078. Mouse experiments were performed in accordance with the recommendations and guidelines of the Federation of the European Laboratory Animal Science Association (FELASA), with all protocols approved by the Landesamt fur Natur, Umwelt und Verbraucherschutz Nordrhein-Westfalen, Germany.

Mouse genotyping

Mutant mice were identified by PCR genotyping using DNA extracted from ear clip biopsy and amplified using GoTaq® G2 DNA Polymerase, and tail clips were taken from mice at death for genotype confirmation. Primers used to genotype as well as expected size of amplicons, of Irs1 wild type, Irs1 knockout, Irs1 LoxP floxed allele, and different Cre lines are listed in Table 5.

Mouse tissue collection

Irs1KO and nKO mice were euthanized by transcardial perfusion with PBS + EDTA, after general anaesthesia with a cocktail of Ketamine (120 mg/kg) and Xylazine (10 mg/kg) with supplementary Isoflurane (5%) until no reflex response was observed. Blood was collected by cardiac puncture in tubes with EDTA, plasma-EDTA was isolated by centrifugation at 1,000g for at least 10 min at 4 °C before aliquoting and storage at −80 °C. Mice were rapidly decapitated, then the skull and body were dissected by two people simultaneously to minimise tissue deterioration. The brain was removed from the skull and different brain regions were isolated and snap-frozen in liquid nitrogen. The same cortical brain region was collected for mitochondrial respirometry and prepared separately. The body of the animal was dissected and organs collected for histology in PFA or for molecular analysis were snap frozen in liquid nitrogen. The same procedure was performed for lKO, mKO and fKO with the exception of perfusion. Mice from lKO, mKO and fKO lines were sacrificed by cervical dislocation followed by rapid tissue removal as mentioned above.

2.1.3 Mouse Metabolic Phenotyping

A longitudinal cohort of mice was assessed at young (Irs1KO = 6 months and lKO, mKO, fKO, and nKO = 4 months) and old (Irs1KO and lKO, mKO, fKO, and nKO = 16 months) age for measurement of general metabolic health outcomes.

Body composition

Body fat and lean mass content were measured in vivo by nuclear magnetic resonance using the minispec LF50H (Bruker Optics).

Collection of blood samples and determination of blood glucose levels

A small drop of blood was obtained from the tail of mice. Blood glucose levels were determined using an automatic glucose monitor (Accu-Check Aviva, Roche). Determination of blood glucose and collection of blood samples were always performed in the morning to avoid deviations due to circadian variations.

Insulin tolerance test

After determination of basal blood glucose levels, each animal received an intraperitoneal injection of insulin (0.75 U/kg body weight) (Sanofi). Blood glucose levels were measured 15, 30 and 60 minutes after insulin injection.

Glucose Tolerance test and glucose-stimulated insulin secretion

Glucose tolerance tests were performed in the morning with animals after a 16 hour fast. After determination of fasted blood glucose levels, each animal received an intraperitoneal injection of 20% (w/v) glucose (10 ml/kg body weight). Blood glucose levels were measured 15, 30, 60 and 120 minute after the glucose injection. Blood samples were collected at indicated time points to analyse glucose-stimulated insulin secretion.

Indirect calorimetry

Indirect calorimetry, locomotor activity, drinking and feeding were monitored for singly housed mice in purpose-built cages (Phenomaster, TSE Systems). Parameters such as food consumption, respiration, and locomotor activity were measured continuously for 48 hours after one day of acclimatisation and two days of training in similar cages. Values for locomotor activity were averaged for active and inactive phases separately for the 48-hour duration with the exception of the first and last hour of each phase due to increased variability. Metabolic rate was assessed by regression analysis using body weight as a covariate as recommended [11,12].

2.1.4 Mouse Cognitive Phenotyping

All behavioural tests were conducted in dedicated behavioural testing rooms starting at 08:00 during the light phase of the light/dark cycle. All mice were handled for multiple subsequent days prior to the start of the phenotyping pipeline. Order of the phenotyping pipeline was performed from the least to most stressful assay. Mice were randomised and experimenters were blinded to genotype, when possible, all experiments were performed by a single, male scientist. Mice were habituated to the room for at least 45 minutes before behavioural experiments started. Mice were not assayed on days when their home cages were changed. Experimental apparatus was cleaned with bacillol foam between tests on different mice.

High and low stress open field

For the high stress open field experiment, mice were left to explore a square arena surrounded by clear walls (50 × 50 × 40 cm) for 5 minutes for Syn1Cre mice and 10 minutes for Irs1KO mice. Different parameters such as total distance travelled, movement speed and time spent in the

central area were recorded. Anxiety was assessed by quantifying time or distance spent in the centre as a percent of total time or distance in the arena. The test chamber was illuminated to 210-220 lux. Data collection was automatic using the TSE-Phenomaster software.

For the low stress non-aversive arena, mice were left to explore a square area surrounded by opaque white acrylic walls (50 × 50 × 40 cm) for 5 minutes for Syn1Cre mice and 10 minutes for Irs1KO mice. The test chamber was illuminated to 20-30 lux. Data collection was automatic using the TSE VideoMot software.

Novel Object Recognition

A short intertrial interval (~1 hour) novel object recognition (NOR) was used to assess spatial working memory. On day one, mice were familiarised to an empty box (50 × 50 × 40 cm) by allowing them to explore the space three times with a 50-minute interval in between familiarisations. On day two, mice were allowed to explore two equidistant and identical objects on opposite sides of the arena before being returned to their cage. Finally, following an approximately 50-minute inter-trial interval, mice were returned to the arena with an identical object to the previous trial and a novel object located on the opposite side. The mice were given 10 minutes to explore the objects, mice that did not explore objects for at least 30 seconds were excluded from analysis. Young Irs1KO mice exhibited normal exploration, only 2 males and 3 females did not reach exploration criteria. Young wild type mice exhibited less exploration, with 8 male and female mice not reaching the criteria for inclusion. However, only one mouse per group and sex were disqualified in old Irs1KO mice and wild type controls. The higher number of excluded mice in the NOR could be linked to the high anxiety-like behaviour we observed in young mice.

Two complex objects were made from Lego and placed 12.5 cm from the wall of the box, based on previous reports [13]. The novel and familiar object designations, as well as the location of the object that was replaced with the novel object, was counterbalanced across mouse genotype and sex.

The time the mice spent exploring each object was assessed by the TSE VideoMot program. Exploration of an object was recorded if the mouse's head was within 2 cm of the object. Novelty preference was calculated as:

(Novel object interaction time − Identical object interaction time)/ Identical object interaction time × 100

Rotarod

We used the rotarod test to test motor coordination and balance. The rotarod uses an accelerating rotarod [14], to measure a mouse's ability to maintain its balance on the rod. The rotation of the rotarod was accelerated from 5 to 40 rpm over a 300 second period. Each mouse was placed twice onto the rod, and latency to fall off the rod was measured and averaged per day. The inter-trial interval was approximately one hour. Mice were tested for four consecutive days to assess motor learning.

Y-maze

Mice were placed in a Y-shaped maze with three opaque black plastic arms at a 120° angle from each other. Mice started at the centre of the maze, then were allowed to freely explore the three arms. Over the course of multiple arm entries, the tendency of a healthy mouse is to enter a less recently visited arm, or to be attracted to the novel arm. The number of arm entries and the number

of ABC alternations (where A, B and C are the three different arms) are recorded in order to calculate the percentage of alternation. An entry occurs when all four limbs are within the arm for longer than 500 ms. Each mouse was placed in the maze for eight minutes.

Hidden platform and visual cued water maze

The hidden platform variation of the water maze was used to examine spatial learning ability and long-term reference memory. We adapted the water maze protocol from a previous report [15]. The water maze consists of a round basin with a diameter of 1.2 metre filled with water made opaque by adding white, non-toxic paint. A transparent glass platform (10 cm) is submerged in the centre of one of the quadrants, denoted as the target quadrant, by approximately one centimetre. Four different high contrast distal cues were placed on the walls surrounding the basin. The water temperature was kept around 24-25 degree Celsius and the light intensity was approximately 220 lux in the centre of the pool.

Each trial started with a mouse being placed on the platform for 30 seconds. Mice were then placed in the water facing the wall pseudo-randomly at one of the six start positions of the basin and allowed to search for the platform or until 60 seconds had elapsed. At the completion of each training trial, the mice were allowed to remain on the platform for 30 seconds. Mice were given 3 trials per day until reaching a criterion threshold of learning by escaping the water in less than 30 seconds. After criterion was reached, a probe trial was conducted in which the platform was removed. Mice were placed facing the wall in the quadrant directly opposite the previous location of the hidden platform and allowed to search for 60 seconds. The day after the probe trial, the mice were given the visually cued test, where the platform location was changed but was marked with a distinct local cue. The distant visual cues were hidden from sight of the mice and visual acuity, swimming ability and motivation for escape were assessed by how well the mice could escape the pool using only the local cue. Three trials were given of the visual cued water maze. Data analysis was carried out by the automated video tracking TSE VideoMot software. If the mouse did not explore the maze but floated upon placement in the water, the data were excluded from the analysis. Mice were also excluded based on standard exclusion criteria: excessive thigmotaxis, obvious visual impairment, excessive corkscrew swimming pattern, and obvious sensorimotor dysfunction. Genotype and sex did not affect likelihood of exclusion. Nine of the twenty Syn1Cre male mice displayed excessive floating, but these mice were not removed as that was a phenotype of the Syn1Cre male mice. This may have been due to the visual deficits in this genotype.

2.2. Molecular biology

Quantitative real time PCR

For the analysis of DNA expression, dissected organs were immediately transferred to a reagent tube and frozen in liquid nitrogen. Tissue was stored at −80 °C until use. RNA was extracted according to the manufacturer's instructions using the TRIzol™ Reagent (ThermoFisher, 15596018) in Lysing Matrix D tubes (speed 6 for 40 seconds) (MP Biomedicals, 6913-500). RNA was precipitated with the aid of GlycoBlue Coprecipitant (ThermoFisher, AM9515) overnight at −80 °C. Isolated RNA was treated with DNase using the DNA-free™ kit (ThermoFisher, AM1906) to remove any contaminating DNA according to manufacturer's instructions. Finally, cDNA was prepared with the SuperScript® III First-Strand Synthesis SuperMix (ThermoFisher, 18080400) for qPCR. Samples of cDNA mixed with the PowerUp SYBR Green Master Mix (ThermoFisher, 4368706) and primers validated using a standard curve, were loaded in technical quadruplicates for qPCR on a QuantStudio™ 6 Flex Real-Time PCR System (ThermoFisher, 4485691). The ΔΔCT

method was used to provide gene expression values after normalising to the known reference gene B2M. Primer sequences used for q-RT-PCR in Chapter 3 and 5 are shown in Table 5. Samples of cDNA mixed with the TaqMan™ Fast Advanced Master Mix (ThermoFisher, 4444557) and TaqMan® Assay probes, were loaded in technical quadruplicates for qPCR on a QuantStudio™ 6 Flex Real-Time PCR System (ThermoFisher, 4485691). The ΔΔCT method was used to provide gene expression values after normalising to the known reference gene *B2M*. Probe catalogue numbers used for q-RT-PCR are shown in Table 5.

2.3. Mitochondrial respirometry

Mitochondrial mediums

Mediums were prepared as described previously [16]. Briefly, solution A contained 250 mM sucrose, 1 g/L BSA, 0.5 mM Na_2EDTA, 10 mM Tris–HCl, pH 7.4. Solution B contained 20 mM taurine, 15 mM phosphocreatine, 20 mM imidazole, 0.5 mM DTT, 10 mM CaEGTA, 5.77 mM ATP, 6.56 mM $MgCl_2$, 50 mM K-MES, pH 7.1. Solution C contained 0.5 mM EGTA, 60 mM K-lactobionate, 20 mM taurine, 10 mM KH_2PO_4, 3 mM $MgCl_2$, 110 mM sucrose, 1 g/L fatty acid free BSA, 20 mM hepes, pH 7.1.

Tissue permeabilization

The protocol was adjusted from previous reports[16]. In brief, cortical pieces (approximately 1 mm × 1 mm × 2 mm) were quickly removed and placed in cold solution A. Then, cortical tissue was weighed for normalisation of oxygen consumption and transferred into 2 mL tubes with 1 mL of cold solution B. Medium was replaced by 2 mL of cold solution B complemented with 20 µL of a freshly prepared 5 mg/mL saponin solution. After 30 minute at 4 °C under gentle agitation on an orbital shaker, samples were rinsed in cold solution C (3× 2 minute), and further incubated on ice until measurements were taken.

Oxygen consumption measurement

We measured oxygen consumption of intact but permeabilized cortical sections using a respirometer (Oxygraph-2k, Oroboros Instruments). Measurements were performed under continuous stirring in 2 mL of solution C at 37 °C. The solution was equilibrated in air for at least 30 minutes before recording, and permeabilized cortical tissue was transferred into the instrument chambers. Mutant mice with respective controls were run in parallel in the instrument's two chambers simultaneously to minimise any day-to-day variability. After stabilisation of the initial mitochondrial oxygen consumption, mitochondrial respiration was stimulated by successive addition of substrates and inhibitors: First, 5 ul of 2M pyruvate and 5 ul of 800 mM Malate were added. Second, 10 ul of 500 mM ADP (with 300 mM free Mg2+) was added to measure O_2 consumption under normal phosphorylating state. Third, 5 ul of 4 mM Cytochrome C was added to check for mitochondrial membrane integrity, any samples that responded with a significant increase in O_2 consumption were removed from further analysis due to technical defects in sample preparation. Fourth, 10 ul of 2 M glutamate was added. Fifth, 20 ul of 1 M succinate was added. Sixth, 1 ul of 5 mM oligomycin, an ATP synthase inhibitor, was added. Then, maximum mitochondrial capacity was assessed by adding gradual volumes of 1 mM Trifluoromethoxy carbonylcyanide phenylhydrazone, Carbonyl cyanide 4-(trifluoromethoxy)phenylhydrazone (FCCP) until maximum oxygen consumption was reached. Then, 1 ul of 1 mM rotenone, a complex one inhibitor, was added to measure complex II activity. Finally, 1 ul of 5 mM antimycin A, a complex

three inhibitor, was added to measure non-mitochondrial O_2 consumption (residual oxygen flux) due to cytosolic oxidases. Residual oxygen flux was subtracted from all other measurements to report baseline mitochondrial oxygen consumption and spare respiratory capacity was calculated by subtracting baseline mitochondrial oxygen consumption from maximum oxygen consumption after FCCP addition. Mitochondrial oxygen consumption was calculated using DataGraph software from the manufacturer (Oroboros Instruments).

2.4 Metabolomics

2-phase metabolite extraction of polar and lipophilic metabolites in brain

For the preparation of polar and lipophilic metabolites between 10 and 30 mg of snap-frozen mouse tissue (Irs1KO young = 5 months and old = 19 months, nKO young = 5 months and old = 22 months) was collected in 2 mL tubes. For the extraction of the snap frozen material, the tissue was homogenised to a fine powder using a ball mill-type grinder (Tissuelyser II Qiagen, 85300). For the homogenization of the frozen material one liquid nitrogen cooled 5 mm stainless steel metal balls was added to each tube and the frozen material was disintegrated for 1 minute at 25 Hz.

Metabolites were extracted by adding 1 mL of pre-cooled (-20°C) extraction buffer (methyl tert-butyl ether (MTBE): UPLC-grade methanol: UPLC-grade water 5:3:2 [v:v:v]), containing an equivalent 0.2 µL of EquiSplash Lipidomix (www. avantilipids.com) as an internal standard. The tubes were immediately vortexed until the sample was well re-suspended in the extraction buffer. The homogenised samples were incubated on a cooled (4°C) orbital mixer at 1500 rpm for 30 min. After this step, the metal ball was removed using a magnet and the samples were centrifuged for 10 min at 21,100 x g in a cooled table top centrifuge (4°C). The supernatant was transferred to a fresh 2 mL Eppendorf tube and 250 µL of MTBE and 150 µL of UPLC-grade water were added to each sample. The tubes were immediately vortexed before incubating them for an additional 10 min on a cooled (15°C) orbital mixer at 1500 rpm, before centrifuging them for 10 min at 15°C and 16,000 x g. After the centrifugation, the tubes contained two distinct phases. The upper MTBE phase contains the lipids, while the lower methanol-water phase contains the polar and semi-polar metabolites.

For the lipidomic analysis 600 µL of the upper lipid phase were collected into fresh 1.5 mL tubes, which were stored at -80°C, until mass spectrometric analysis. The remaining polar phase (~800 µL) was immediately dried in a SpeedVac concentrator and stored dry at -80°C until mass spectrometric analysis.

Semi-targeted LC-HRS-MS analysis of amine-containing metabolites in brain

The LC-HRMS analysis of amine-containing compounds was performed using an adapted benzoyl chloride-based derivatization method[17].

In brief: The polar fraction of the metabolite extract was re-suspended in 200 µL of LC-MS-grade water (Optima-Grade, Thermo Fisher Scientific) and incubated at 4°C for 15 min on a thermomixer. The re-suspended extract was centrifuged for 5 min at 21.100 x g at 4°C and 50 µL of the cleared supernatant were mixed in an auto-sampler vial with a 200 µL glass insert (Chromatography Accessories Trott, Germany). The aqueous extract was mixed with 25 µl of 100 mM sodium carbonate (Sigma), followed by the addition of 25 µl 2% [v/v] benzoyl chloride (Sigma) in acetonitrile (Optima-Grade, Thermo Fisher Scientific). Samples were vortexed and kept at 20°C until analysis.

For the LC-HRMS analysis, 1 µl of the derivatized sample was injected onto a 100 x 2.1 mm HSS T3 UPLC column (Waters). The flow rate was set to 400 µl/min using a binary buffer system consisting of buffer A (10 mM ammonium formate (Sigma), 0.15% [v/v] formic acid (Sigma) in LC-MS-grade water (Optima-Grade, Thermo Fisher Scientific). Buffer B consisted solely of acetonitrile (Optima-grade, Thermo Fisher-Scientific).

The column temperature for Irs1KO brain samples was set to 40°C, while the LC gradient was: 0% B at 0 min, 0-15% B 0- 4.1min; 15-17% B 4.1 – 4.5 min; 17-55% B 4.5-11 min; 55-70% B 11 – 11.5 min, 70-100% B 11.5 - 13 min; B 100% 13 - 14 min; 100-0% B 14 -14.1 min; 0% B 14.1-19 min; 0% B.

The column temperature for nKO brain samples was set to 40°C, while the LC gradient was: 0% B at 0 min, 0-15% B 0- 0.1min; 15-17% B 0.1 – 0.5 min; 17-55% B 5.5-14 min; 55-70% B 14 – 14.5 min, 70-100% B 14.5 - 18 min; B 100% 18 - 19 min; 100-0% B 19 -19.1 min; 0% B 19.1-28 min; 0% B.

The mass spectrometer (Orbitrap ID-X, Thermo Fisher Scientific) was operating in positive ionisation mode recording the mass range m/z 100-1000. The heated ESI source settings of the mass spectrometer were: Spray voltage 3.5 kV, capillary temperature 300°C, sheath gas flow 60 AU, aux gas flow 20 AU at a temperature of 340°C and the sweep gas to 2 AU. The RF-lens was set to a value of 60%. Semi-targeted data analysis for the samples was performed using the TraceFinder software (Version 4.1, Thermo Fisher Scientific). The identity of each compound was validated by authentic reference compounds, which were run before and after every sequence. Peak areas of $[M + nBz + H]^+$ ions were extracted using a mass accuracy (<5 ppm) and a retention time tolerance of <0.05 min. Areas of the cellular pool sizes were normalised to the internal standards (U-^{15}N; U-^{13}C amino acid mix (MSK-A2-1.2), Cambridge Isotope Laboratories), which were added to the extraction buffer, followed by a normalisation to the fresh weight of the analysed sample.

Anion-Exchange Chromatography Mass Spectrometry (AEX-MS) for the analysis of anionic metabolites of brain tissue

Extracted metabolites were re-suspended in 150-200 µl of Optima UPLC/MS grade water (Thermo Fisher Scientific). After 15 min incubation on a thermomixer at 4°C and a 5 min centrifugation at 21,100 x g at 4°C, 100 µl of the cleared supernatant were transferred to polypropylene autosampler vials (Chromatography Accessories Trott, Germany) before AEX MS analysis.

The samples were analysed using a Dionex ion chromatography system (Integrion, Thermo Fisher Scientific) as described previously18. In brief, 5 µL of polar metabolite extract were injected in push partial mode using an overfill factor of 1, onto a Dionex IonPac AS11-HC column (2 mm × 250 mm, 4 µm particle size, Thermo Fisher Scientific) equipped with a Dionex IonPac AG11-HC guard column (2 mm × 50 mm, 4 µm, Thermo Fisher Scientific). The column temperature was held at 30°C, while the auto sampler was set to 6°C. A potassium hydroxide gradient was generated using a potassium hydroxide cartridge (Eluent Generator, Thermo Scientific), which was supplied with deionized water. The metabolite separation was carried at a flow rate of 380 µL/min, applying the following gradient conditions: 0-3 min, 10 mM KOH; 3-12 min, 10−50 mM KOH; 12-19 min, 50-100 mM KOH, 19-21 min, 100 mM KOH, 21-22 min, 100-10 mM KOH. The column was re-equilibrated at 10 mM for 8 min.

For the analysis of metabolic pool sizes in Irs1KO brains, the eluting compounds were detected in negative ion mode using full scan measurements in the mass range m/z 50 – 750 on a Q-Exactive HF high resolution MS (Thermo Fisher Scientific). The heated electrospray ionisation (ESI) source settings of the mass spectrometer were: Spray voltage 3.2 kV, capillary temperature was set to 300°C, sheath gas flow 60 AU, aux gas flow 20 AU at a temperature of 300°C and a sweep gas glow of 2 AU. The S-lens was set to a value of 60. The semi-targeted LC-MS data analysis was performed using the TraceFinder software (Version 4.1, Thermo Fisher Scientific). The identity of each compound was validated by authentic reference compounds which were at the beginning and the end of the sequence.

For the analysis of metabolic pool sizes in nKO brains, the eluting compounds were detected in negative ion mode [M-H]- using multiple reaction monitoring (MRM) mode with the following settings: Capillary voltage 2.7 kV, desolvation temperature 550°C, desolvation gas flow 800 l/h, collision cell gas flow 0.15 ml/min. The detailed quantitative and qualitative transitions and electronic settings for the analysed metabolites are summarised in Table 2. The MS data analysis was performed using the TargetLynx Software (Version 4.1, Waters).

For data analysis the area of the deprotonated [M-H+]- monoisotopic mass peak of each compound was extracted and integrated using a mass accuracy <5 ppm and a retention time (RT) tolerance of <0.1 min as compared to the independently measured reference compounds. Areas of the cellular pool sizes were normalised to the internal standards (citric acid D4), which were added to the extraction buffer, followed by a normalisation to the fresh weight of the analysed sample.

2.5 Statistics

Animals were checked every morning for survival. Mean lifespan was assessed, and survivorship was analysed using log-rank test or Cox proportional hazard analysis. Two-group comparisons were made using two-tailed, unpaired Student's t-test unless otherwise stated. However, if data was not normally distributed then Mann Whitney U test was performed. For comparisons of multiple factors (for example, phase * genotype or sex*genotype), two-way ANOVA was reported, followed by Sidak's post-test if interaction between main effects was significant.

Numbers of mice were estimated to be sufficient to detect statistically meaningful differences of at least 20% between or among groups using standard power calculations with $\alpha = 0.05$ and power of 0.8 on the basis of similar experiments conducted in our group. Homogeneity of variance and normality of residuals were assessed, and appropriate corrections were made if necessary. All experiments were performed in a randomised and blinded fashion when possible. Data were analysed statistically using GraphPad Prism 9.0, outliers were removed from analysis based on a Grubb's test. The value of α was 0.05, and data are expressed as $^{*}P < 0.05$; $^{**}P < 0.01$; $^{***}P < 0.001$; $^{****}P < 0.0001$. Number of animals reported at the bottom of the bars for each condition or in figure legends. All error bars correspond to standard deviation except for longitudinal glucose and insulin sensitivity where standard error of the mean is reported. ANCOVA analyses were plotted with 95% confidence interval bands. Detailed P values for non-significant comparisons, test statistic values, and degrees of freedom for Chapter 3, 4 and 5 are included in Table 1, 3 and 4 respectively.

3. Reduced insulin signalling in neurons induces sex-specific health benefits

Author contributions:

Conception of the study predominantly by Maarouf Baghdadi and Linda Partridge. Maarouf Baghdadi, Tobias Nespital, and Linda Partridge conceived of lifespan experiments. Maarouf Baghdadi, Andrea Mesaros and Linda Partridge conceived of metabolic phenotyping experiments

Execution of experiments predominantly by Maarouf Baghdadi and Tobias Nespital. Maarouf Baghdadi and Sandra Buschbaum performed tissue collection experiments. Maarouf Baghdadi, Andrea Mesaros and Martin Purrio performed metabolic phenotyping

Evaluation of data by Maarouf Baghdadi

Graphical representation by Maarouf Baghdadi

Writing of the manuscript predominantly by Maarouf Baghdadi, Sebastian Grönke and Linda Partridge

Reduced insulin signalling in neurons induces sex-specific health benefits

Authors:

Maarouf Baghdadi [1], Tobias Nespital [1], Andrea Mesaros [1], Sandra Buschbaum [1], Martin Purrio[1], Dominic Withers [2], Sebastian Grönke [1], Linda Partridge [1 3]

Affiliations:

1. Max-Planck Institute for Biology of Ageing, Cologne, Germany
2. Institute of Clinical Sciences (ICS), Faculty of Medicine, Imperial College London, London, UK
3. Institute of Healthy Ageing, and GEE, UCL, London, UK

3.1 Introduction

Human lifespan has been increasing in many parts of the world for the past two centuries, but healthy lifespan has not kept pace[19]. Ageing is characterised both by increased prevalence of multiple age-related diseases, including cancers and cardiovascular and neurodegenerative diseases, and by a general decline in physiological function. Moreover, the prevalence of age-related disease shows a clear sex difference in humans, whereby women live longer on average but suffer greater age-associated morbidity[20]. Research into the mechanisms of ageing has revealed that it is a malleable process that can be ameliorated by genetic, dietary or pharmaceutical interventions with the potential to delay or even compress age-associated morbidity[21]. However, the response to longevity interventions have demonstrated differences due to sex[20], demanding its addition as a variable in longevity studies.

Reduced activity of the insulin/insulin-like growth factor 1 (IGF1) signalling (IIS) pathway is associated with longevity and stress resistance in animal models, including worms[22], flies[23], fish[24] and mice [25–28]. Moreover, studies in mice have found that the role of IIS manipulation on lifespan and health in C57BL/6J mice shows significant sex differences[1,26,27]. Due to its high evolutionary conservation, this central and conserved signalling network was presumed to be involved in human longevity. Indeed, recent GWAS studies have implicated variants in IIS pathway loci with longevity[29], and studies of rare genetic variants have found enrichment of IIS variants in centenarians, suggesting a relationship between IIS and longevity in humans[30]. The finding that a longevity-associated allele reduced IIS activity in cell culture[31] further supports this link. Therefore, understanding how reduced IIS mediates longevity will help to decipher the underlying biological mechanisms of ageing and the development of therapeutics for healthy ageing in the future.

The IIS pathway is a signalling network that plays a central role in regulating growth, survival and metabolism. In mammals, intracellular IIS activity is initiated by two receptors, the insulin receptor (IR) and IGF1 receptors. The IR and the IGF1 receptor are tyrosine kinases that upon ligand binding phosphorylate insulin receptor substrate (IRS) proteins, which are key downstream mediators of pathway activity. While mice have four IRS proteins (IRS1-4), IRS3 is not present in humans[32]. Interestingly, mice globally lacking Irs1 activity (Irs1KO) are long lived[1]. In contrast, Irs2 knockout mice showed reduced survival, suggesting a specific function for IRS1 in the regulation of longevity[1]. Importantly, Irs1KO mice were not only long-lived but also showed resistance to a variety of age-related diseases including adiposity, ulcerative dermatitis, reduced bone volume, motor dysfunction and age-related glucose intolerance[1]. However, lifelong, whole body reduction of IIS has drawbacks such as reduced body size, compromised wound healing, and reduced

fertility. However, in which tissues IRS1 acts to affect longevity and the underlying molecular mechanisms are currently unknown.

Transcriptomic analysis in livers of Irs1KO mice have linked altered IIS to mitochondrial function[1], and subsequent molecular studies have found that livers of IIS mutant mice exhibit reduced mitochondrial respiration, ATP generation and membrane potential[33]. Mitochondria are cellular organelles with a central role in energy production, cellular stress response and apoptosis. Mitochondrial function has long been associated with health and longevity, and mitochondrial dysfunction can cause complex multi tissue diseases, including metabolic and neurodegenerative disorders [34,35]. A recent study has identified activating transcription factor 4 (ATF4) as a key mediator of mitochondrial stress in response to mitochondrial proteostasis perturbations[36]. ATF4 modulates responses to amino acid availability and is up-regulated in mouse liver in response to a wide variety of lifespan-extending interventions, such as methionine restriction, rapamycin and acarbose treated[37]. Furthermore, over-expression of the ATF4 target gene fibroblast growth factor 21 (*Fgf21*) can extend lifespan in mice, suggesting that the ISR might also ameliorate ageing in mammals[38]. Different mitochondrial stressors, affecting mitochondrial translation, oxidative phosphorylation (OXPHOS) stability, mitochondrial membrane potential disruption and impairment of mitochondrial import, activate ATF4, which then up-regulates expression of cytoprotective genes that result in a down-regulation of mitochondrial respiration and activation of the integrated stress response (ISR) through cellular metabolic rewiring[36]. Moreover, in response to stress ATF4 activates ATF5[39], with downstream consequences on rescuing mitochondrial activity[40]. These adaptations lead to increased cellular resistance and protect cells from mitochondrial stress and apoptosis.

In this study, we addressed whether the benefits observed in Irs1KO mice were due to a protection from age-associated decline or reflected an age-independent effect. Moreover, we extended the phenotypic characterisation to include male Irs1KO mice. Then, we deleted IRS1 specifically in liver, muscle, fat and brain tissue of male and female mice and assessed adult survival, but did not detect any significant lifespan extension in any single tissue. We tested all tissue-specific IRS1 deletion models for general health parameters that decline with age[41] to identify which tissues contribute to the benefits observed in Irs1KO mice. We found that neuron-specific IRS1 deletion was unique in improving energy expenditure (EE), locomotor activity and insulin sensitivity in male mice. Furthermore, reduced neuronal IIS induces an associated male-specific and age-dependent mitochondrial dysfunction leading to an up-regulation of brain ISR and a shift in cellular metabolism.

3.2 Results

3.2.1 Increased lifespan and health parameters in Irs1KO mice

The effects of reduced IIS on metabolism and longevity are often sex-specific[20]. For instance, female Irs1KO mice in a C57BL/6J background showed greater lifespan extension than did the mutant male mice[25]. The females were also healthier than controls at old age[1]. The health status of the mutant males was not reported. The improved health at old age in females could indicate protection against the effects of ageing, or reflect an age-independent effect. To address these questions, we measured health parameters in 5 months (young) and 16 months (old) female and male Irs1KO mice and their genetic background controls. We set out to perform these experiments using Irs1KO mice in a C57BL/6N background. However, homozygous mutant animals were not

born in the expected Mendelian ratio and only 4% of homozygous Irs1KO animals were retrieved from matings between heterozygous females and males (10 males and 13 females out of 510 pups). In an earlier study[1], there was also a deficit of Irs1KO pups from double heterozygous matings in the C57BL/6 background, particularly for males (pers. comm.). We therefore generated these animals in the C3B6F1 hybrid background, in which homozygous animals were born in the expected 25% ratio. We therefore assessed health parameters of young and old male and female Irs1KO mice in the C3B6F1 hybrid background.

Lifespan

To determine if lack of IRS1 can also extend lifespan in the C3B6F1 background, we measured adult survival of hybrid C3B6F1 Irs1KO mice and their wildtype littermates. Deletion of IRS1 led to an extension of median lifespan by 7% and 11% and of maximum lifespan, as defined by the 80th percentile age, by 12% and 10% for males (Fig. 1a) and females (Fig. 1b), respectively. The lifespan-extending effect of loss of IRS1 is therefore robust to different genetic backgrounds. Interestingly, there was no gender bias in lifespan extension in the C3B6F1 hybrid background (Cox proportional hazard test, sex*genotype interaction P = 0.4844), in contrast to C57BL/6J[1], indicating that sex-specific effects on IIS mediated longevity are affected by genetic background.

Insulin mutant animals are not only long-lived but also show resistance to age-related diseases. Given the replication of the Irs1KO lifespan extension phenotype in a new mouse background, we assessed whether female hybrid Irs1KO mice also presented with improved age-associated outcomes as reported in the original study[1], and extended the characterisation to include male Irs1KO mice.

Body weight and composition

Irs1KO C3B6F1 mice were dwarves, with a sex-specific reduction in body weight of 46% and 36% in young male and female mice, respectively (two-way ANOVA, sex*genotype interaction P<0.0001; F (1,76) =22.74, Fig. 2a). The greater effect of the mutation on male body weight may have been in part attributable to differences in fat content, as young male Irs1KO mice showed a sex-specific reduction in fat mass, with no significant change in females (two-way ANOVA, sex*genotype interaction P=0.0041; F (1,76) =8.76, Fig. 2a). Body weight and fat content were reduced in mutant mice of both sexes at old age, with no significant sex-specificity (two-way ANOVA, body weight sex*genotype interaction term P=0.9049; F (1,74) =0.0144, fat content sex*genotype interaction term P=0.1787; F (1,74) =1,844, Fig. 1c). The decreased adiposity of old Irs1KO mice was not due to reduced food intake, because there was no difference in food consumption relative to body weight between old mutant and wild type animals of either sex (Fig. 3a). In contrast, young Irs1KO mice of both sexes ate more food relative to their body weight (Fig. 2b), while not showing increased fat mass, suggesting changes in EE.

Energy expenditure

Indirect calorimetry showed increased daytime EE in young Irs1KO mice of both sexes (Fig. 2c), consistent with the hypothesis that body size and body weight-adjusted EE are inversely correlated[42]. We also found increased EE in old Irs1KO mice of both sexes during daytime (Fig. 1d) and nighttime (Fig. 3b). The decrease in adiposity was therefore not mediated by increased EE as young female Irs1KO mice show increased EE but no significant difference in adiposity (Fig. 2a).

We next measured spontaneous home cage locomotor activity to investigate if an increase in movement could account for the decreased adiposity observed in Irs1KO mice. Young male and female Irs1KO mice showed no significant difference in activity levels (Fig. 2d). However, there was a trend that did not reach significance in nighttime male Irs1KO activity (Fig. 2d) that may have contributed to the sex-specific reduction in adiposity observed in young male Irs1KO mice (Fig. 2a). Analysis of activity levels in old male and female Irs1KO mice revealed a significant increase in nighttime, but not daytime activity (Fig. 1e). Thus, increased locomotor activity might contribute to the reduced adiposity of old male and female Irs1KO mutant mice, but it cannot explain the reduced fat mass of young male Irs1KO mice.

Consistent with previous findings in female C57BL/6J Irs1KO mice, female hybrid Irs1KO developed an age-dependent reduction in adiposity[1]. However, adiposity presented in a sex-specific manner, where male hybrid Irs1KO mice had significantly decreased fat content independent of age. Moreover, we detected a significant increase in locomotor activity in old male and female Irs1KO mice. One potential explanation could be an amelioration of the age-dependent decrease in locomotor activity observed in wild type mice[43]. Interestingly, this is consistent with the original report in C57BL/6J female Irs1KO mice, where they reported a delay in age-dependent loss of locomotor coordination on the rotarod[1].

Peripheral metabolism

Increased insulin resistance due to elevated circulating insulin is an age-dependent phenomenon contributing to obesity, type-2 diabetes and metabolic syndrome [44]. Therefore, we assessed if Irs1KO mice had improved metabolic health. We assessed glucose metabolism by insulin tolerance (ITT) and glucose tolerance tests (GTT) of young and old Irs1KO mice of both sexes as a read out for insulin sensitivity and pancreatic beta cell function, respectively. Area under the curve (AUC) analysis of ITT revealed that male Irs1KO mice had significantly enhanced blood glucose uptake in response to the insulin challenge compared to controls at both young (Fig. 2e) and old age (Fig. 1f). In contrast, Irs1KO knockout has no effect on insulin sensitivity in young females (Fig. 2f) but caused insulin resistance in old females (Fig. 1g), consistent with results of female Irs1KO C57BL/6J mice [1]. Old male Irs1KO mice had significantly reduced response to glucose challenge (Fig. 3c), but there was no difference in glucose clearance in young male Irs1KO mice (Fig. 2g). Conversely, young female Irs1KO mice presented with glucose intolerance (Fig. 2h) while we did not detect any significant difference in glucose tolerance in old Irs1KO females (Fig. 3d). These findings are consistent with previous reports, which also detected no change in glucose tolerance in 16-month-old female Irs1KO C57BL/6J mice[1].

Interestingly, we detected age-independent improvement in male Irs1KO insulin sensitivity, while male Irs1KO mice suffered from an age-associated reduction in glucose sensitivity. Female Irs1KO mice recapitulated all the phenotypes observed in C57BL/6J female Irs1KO [1].

Thus, in hybrid Irs1KO mice, there were no sex differences in lifespan or metabolic health parameters such as reduced adiposity, increased EE, and higher locomotor activity at old age, and a sex-specific benefit only to insulin sensitivity in young and old male Irs1KO mice.

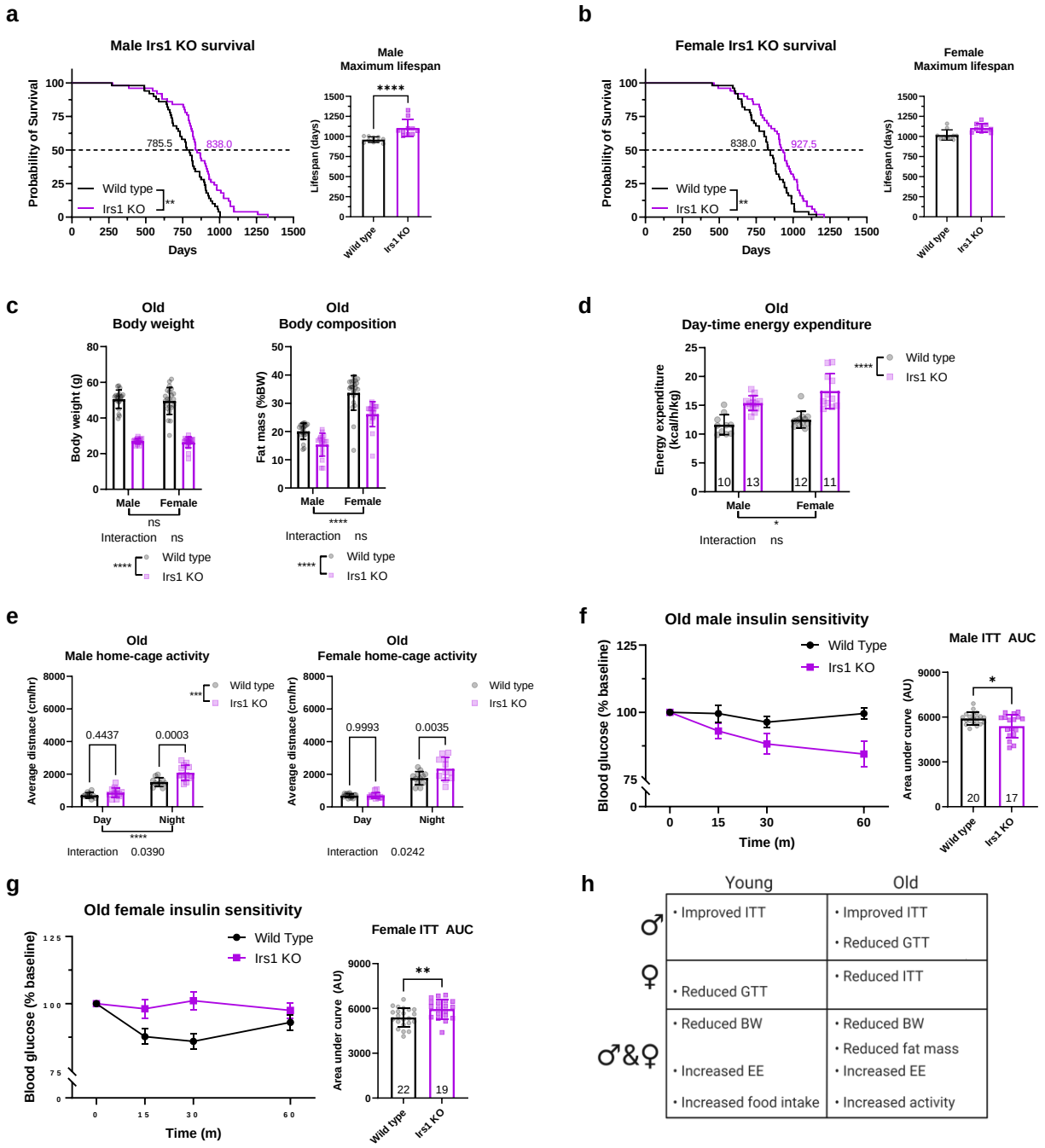

Figure 1: Increased lifespan and improved health parameters in Irs1KO mice

(A) Male and **(B)** female wild type and whole body Irs1KO mice (n=50 biologically independent animals per sex and genotype). **(C)** Body weight and composition of Irs1KO mice was measured at old age (16 months) (Wild type males n=20, Irs1KO males n=17, Wild type females n=21, Irs1KO females n=19). **(D)** Body weight normalised energy expenditure of singly housed old Irs1KO mice during daytime. **(E)** Spontaneous activity of old Irs1KO single housed mice during daytime (inactive phase) and nighttime (active phase) (Wild type males n=10, Irs1KO males n=13, Wild type females n=12, Irs1KO females n=11). Insulin tolerance test (ITT) performed on male **(F)** and female **(G)** Irs1KO mice at old age with respective AUC analysis revealed significantly higher insulin sensitivity in male Irs1KO mice but significantly lower insulin sensitivity in female Irs1KO mice. **(H)** Table summarising the phenotypes unique to and shared between male and female mutant mice. All error bars correspond to standard deviation except for longitudinal insulin sensitivity where standard error of the mean was reported. Number of animals reported at the bottom of the bars or in figure legends. Detailed statistical values found in Table 1.

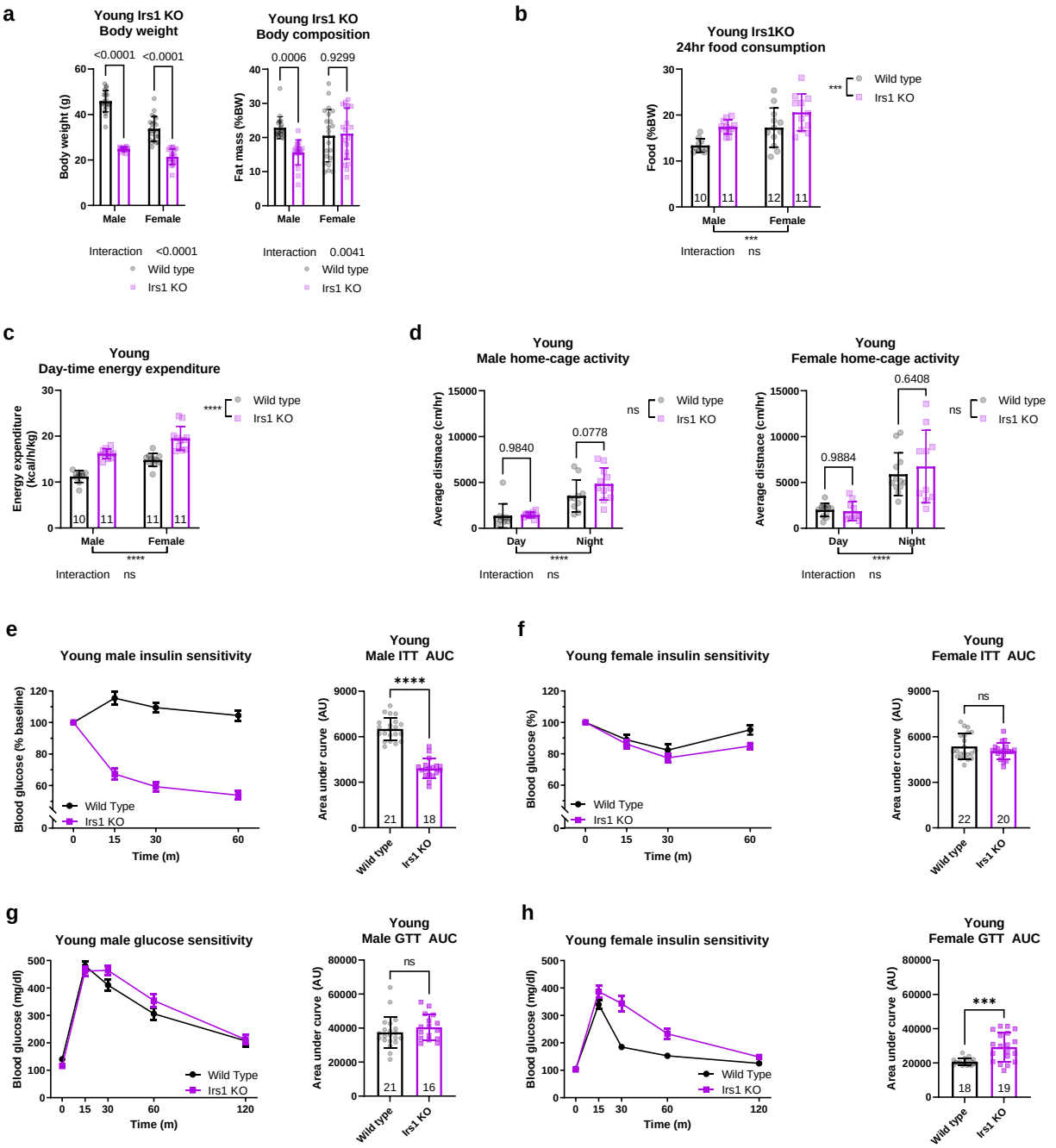

Figure 2: Characterisation of young Irs1KO

(A) Body weight and body composition of Irs1KO mice measured at young age (5 months) (Wild type males n=21, Irs1KO males n=18, Wild type females n=22, Irs1KO females n=19). **(B)** Measurement of food consumption of young Irs1KO and wild type mice revealed a significant increase in food consumption of single housed Irs1KO male and female mice. **(C)** Young body weight normalised energy expenditure of singly housed male and female mice during daytime as assessed by metabolic chambers showing an increase in energy expenditure in Irs1KO mice. **(D)** Spontaneous activity of Irs1KO single housed mice during their inactive cycle or daytime showed no significant difference in activity at young age (Wild type males n=10, Irs1KO males n=11, Wild type females n=12, Irs1KO females n=10). Insulin tolerance test (ITT) of young male **(E)** Irs1KO mice revealed a clear enhanced systemic insulin sensitivity in male Irs1KO mice, while no difference was observed between female **(F)** Irs1KO mice and their wild type littermates. **(G)** Glucose tolerance test (GTT) did not show any significant difference in glucose tolerance in young male Irs1KO and wild type littermate mice. **(H)** AUC analysis of GTT in young female Irs1KO mice revealed a significantly reduced glucose tolerance in Irs1KO females compared to wild type littermate mice. All error bars correspond to standard deviation except for longitudinal glucose and insulin sensitivity where standard error of the mean is reported. Number of animals reported at the bottom of the bars for each condition. Detailed statistical values found in Table 1.

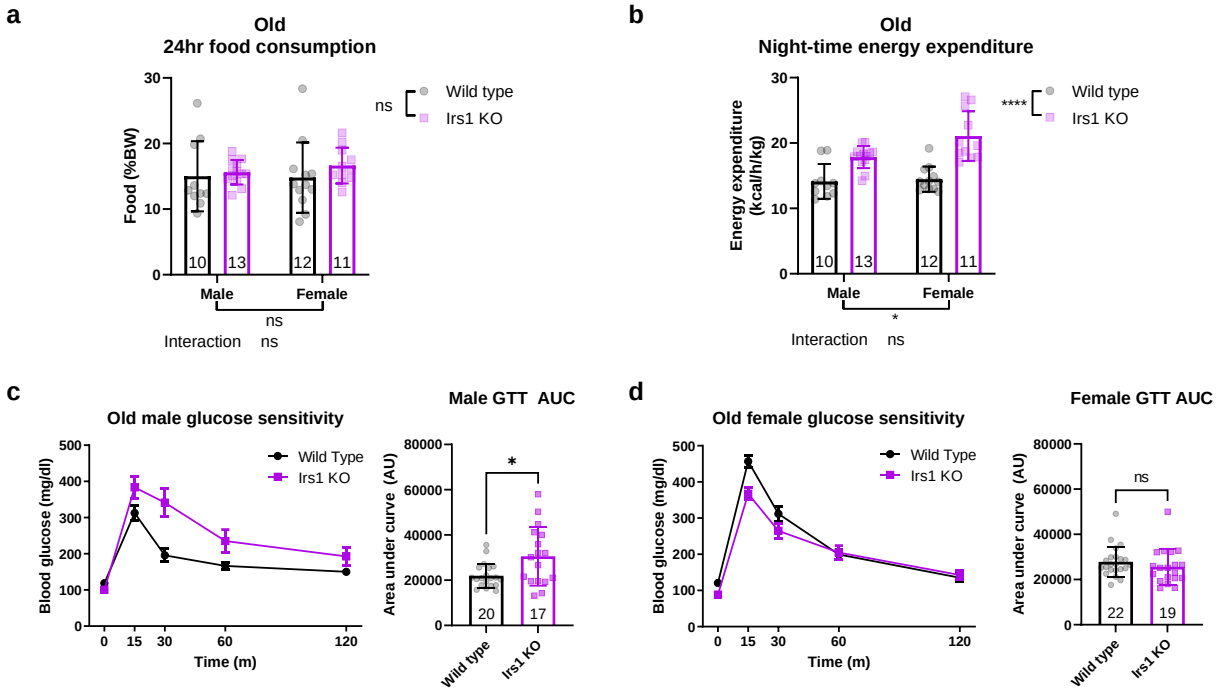

Figure 3: Additional parameters of old Irs1KO

(A) Old (16 months) Irs1KO and wild type food consumption measured in single housed animals shows no significant differences. **(B)** Body weight normalised energy expenditure of old Irs1KO mice during nighttime in individually housed animals showing significant increase in old Irs1KO mice. Glucose tolerance test (GTT) was administered to old male **(C)** and female **(D)** Irs1KO mice, by measuring blood glucose levels in response to a body weight adjusted glucose bolus. Old male Irs1KO mice showed significant reduction in glucose sensitivity. Detailed statistical values found in Table 1.

3.2.2. Tissue-specific Irs1 knockout mice

3.2.2.1 Generation and validation of tissue-specific Irs1 knockout mice

We next investigated the role of different tissues in mediating the effect of IRS1 deficiency on murine longevity and health. Given our findings that hybrid Irs1KO mice recapitulated the majority of the original findings in C57BL/6J Irs1KO mice[1], we used C57BL/6N mice as that is the mouse strain containing the LoxP floxed Irs1 allele and the Cre drivers used to target the five major insulin-responsive metabolic organs: the liver, muscle, fat, gut and nervous system.

Liver-specific Irs1 knockout mice were generated using Alfp-CreT (lKO)[4], muscle-specific (targeting skeletal and cardiac muscle tissue) using Ckmm-CreT (mKO)[5], fat-specific (targeting white adipose tissue (WAT) and brown adipose tissue (BAT)) using Adipoq-CreT (fKO)[6], gut-specific (targeting small and large intestine) using Villin1-CreT (gKO)[7] and neuron-specific using Syn1-CreT (nKO)[8] mice. Male C57BL/6N mice carrying the corresponding CreT transgenic constructs were mated to LoxP floxed Irs1[3] mutant C57BL/6N females to generate tissue-specific Irs1 knockout mice (CreT/+: Irs1fl/fl) and their corresponding LoxP floxed Irs1 littermate controls (Cre+/+: Irs1fl/fl). We first validated the efficiency of IRS1 depletion by measuring *Irs1* transcript levels by quantitative real-time PCR (Q-RT-PCR) in the corresponding target tissue (Fig. 4a-f). This was done using old male and female mice to verify that the depletion of IRS1 is stable throughout life. Primers and conditions were validated with cortical brain samples from Irs1KO mice (Fig 4a). *Irs1* transcripts

were strongly depleted in liver tissue of lKO (Fig. 4b), hindlimb muscle tissue of mKO (Fig. 4c), BAT tissue (subscapular) of fKO (Fig. 4d) and partly depleted in cortical brain tissue of nKO mice (Fig. 4e). The partial reduction in the cortex is probably explained by the residual expression of *Irs1* in glial cells, which are not targeted by the Syn1Cre [8]. In contrast, we did not detect depletion of *Irs1* transcripts in the small intestine (ileum) of gKO mice (Fig. 4f), suggesting that *Irs1* mutant cells were outcompeted by wild type cells in the gut epithelium during ageing. Therefore, gKO mice were excluded from further analysis.

We next tested the specificity of the tissue-specific knockout lines by measuring *Irs1* expression levels in non-targeted tissues, namely brain cortex for lKO, mKO and fKO (Fig. 4g) and liver tissue for the nKO (Fig. 4h), respectively. There was no significant difference in the expression level of *Irs1* in the non-targeted tissues, demonstrating the specificity of the generated tissue-specific knockout lines. As IRS1 and IRS2 have been suggested to have redundant functions, we used Q-RT-PCR to measure *Irs2* levels in the IRS1 tissue-specific knockout lines. However, except for a slight up-regulation of *Irs2* transcript levels in the liver of male lKO mice (Fig. 4b), there was no compensatory up-regulation of *Irs2* gene expression in any of the tested knockout lines (Fig. 4a-e). In summary, the four IRS1 tissue-specific knockout lines had efficient depletion of *Irs1* expression, without unspecific effects in other tissues or compensatory regulation of *Irs2* expression. Thus, these lines were suitable for addressing how tissue-specific depletion of IRS1 affects health and longevity.

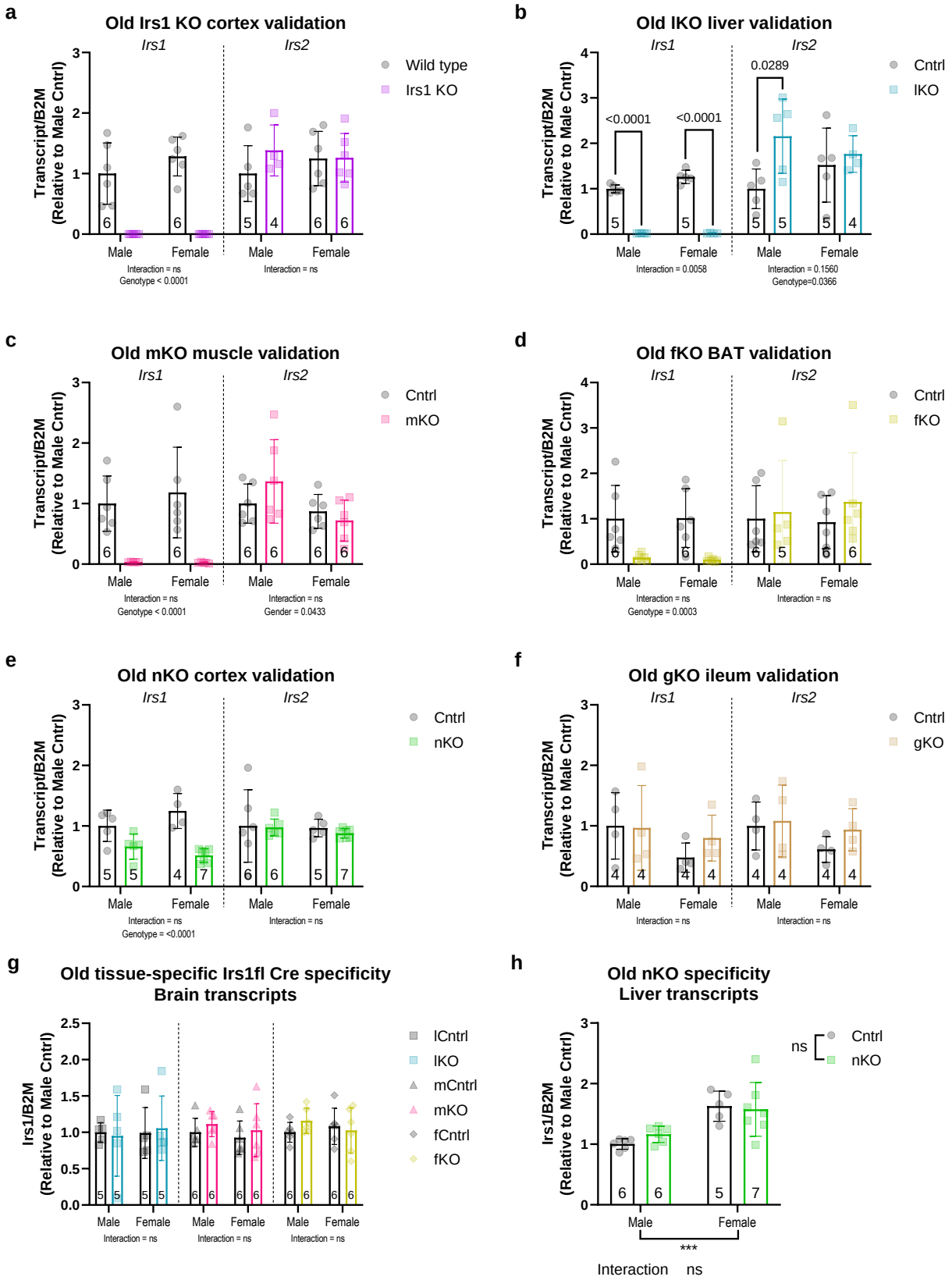

Figure 4: Validation of mouse models used in the study

(A) Quantitative real-time PCR of cortical tissue in Irs1KO mice shows depletion of Irs1 transcripts. Irs2 transcript levels show no compensatory effect. **(B)** Liver samples of IKO mice show depletion of Irs1 transcripts and compensatory Irs2 upregulation in male IKO mice. **(C)** Hindlimb muscle samples revealed depletion of Irs1 transcript levels in mKO mice, but no effect on Irs2 transcript

levels. **(D)** Supraclavicular brown adipose tissue (BAT) samples of fKO mice show depletion of Irs1 transcripts with no compensatory Irs2 upregulation. **(E)** Cortex samples of nKO mice show significant reduction but not depletion of Irs1 transcripts in nKO mice, with no effect on Irs2 transcript levels. **(F)** lKO, mKO and fKO cortical samples used to assess Irs1 transcript levels did not reveal any non-specific Irs1 deletion in brain tissue. **(G)** Liver samples from nKO mice not showing any non-specific Irs1 deletion in liver tissue. All error bars correspond to standard deviation. Number of animals reported at the bottom of the bars or in figure legends. Detailed statistical values found in Table 1.

3.2.2.2 Tissue-specific knockout of Irs1 in liver, muscle, fat or neurons does not extend lifespan in mice

Lifespan

As global loss of IRS1 results in lifespan extension, we measured survival of tissue-specific Irs1 mutant male and female mice, to address which tissue might underlie the longevity effect. However, there was no change in lifespan detected by log-rank test in male lKO (Fig. 5a), mKO (Fig. 5c), fKO (Fig. 5e) and nKO (Fig. 5g). We observed a slight trend towards lifespan reduction in male mKO mice (log-rank test P=0.0605) (Fig. 5c). Maximum lifespan analysis of male tissue-specific Irs1 knockout mice revealed a reduction in lKO (Fig. 5a) and mKO (Fig. 5c) maximum lifespan compared to littermate controls. Median survival and maximum lifespan for female lKO (Fig. 5b), mKO (Fig. 5d) and nKO (Fig. 5h) were not significantly different compared to their respective littermate controls. However, there was a significant reduction in female fKO median lifespan of approximately 17% and maximum survival by approximately 9% (Fig. 5f), potentially highlighting a critical female-specific role of IRS1 in adipose tissue. Previous reports of a fat specific IR knockout model showed significant extension in lifespan of approximately 18%[45]. However, the data was not separated by sex to determine whether one sex responded differently to the intervention.

In summary, we did not detect lifespan extension in any of the tested *Irs1* tissue-specific KO lines, suggesting that reduction of IIS in more than one tissue or in a tissue we have not targeted is required for lifespan extension in mice.

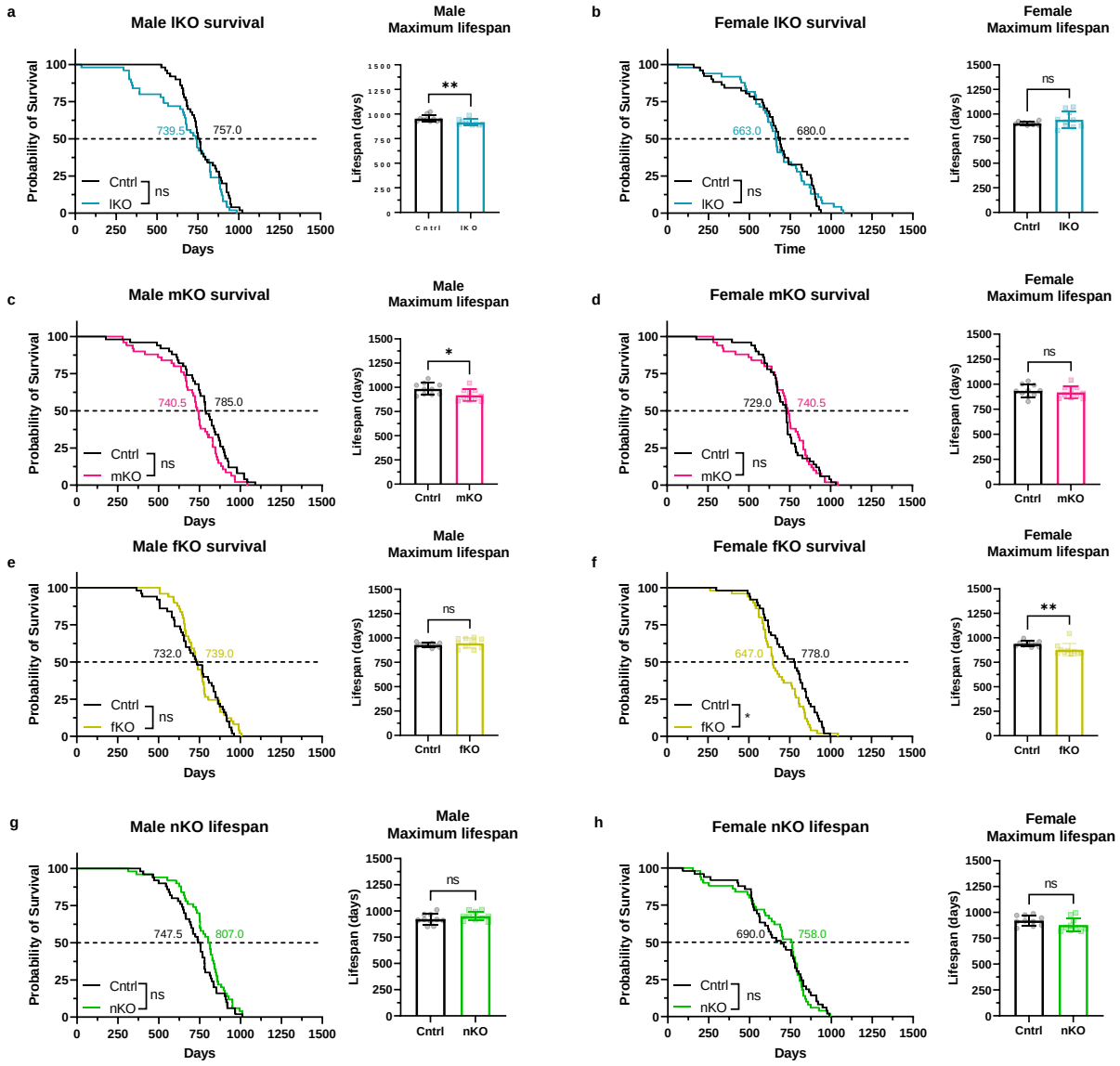

Figure 5: Tissue-specific deletion of IRS1 is not sufficient for lifespan extension

Kaplan Meier plots depicting survival of male and female mice. Log-rank tests were used to compare median survival (labelled on 50% survival probability line in days) and Mann Whitney tests to compare maximum lifespan (inset shows top 20% longest-lived mice) of all mutant mice. **(C)** Male and **(D)** female control (Cntrl) and liver-specific Irs1 knockout (lKO) mice (n=50 biologically independent animals for all groups). **(E)** Male and **(F)** female control (Cntrl) and muscle-specific Irs1 knockout (mKO) mice (n=50 biologically independent animals for all groups). **(G)** Male and **(H)** female control (Cntrl) and fat-specific Irs1 knockout (fKO) mice (n=50 biologically independent animals for all groups, n=49 for male fKO mice). **(I)** Male and **(J)** female control (Cntrl) and neuron-specific Irs1KO (nKO) mice (n=50 biologically independent animals for all groups, n=49 for female control). Detailed statistical values found in Table 1.

3.2.2.3 IRS1 deletion in liver, muscle or fat does not improve health

Body weight and composition

In order to ask whether tissue-specific deletion of IRS1 would lead to health benefits, we characterised male and female *Irs1* tissue-specific knockout lines. In contrast, to whole body Irs1KO animals, which are dwarfs, there was no difference in body weight in young lKO, mKO or

fKO animals (Fig. 6a, e and i), indicating that deletion of IRS1 in these tissues did not interfere with overall growth.

The liver stores glucose after a meal as glycogen or converts excess glucose to fatty acids. It also oxidises fatty acids to provide energy for gluconeogenesis during fasting. Moreover, sex affects liver physiology, with significant consequences for systemic metabolism[46]. We observed sex differences in the metabolic phenotypes of Irs1KO mice, therefore, we investigated the contribution of liver-specific IRS1 deletion to the metabolic phenotypes in male and female Irs1KO mice. Deletion of IRS1 in muscle revealed an important role for IRS1 in muscle growth and for insulin-stimulated glucose transport into muscle [47,48]. However, the sex-specific role of IRS1 in muscle tissue has not been fully characterised. Therefore, we assessed whether muscle contributed to the sex-specific health benefits observed in Irs1KO mice. The contribution of adipose tissue to the physiological insulin response is not certain. However, fat-specific IR knockout mice are protected against age-associated glucose intolerance and insulin insensitivity[49], and show enhanced lifespan[45]. However, the role of a relatively modest IIS reduction in IRS1 deletion and the role of sex have not been assessed.

lKO mice showed a sex-specific reduction in body weight only in old males (two-way ANOVA, sex*genotype interaction P=0.0015; F (1,45) =11.38, Fig. 6c), which was probably due to a sex-specific decrease in fat mass (two-way ANOVA, sex*genotype interaction P=0.0284; F (1,45) =5.132, Fig. 6d). Male and female mKO mice showed no change in body weight (Fig. 6e and g), but a significant increase in fat mass relative to body weight at both young and old age in both sexes (Fig. 6f and h). Potentially, the increase in fat mass in old mKO could be specific to the male mice, however, the high variability in the control males prevented the interaction term from reaching statistical significance (P=0.0629) (Fig. 6h). These results are consistent with findings using muscle-specific IR knockout animals, which also showed increased fat mass and reduced muscle mass[50]. Although male and female fKO showed no change in body weight (Fig. 6i and k), we measured a significant reduction in fat mass at young and old age in both male and female fKO mice (Fig. 6j and l), suggesting that, similar to fat-specific IR knockout mice [49,51], fKO mice also have reduced WAT mass. Changes in body weight and composition was not a result of altered food consumption as no significant difference was observed in young and old lKO, mKO or fKO animals (Fig. 6m-r). There has been controversy whether IIS in fat can modulate feeding, as one report found a significant increase in fat-specific IR knockout mice[51], while another study found no difference[49]. We did not detect any significant changes in food intake of young or old fKO mice of either sex (Fig. 6q and r), which might be due to the less severe interruption of IIS upon loss of IRS1 compared to the IR.

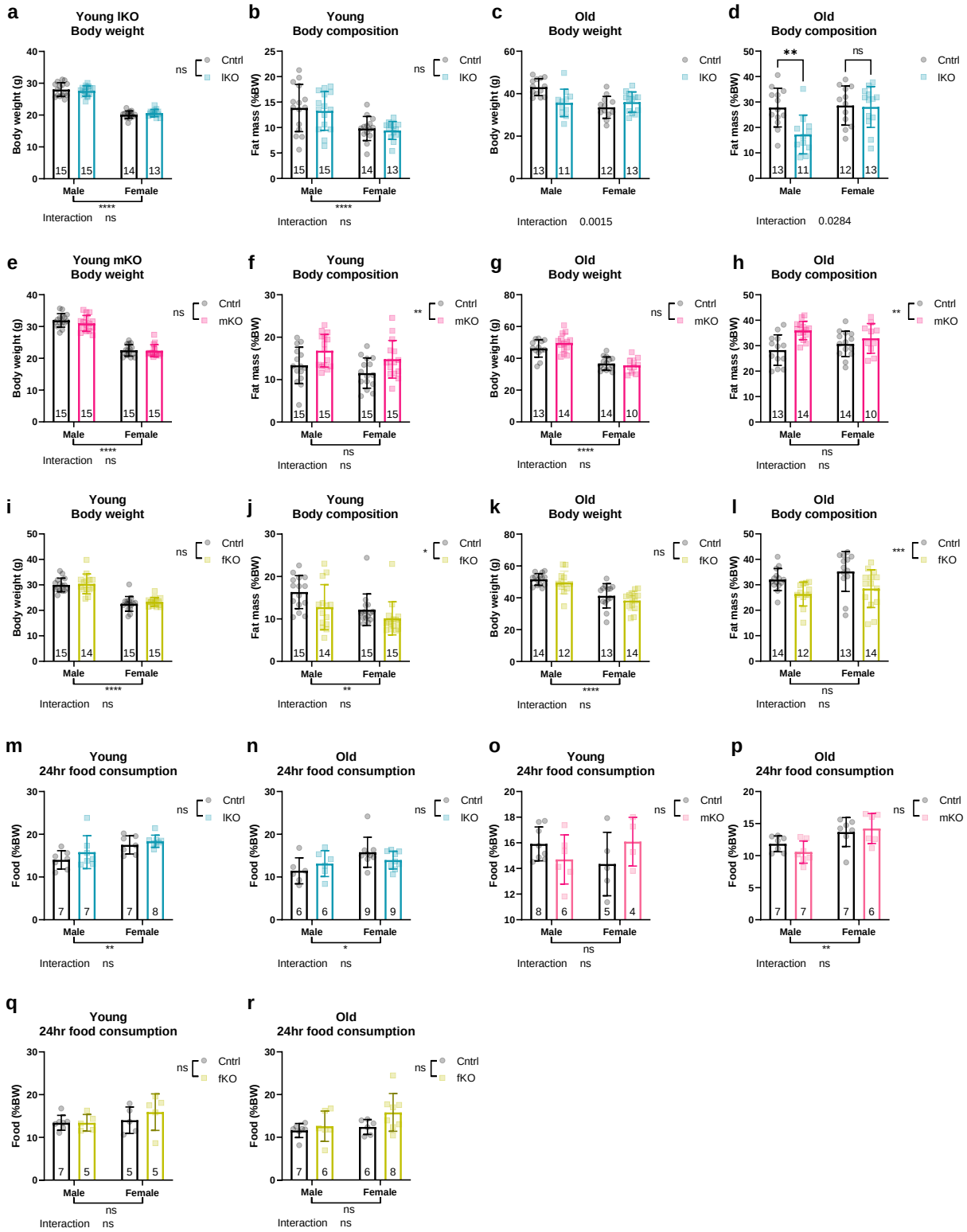

Figure 6: Body weight and composition of tissue-specific Irs1KO mice

Body weight **(A)** and body composition **(B)** of young (4 months) male and female lKO mice revealed no significant difference between lKO and control littermates. **(C)** Body weight of old (16 months) male and female lKO revealed a sex-specific significant reduction in body weight of male lKO mice. **(D)** Body composition at old age also revealed sex-specific significant reduction in body weight adjusted fat mass of male lKO mice. Body weight of young **(E)** (4 months) and old **(F)** (16 months) mKO mice showed no significant difference. Body composition in young **(G)** and old **(H)** mKO mice revealed a significant age-independent increase in fat mass of mKO mice compared to control littermates. Body weight of young **(I)** (4 months) and old **(K)** (16 months) fKO mice showed

no significant difference. Body composition in young **(J)** and old **(L)** fKO mice revealed a significant age-independent decrease in fat mass of fKO mice compared to control littermates. Measurement of food consumption of young lKO **(M)** and old lKO **(N)** revealed no significant difference in food consumption of single housed animals relative to the corresponding littermate controls. Measurement of food consumption of young mKO **(O)** and old mKO **(P)** revealed no significant difference in food consumption of single housed animals relative to the corresponding littermate controls. Measurement of food consumption of young fKO **(Q)** and old fKO **(R)** revealed no significant difference in food consumption of single housed animals relative to the corresponding littermate controls. Number of animals reported at the bottom of the bars for each condition. Detailed statistical values found in Table 1.

Energy expenditure

Consistent with the lack of differences in young lKO body weight and composition, we did not detect any significant differences in EE of young male (Fig. 7a) or female (Fig. 7b) lKO mice. Although we detected a sex-specific reduction in body weight and composition in old male lKO mice, we did not detect any significant difference in EE of old males (Fig. 7c) or females (Fig. 7d). However, the slopes of the regression analysis were significantly different in old lKO mice, preventing comparison of EE. IRS1 deficiency in muscle and fat tissue did not lead to a significant difference in EE in young or old male and female mKO and fKO mice (Fig. 7e-l). Spontaneous locomotor activity did not reveal any significant difference in young or old male and female lKO (Fig. 8a-b). Young male mKO mice showed increased spontaneous locomotor activity specifically during nighttime (Fig. 8c), while no change was observed in mKO females or old mKO males (Fig. 8d). Reduced IIS in the fat was insufficient to affect spontaneous activity on young or old fKO mice of either sex (Fig. 8e and f).

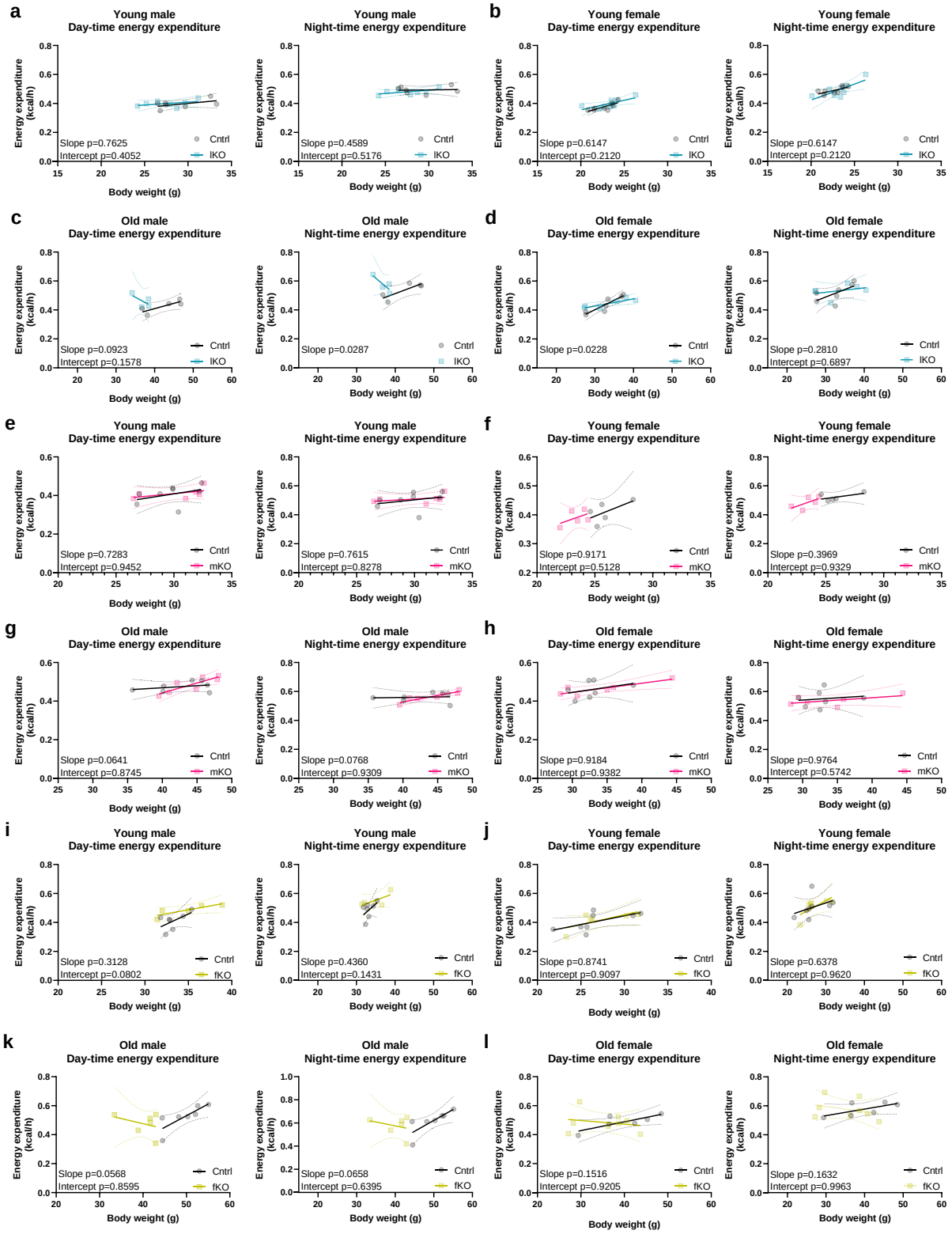

Figure 7: Energy expenditure of tissue-specific Irs1KO mice

Daytime and nighttime energy expenditure were analysed by linear regression of energy expenditure by body weight (ANCOVA). No difference in energy expenditure was detected in young male **(A)** or female **(B)** IKOs (male control and IKO n=7, female controls and IKO n=8) or old male **(C)** and female **(D)** IKOs (male control n=5 and IKO n=4, female controls n=7 and IKO n=6). No difference in energy expenditure was detected in young male **(E)** and female **(F)** mKOs (male control n=8 and mKO n=6, female controls and mKO n=5) or old male **(G)** and female **(H)** mKOs (male control and mKO n=7, female control n=7 and mKO n=6). No difference in energy expenditure was detected in young male **(I)** and female **(J)** fKOs (male control n=7 and fKO n=5, female control n=8 and fKO

n=6) or old male **(K)** and female **(L)** fKOs (male control n=7 and fKO n=6, female control n=6 and fKO n=8). Detailed statistical values found in Table 1.

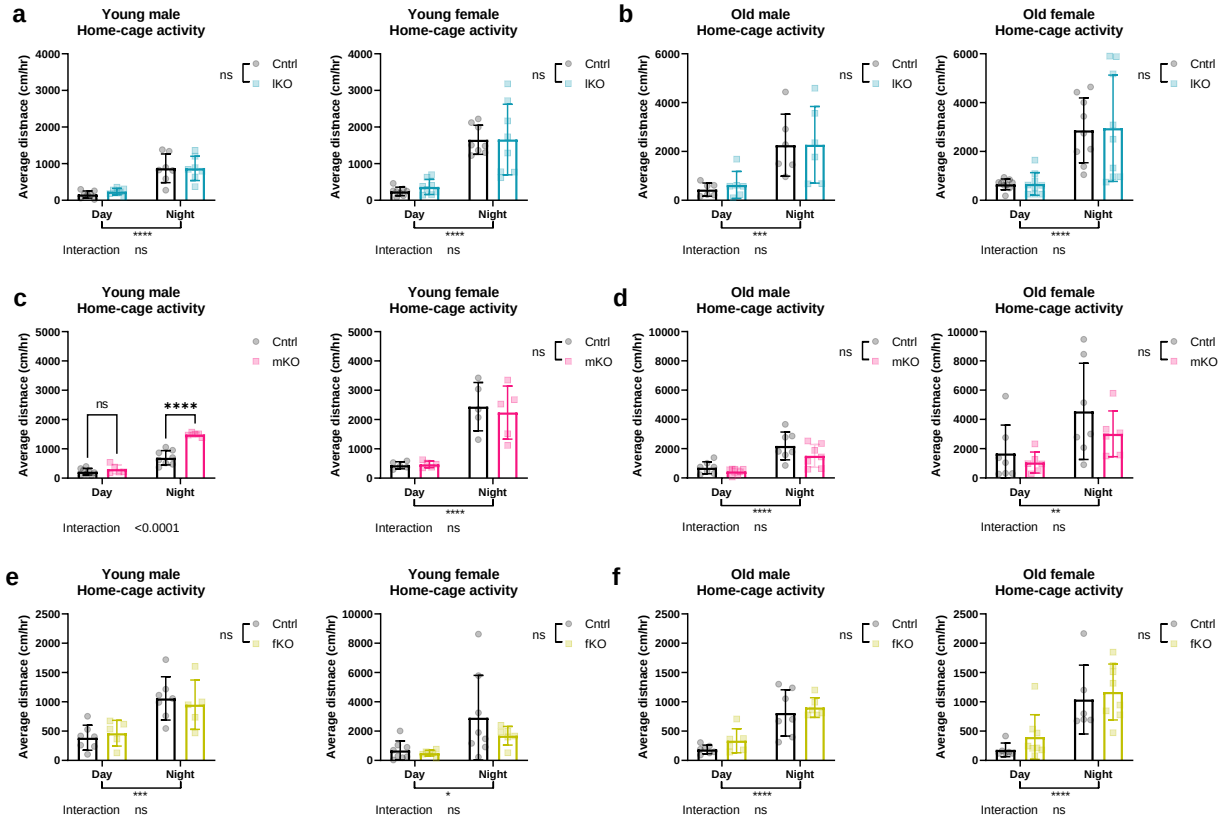

Figure 8: Locomotor activity of tissue-specific Irs1KO mice

Measurement of spontaneous locomotor activity of singly housed young IKO **(A)** (male control and IKO n=7, female controls and IKO n=8) and old IKO **(B)** (male control and IKO n=6, female controls and IKO n=9) mice during daytime and nighttime did not reveal any significant difference due to genotype. Spontaneous locomotor activity of singly housed young male mKO mice **(C)** (control n=8 and mKO n=5) revealed higher activity levels during nighttime compared to controls. Spontaneous activity of young female mKO **(C)** (control and mKO n=5), old male mKO **(D)** (control and mKO n=7) or old female mKO **(D)** (control n=7 and mKO n=6) mice during daytime and nighttime did not reveal any significant difference due to genotype. Spontaneous locomotor activity of singly housed young fKO **(E)** (male control n=7 and fKO n=5, female controls n=8 and fKO n=6) and old fKO **(F)** (male control n=7 and fKO n=6, female controls n=6 and fKO n=8) mice during daytime and nighttime did not reveal any significant differences. Detailed statistical values found in Table 1.

Peripheral metabolism

Insulin sensitivity was unaffected in young or old male and female IKO mice (Fig. 9a-d). Insulin sensitivity was not significantly changed in mKO mice (Fig. 9e-h), consistent with data from muscle-specific IR and IGF1R knockout mice, which had reduced activated IRS1 levels but no change in insulin sensitivity [5,52]. Insulin sensitivity was slightly but significantly reduced in young male fKO mice (Fig. 9i), while young female fKO mice showed no significant difference (Fig. 9j). Insulin sensitivity of old male fKO mice was not significantly changed (Fig. 9k), however, old female fKO mice had significantly reduced insulin sensitivity (Fig. 9l).

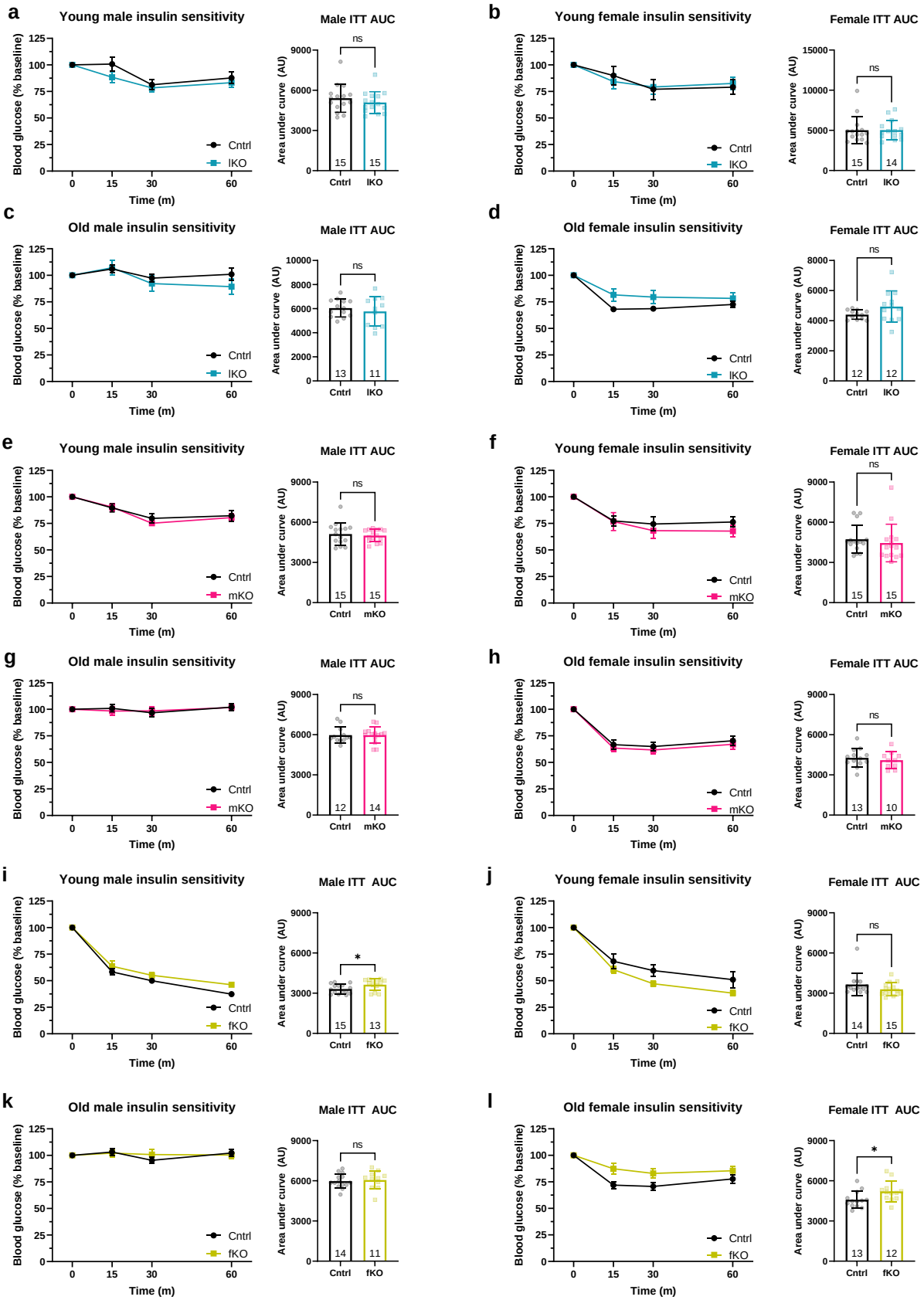

Figure 9: Insulin tolerance test of tissue-specific Irs1KO mice

Insulin tolerance test (ITT) revealed no significant difference in insulin sensitivity of young male lKO **(A)**, young female lKO **(B),** old male lKO **(C)** and old female lKO **(D)** compared to their respective control littermates as assessed by AUC analysis. No significant

difference in insulin sensitivity of young male mKO **(E)**, young female mKO **(F),** old male mKO **(G)** and old female mKO **(H)** compared to their respective control littermates as assessed by AUC analysis. ITT of young male fKO **(I)** revealed a significant reduction in insulin sensitivity between fKO and control littermates. ITT analysis of young female fKO **(J)** and old male fKO **(K)** did not detect any significant differences between fKO mice and their control littermates. ITT of old female fKO **(L)** revealed a significant reduction in insulin sensitivity between fKO and control littermates. Detailed statistical values found in Table 1.

Consistent with previous studies[53], male lKO mice showed reduced glucose sensitivity at young (Fig. 10a), but not old age (Fig. 10c). This suggests that the liver-specific loss of IRS1 function can be compensated for during ageing, potentially due compensatory increase in *Irs2* expression (Fig. 4b). In contrast to the males, female lKO mice showed no difference in glucose sensitivity at young or old age (Fig. 10b and d). Young male and female mKO animals showed a significant reduction in glucose sensitivity (Fig. 10e and f), which was surprising, given that IR or IRS1+2 knockout mice did not show this effect[5,48]. However, the reduction in glucose sensitivity was also observed in old male (Fig. 10g), but not in old female mKO mice (Fig. 10h). Glucose sensitivity was significantly reduced in young female fKO mice (Fig. 10j), but unaffected in young males (Fig. 10e). Old female fKO mice were more glucose-sensitive than controls (Fig. 10l), but only a trend in old male glucose sensitivity (Fig. 10k).

Overall, our data suggest that loss of IRS1 in the liver predominantly affects male body composition and glucose sensitivity, while loss of IRS1 in muscle leads to consistent differences in males and females, with the exception of the locomotor activity at young age. Loss of IRS1 in fat tissue mostly affected females, leading to significant differences in peripheral metabolism, potentially linked to the female-specific decrease in lifespan we observed (Fig. 5f).

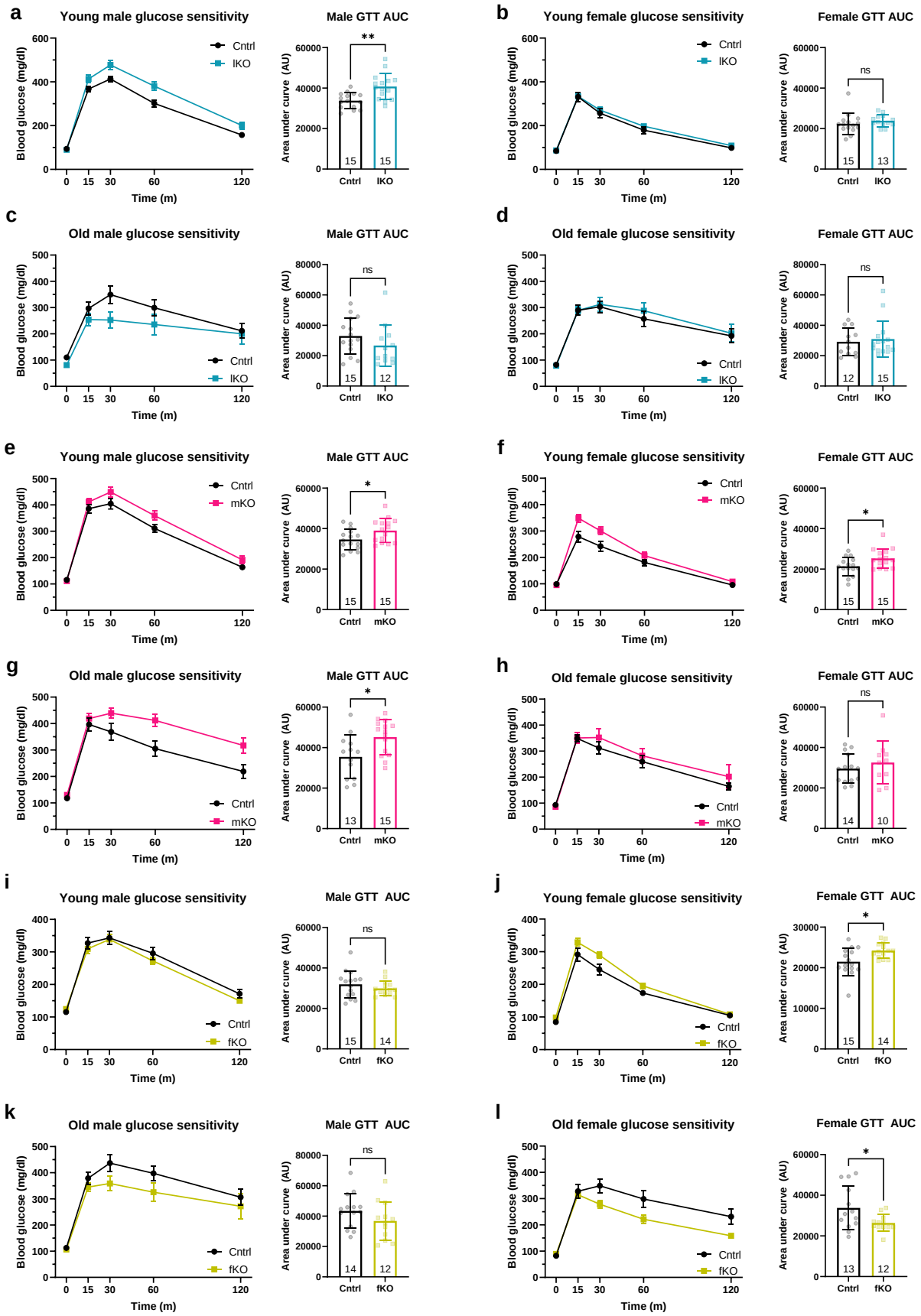

Figure 10: Glucose tolerance test of tissue-specific Irs1KO mice (below)

Glucose tolerance test (GTT) revealed a significant reduction in glucose tolerance of young male lKO **(A)** compared to control mice as assessed by AUC analysis. AUC analysis of GTT of young female lKO **(B)**, old male lKO **(C)** and old female lKO **(D)** did not detect any significant differences between lKO mice and their control littermates. GTT revealed a significant reduction in glucose tolerance of young male mKO **(E)**, young female mKO **(F)** and old male mKO **(G)** as assessed by AUC analysis. GTT of old female mKO **(H)** did not detect any significant differences between mKO mice and their control littermates. GTT of young male fKO **(I)** did not detect any significant differences between fKO mice and their control littermates. GTT of young female fKO **(J)** revealed a significant reduction in glucose tolerance as assessed by AUC analysis. GTT of old male fKO **(K)** and old female fKO **(L)** did not detect any significant differences between fKO mice and their control littermates. Detailed statistical values found in Table 1.

3.2.2.4 Neuron-specific Irs1 knockout mice show male-specific improvement in metabolic health

The brain is a central mediator of metabolic function[54], and reduced IIS in the brain has been associated with changes in body weight, fat mass, glucose metabolism and feeding behaviour[55]. However, peripheral, off-target recombination has been reported in kidney, pancreas and muscle of some of the Cre-driver lines used in these studies[56]. We therefore phenotyped male and female nKO mice at young and old age using the Syn1Cre gene driver, drives pan-neuronal Cre expression. There was a slight sex-specific reduction in body weight in old male nKO mice (two-way ANOVA, sex*genotype interaction $P<0.0172$; $F(1,51)=6.069$, Fig. 11a) with no significant change in body composition of either young (Fig. 12a) or old nKO (Fig. 11a) mice of either sex. As brain insulin signalling has been implicated in feeding and satiety[57], we measured food consumption in nKO mice, but we could not detect any differences in young (Fig. 12b) or old (Fig. 13a) mice of either sex. Previous studies have uncovered a direct role of the brain in mediating EE through peripheral tissues such as BAT [58,59]. In young animals, there was no effect on EE in either male or female nKO mice (Fig. 12c). However, EE was specifically increased in old male, but not female nKO mice during daytime (Fig. 11b) and nighttime (Fig. 13b), indicating that nKO mice show an age-dependent and sex-specific increase in EE. Given the role of neuronal IIS in locomotor activity[60] we next measured spontaneous home-cage activity. Locomotor activity was not changed in young nKO males (Fig. 12d), but was increased in young females during both daytime and nighttime. In contrast, old male nKO mice showed a significant increase in activity only during nighttime, while there was no change in old nKO females (Fig. 11c). The male specific increase in activity was not observed during daytime, suggesting that the effect seen at old age was not due to general hyperactivity of old male nKO mice. As neuronal IIS function has been implicated in mediating insulin sensitivity through circuitry with peripheral metabolic organs[60], we assessed insulin sensitivity in young and old nKO mice of both sexes. Consistent with male Irs1KO mice, insulin sensitivity was increased in young (Fig. 12e) and old (Fig. 11d) male nKO mice. However, the opposite occurred in young female nKO mice, with a significant reduction in insulin sensitivity (Fig. 12f), which was lost at old age (Fig. 11e). Importantly, none of the phenotypes in the nKO mice were present in the Syn1Cre control mice (Fig. 14a-j). Thus, IRS1 deletion only in neurons was sufficient to induce male-specific benefits in metabolic outcomes that in part recapitulated the phenotypes of the global Irs1KO. Moreover, nKO mice successfully avoided the negative consequences of Irs1KO mice such as reduced body size and glucose sensitivity (Fig. 13 c and d).

In summary, all mutant mice successfully avoided the dwarf phenotype in Irs1KO mice, but, IRS1 deficiency in liver, muscle or fat did not recapitulate the health benefits observed in old Irs1KO mice. On the other hand, deletion of IRS1 in neurons induced all of the health benefits observed in Irs1KO mice, without the negative effects on glucose sensitivity, but in a male-specific manner. In summary, neuronal IIS in male mice may play a key role in the improved insulin sensitivity, excess EE and amplified activity of whole body knockout mice.

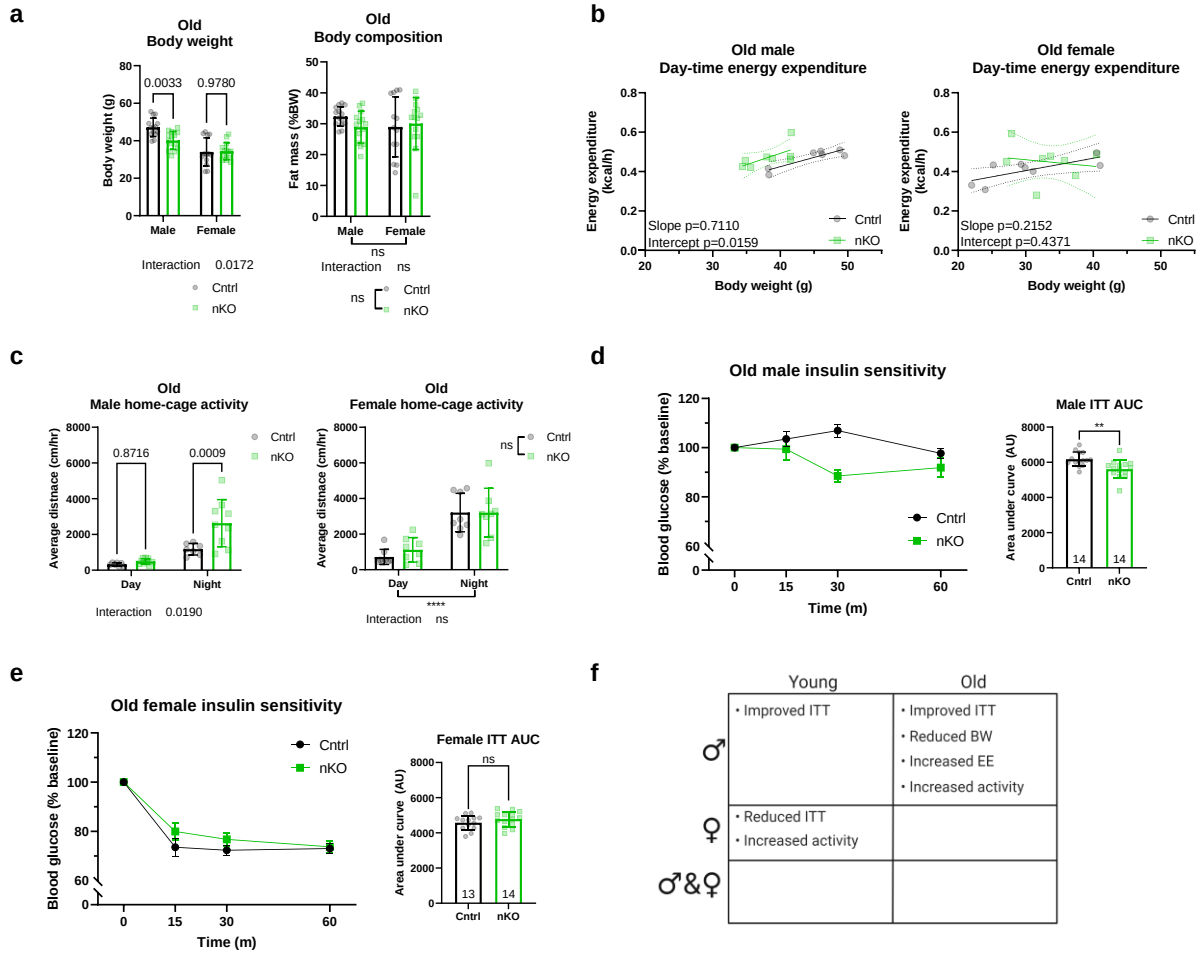

Figure 11: Neuron-specific Irs1 knockout (nKO) mice show male-specific improvement in metabolic health

(A) Body weight and composition of nKO mice was assessed at old age (16 months) (n = 14 biologically independent animals for all groups). **(B)** Daytime energy expenditure of male (control n=7 and nKO n=8) and female (n=8 female control and nKO) mice was analysed by linear regression of energy expenditure by body weight (ANCOVA). **(C)** Plotted spontaneous home-cage activity of old male (control n =7 and nKO n=9) and female (control n=7 and nKO n=9) single housed nKO mice showed a nighttime specific increase in activity of male nKO mice. **(D)** Analysis of insulin tolerance test (ITT) curves and AUC values of old male nKO showed a significant improvement in insulin sensitivity in nKO mice compared to controls. **(E)** Analysis of ITT curves and AUC values of old female nKO did not reveal any significant difference compared to controls. **(F)** Table summarising the phenotypes unique to and shared between male and female mutant mice, highlighting the enrichment of male-specific phenotypes in nKO mice. All error bars correspond to standard deviation except for longitudinal insulin sensitivity where standard error of the mean was reported. For ANCOVA analysis the 95% confidence interval is plotted. Number of animals reported at the bottom of the bars or in figure legends. Detailed statistical values found in Table 1.

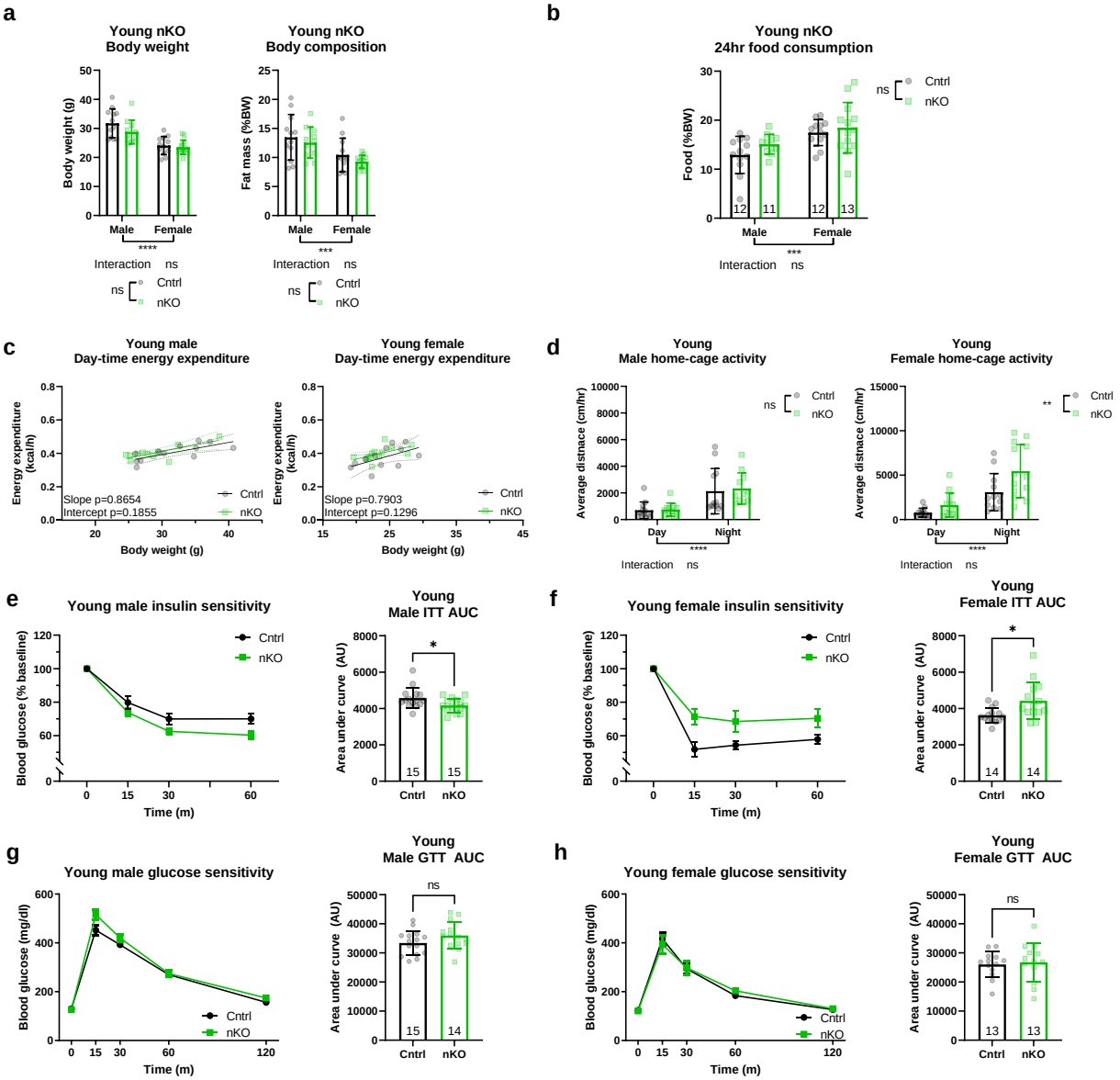

Figure 12: Characterisation of young nKO

(A) No significant difference was observed in body weight or body composition at young age (3 months) of nKO and control littermates (male nKO and controls n=15, female nKO and control n=14). **(B)** Measurement of food consumption of young nKO and control mice revealed no significant difference in food consumption of single housed animals. **(C)** Daytime energy expenditure of male nKO and female nKO and control mice was analysed by linear regression of energy expenditure by body weight (ANCOVA). No difference in energy expenditure between young male nKO (n=11) and controls (n=12) or female nKO (n=13) and controls (n=12) was observed. **(D)** No significant difference was observed in spontaneous activity of young single-housed male nKO (n=12) and littermate control (n=11) mice. A significant increase in daytime and nighttime activity was observed between female nKO (n=13) and littermate control (n=12) mice. Insulin sensitivity of male nKO and control mice **(E)** showed a significantly improved insulin sensitivity in male nKO mice. However, a significant reduction in insulin sensitivity was detected between female **(F)** nKO and control mice. Analysis of GTT of male **(G)** and female **(H)** nKO mice did not reveal any significant difference in young nKO glucose tolerance compared to control littermates. All error bars correspond to standard deviation except for longitudinal glucose and insulin sensitivity where standard error of the mean is reported. Number of animals reported at the bottom of the bars for each condition. Detailed statistical values found in Table 1.

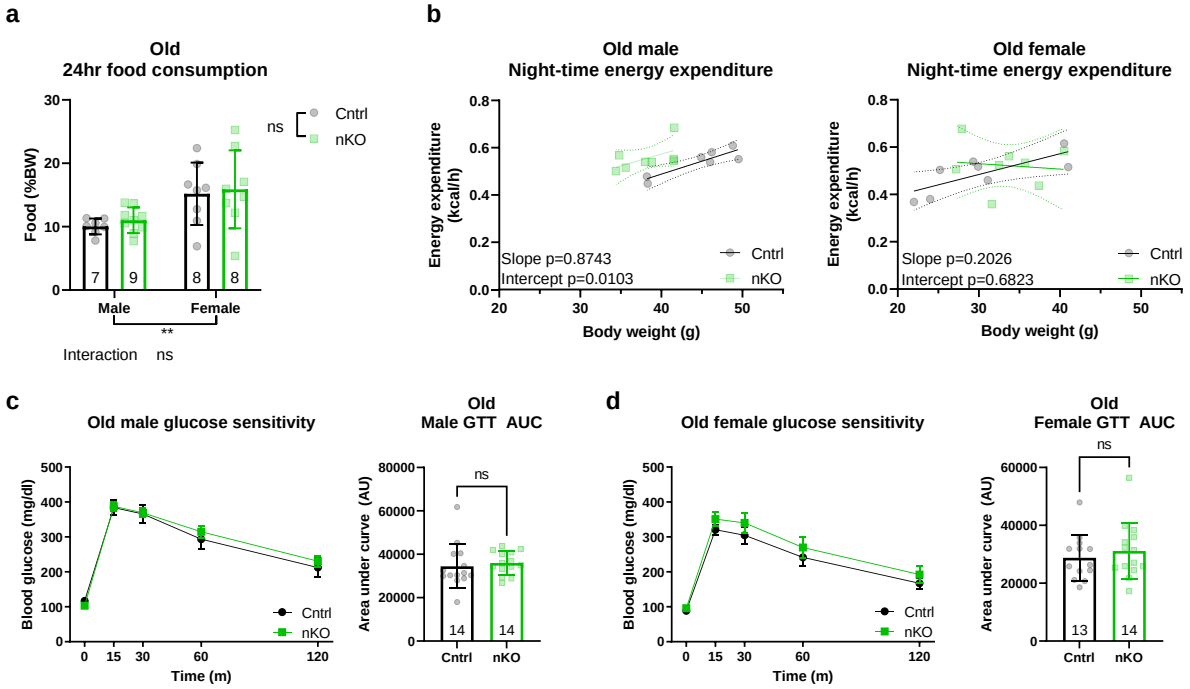

Figure 13: Additional parameters of old nKO

(A) No difference in food consumption was detected in single housed old (16 months) nKO and control littermates. **(B)** Nighttime energy expenditure of male and female mice was analysed by linear regression of energy expenditure by body weight (ANCOVA). Unlike female nKO mice (n=8 female control and nKO mice) where no significant difference between intercepts was detected, male nKO (n=8) mice showed significant increase in energy expenditure compared to male controls (n=7). Analysis of GTT did not detect any significant difference between the ability of old male **(C)** and female **(D)** nKO mice compared to their respective littermate controls in lowering blood glucose levels. All error bars correspond to standard deviation except for longitudinal glucose sensitivity where standard error of the mean is reported. Number of animals reported at the bottom of the bars for each condition. Detailed statistical values found in Table 1.

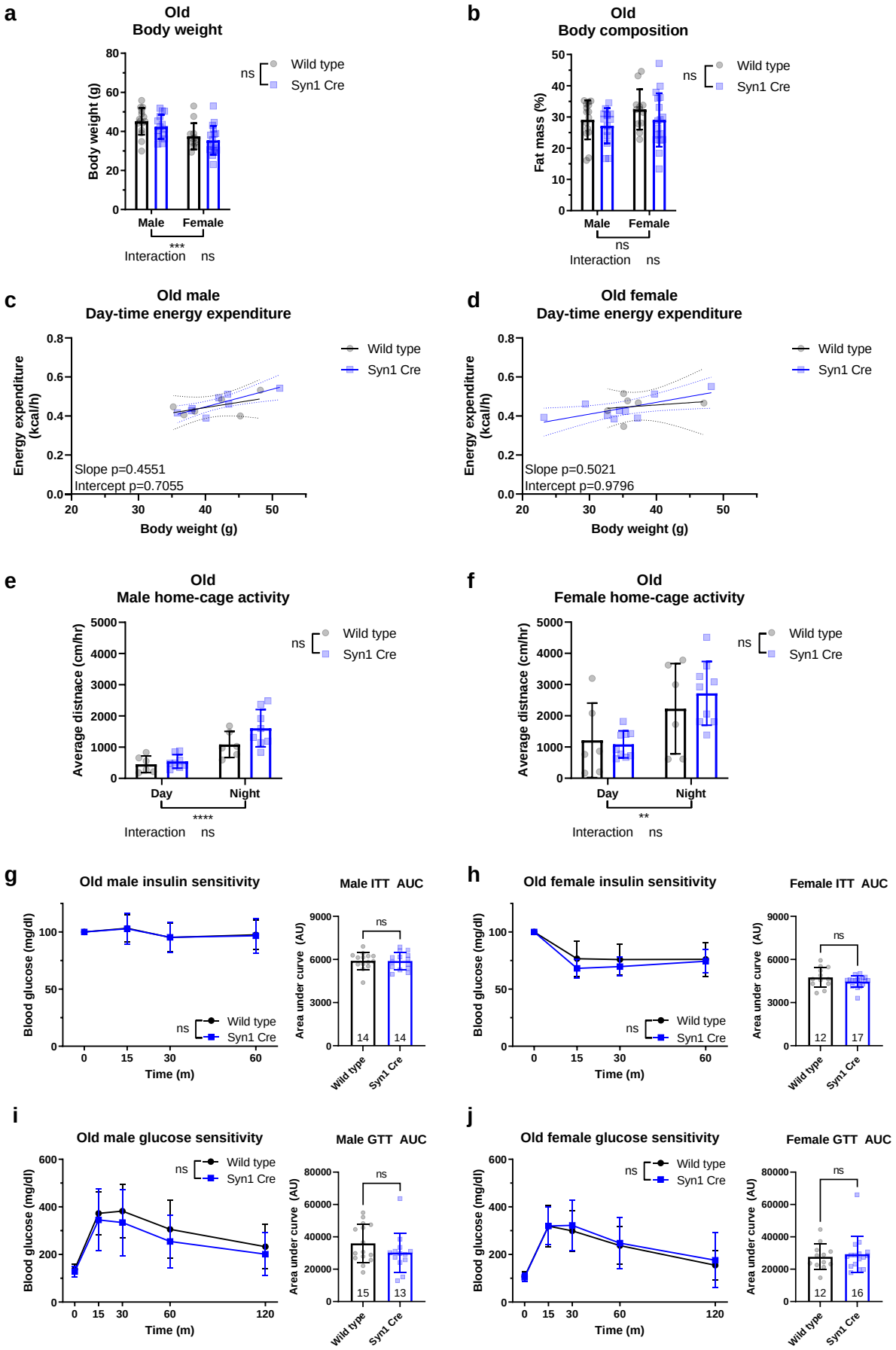

Figure 14: Neuronal Syn1Cre expression does not affect peripheral metabolism (below)

(A) No significant difference was observed in body weight or **(B)** body composition at old age (16 months) of Syn1Cre and wild type littermates (male wild type n=15 and Syn1Cre n=14, female wild type n=12 and Syn1Cre n=17). Daytime energy expenditure of **(C)** male and **(D)** female Syn1Cre and wild type mice was analysed by linear regression of energy expenditure by body weight (ANCOVA). No difference in energy expenditure between old male Syn1Cre (n=8) and wild type (n=6) as well as between female Syn1Cre (n=9) and wild type (n=6) was observed. No significant difference was observed in spontaneous activity of old single-housed **(E)** male Syn1Cre (n=8) and littermate wild type (n=6) mice or female **(F)** Syn1Cre (n=9) and wild type (n=6) mice. Insulin sensitivity of old **(G)** male or **(H)** female Syn1Cre and wild type mice showed no significant difference in insulin sensitivity. Analysis of GTT of male **(I)** and female **(J)** Syn1Cre mice did not reveal any significant difference in old Syn1Cre glucose tolerance compared to wild type littermates. All error bars correspond to standard deviation except for longitudinal glucose and insulin sensitivity where standard error of the mean is reported. Number of animals reported at the bottom of the bars for each condition. Detailed statistical values found in Table 1.

3.2.3. Characterisation of mitochondrial function in Irs1KO and nKO brains

3.2.3.1 Irs1KO and nKO brains exhibit sex-specific, age-dependent mitochondrial dysfunction

Given the improved health observed in male nKO mice, we explored possible molecular and cellular mechanisms in the brain that could contribute to the observed health effects. A previous study conducted a candidate gene differential expression analysis in Irs1KO liver tissue, and found an up-regulation of genes associated with oxidative stress, oxidative phosphorylation, and tricarboxylic acid cycle [1], suggesting a link to altered mitochondrial function. Furthermore, a later study established a causal link between reduced IIS and hepatic mitochondrial function, by demonstrating a reduction in mitochondrial electron transport chain activity and respiratory control ratio in response to FOXO1 activation[33]. Mitochondrial function in neurons is essential for neurotransmission, synaptic maintenance and calcium homeostasis[34]. Moreover, the effect of reduced IIS on mitochondrial function has not been investigated in the mammalian brain. Therefore, we assessed the effect of loss of IRS1 in the brain on OXPHOS by performing high-resolution respirometry on permeabilized brain tissue of young and old Irs1KO mice. There was no difference in basal respiration in old (Fig. 15a) or young (Fig. 16a) or Irs1KO mice of either sex.

Next, we measured oxygen consumption after saturating the mitochondria with substrates and titrating a protonophore (FCCP) until maximum mitochondrial respiration was measured. Basal mitochondrial respiration was then subtracted from maximal mitochondrial respiration to determine the mitochondrial spare capacity. Spare respiratory capacity can indicate how close a cell is operating to its bioenergetic limit or how much capacity a cell has to deal with acute additional energy demand. A neuronal reduction in spare respiratory capacity leads to a vulnerability to cell death linked to age-associated neurodegenerative disorders such as Parkinson's disease [61–63]. Old male Irs1KO mice showed a significantly reduced mitochondrial spare respiratory capacity (Fig. 15c), but this was unaffected in old females and young animals (Fig. 16b). To address whether this phenotype was caused specifically by the lack of IRS1 in neurons, we also measured spare respiratory capacity in nKO mice. Consistent with the results in Irs1KO mice, nKO mice showed a male-specific reduction in spare respiratory capacity only at old age (Fig. 15b, d). Thus, reduced neuronal IIS lowered mitochondrial spare respiratory capacity in old male Irs1KO and nKO mice, effects that were absent in control Syn1Cre mice (Fig. 17a and b).

3.2.3.2 Irs1KO and nKO brains have sex-specific and age-dependent ISR up-regulation

Impaired mitochondrial function has been shown to activate Atf4 signalling [36] and thereby the ISR[64,65]. Moreover, an increase in ATF4 activity has been identified as a common feature shared among different interventions that induced increased lifespan in mice[37]. Therefore, we investigated whether *Atf4* signalling was up-regulated in the brains of Irs1KO mice. We measured *Atf4* transcript levels by Q-RT-PCR, as neuronal ATF4 protein is usually rapidly degraded[66]. Interestingly, *Atf4* mRNA levels were increased only in old but not young male Irs1KO mice and unchanged in female mice (Fig. 15e and Fig. 16c), consistent with the observed age- and sex-specific mitochondrial dysfunction. In line with this finding, *Atf5* levels were also only significantly up-regulated in old male Irs1KO mice (Fig. 15e). Expression level of *Chop*, an *Atf4* target gene commonly up-regulated in long lived mice[37], was also up-regulated specifically in male Irs1KO mice (Fig. 15e). These results suggest that lack of IRS1 induces ISR in the brain at old age and only in males. To address whether deletion of Irs1 in neurons is sufficient to activate the ISR, we measured *Atf4*, *Atf5* and *Chop* expression in the brain of nKO mice. As in Irs1KO mice, no significant change in expression in these genes was observed in young male or in female nKO mice (Fig. 16d), while *Atf5* and *Chop* were significantly and *Atf4* non-significantly up-regulated in old male nKO mice (Fig. 15f). Moreover, consistent with the lack of mitochondrial dysfunction in Syn1Cre mice, we did not detect any difference in ISR (Fig. 17c). Thus, neuronal IRS1 loss was sufficient to trigger ISR in the brain of old male mice and not in young male or female mice.

3.2.3.3 Sex-specific ISR up-regulation leads to neuronal metabolic adaptation

The ISR pathway has been shown to trigger ATF4-dependent cytoprotective metabolic adaptations[36] and has been suggested to be particularly relevant in mitochondrial stress mediated metabolic rewiring [67–69]. Therefore, we performed targeted metabolomics on brains of young and old Irs1KO mice of both sexes to measure metabolite levels of the pathways that have been associated with the ISR response. We detected a significant increase in purine nucleotide abundance in the brains of both old male and female Irs1KO mice (Fig. 16e), a characteristic of increased ATF4 signalling through inhibition of the mTOR pathway, an important branch of the IIS network[70]. Previous reports have highlighted the up-regulation of amino acid biosynthesis pathways in response to ISR, specifically threonine[36], methionine[71], glycine and serine[72] metabolism. However, the up-regulation of these amino acids is context-specific, depending on the tissue and stress mediating the ISR. For example, in the brain an up-regulation of serine, among other metabolites, was detected in response to disrupted mitochondrial fusion dynamics[72], while in the liver a signature of methionine but not serine up-regulation was detected in response to mTORC1 inhibition[71]. In our samples, the majority of detected metabolites were up-regulated in old male and female Irs1KO mice compared to wild type littermates, however only a subset was statistically significant (Fig. 15g).

Arginine and 2-phosphoglyceric acid (2PG) were up-regulated in both old male and female Irs1KO mice, methionine, asparagine, threonine, fructose-1-phosphate (F1P), fructose-1,6-bisphosphate (FBP) and glucose-1-phosphate (G1P) levels in old male but not female Irs1KO mice, while in female Irs1KO mice phosphoenol-pyruvate and glucose-6-phosphate (G6P) were significantly up-regulated (Fig. 15g). In contrast, most of the significantly regulated metabolites in young male Irs1KO mice were down-regulated. Young female Irs1KO mice were unique in having a higher number of differentially abundant metabolites at young age compared to old age, with a significant

change in of G6P, glutamic acid, homocysteine, serine, alanine and pentose-5-phosphates levels (Fig. 16f). Interestingly, neuronal IRS1 deletion in nKO mice resulted in no changes in metabolites in young mice of either sex (Fig. 16g). However, as nKO mice aged, we observed a significant up-regulation in metabolites only in males, including some of the metabolites in the pathways attributed to the ISR pathway up-regulation (Fig. 15h) such as threonine[36], methionine[71], glycine and serine[72]. Consistent with the lack of mitochondrial dysfunction and ISR upregulation, there was no significant change in metabolite abundance in old female nKO mouse brains, suggesting that neuronal IRS1 deletion is not sufficient to induce metabolic adaptation. All together we detect a metabolic adaptation in the brains of old male mice that have a signature of mitochondrial stress that is indicative of a cytoprotective program to increase cellular resilience in cells[36] and in mouse brains[72].

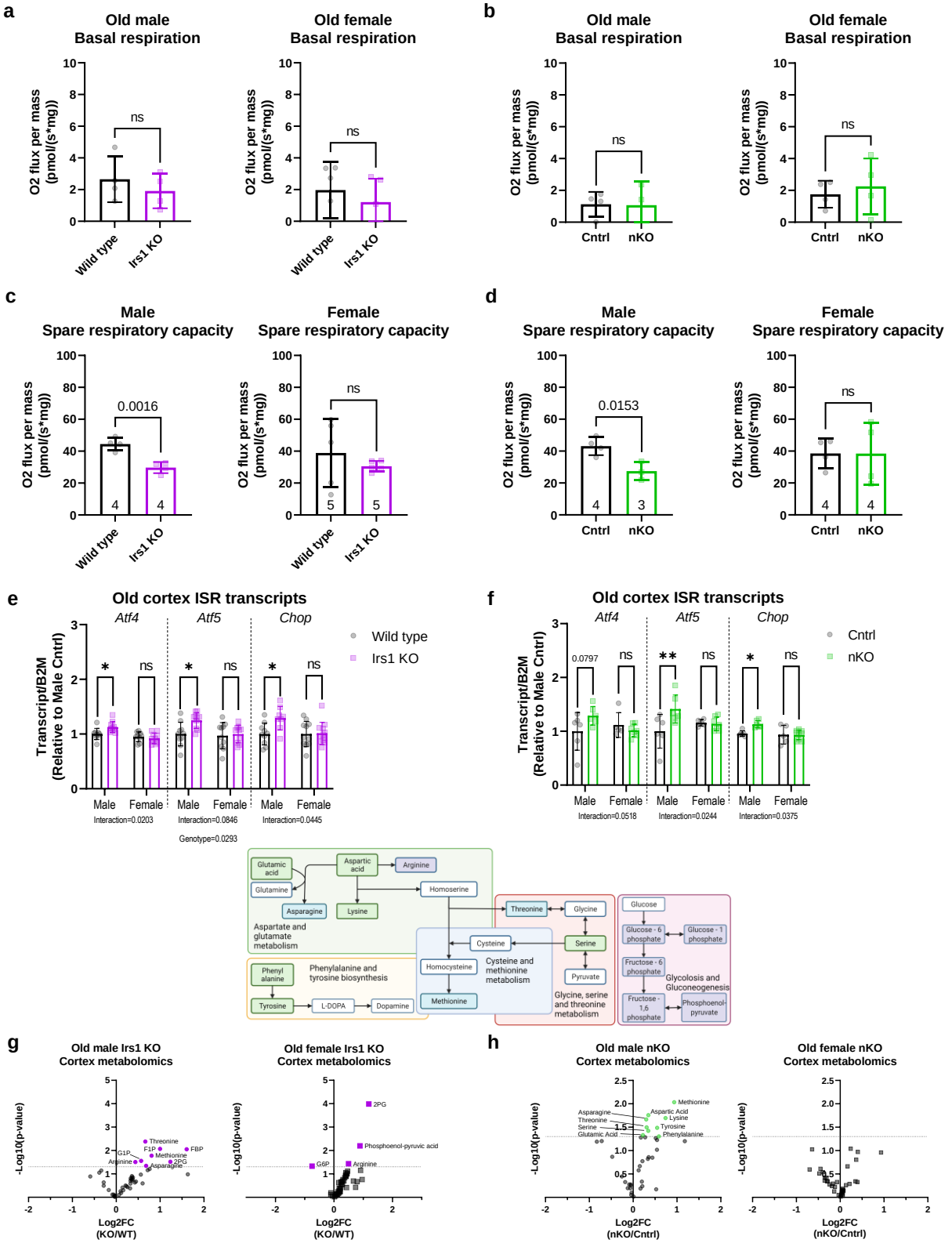

Figure 15: Investigation of mitochondrial function implicated the integrated stress response

(A) Measurement of basal oxygen consumption of brain tissue from old (19 months) Irs1KO mice did not detect any differences (male wild type and Irs1KO n=4, female wild type and Irs1KO n=5). **(B)** Measurement of basal oxygen consumption of brain tissue from old (22 months) nKO mice did not detect any differences (male control n=4 and nKO n=3, female control and nKO n=4). **(C)** Spare mitochondrial capacity in brain tissue of old Irs1KO mice was measured, after titration of a protonophore (FCCP) and subtracting the basal respiration, revealing significant reduction in male but not female Irs1KO brains (male wild type and Irs1KO

n=4, female wild type and Irs1KO n=5). **(D)** Spare mitochondrial capacity in brain tissue of old nKO mice also revealed significant reduction in male but not female nKO brains (male control n=4 and nKO n=3, female control and nKO n=4). **(E)** Quantitative real-time PCR performed to measure transcript levels of several integrated stress response (ISR) markers on brain tissue of old Irs1KO mice and their wild type littermates found significant sex-specific up-regulation of ISR in male Irs1KO mice (male wild types n=9 and Irs1KO n=10, female wild types n=9 and Irs1KO n=10). **(F)** Transcripts of ISR markers were measured in brain tissue of old (16 months) nKO mice and their control littermates found significant sex-specific up-regulation of ISR in male nKO mice (male control and nKO n=6, female control n=5 and nKO n=7). **(G)** Semi-targeted metabolomics revealed only up-regulation of some metabolites in old brain tissue of Irs1KO mice compared to littermate wild types (male wild type n=5 and Irs1KO n=6, and female wild type and Irs1KO n=6). **(H)** While metabolomics analysis in old nKO mice also revealed only up-regulated metabolites, but exclusively in male brain tissue (male control and nKO n=6, female control and nKO n=5). Included above the volcano plots is a schematic of the metabolic pathways affected by reduced IIS in the brain, highlighting metabolites up-regulated in old Irs1KO only (purple box), old nKO males only (green boxes) and old Irs1KO and nKO males (blue boxes). All error bars correspond to standard deviation. Detailed statistical values found in Table 1. Full metabolites measured in Table 2.

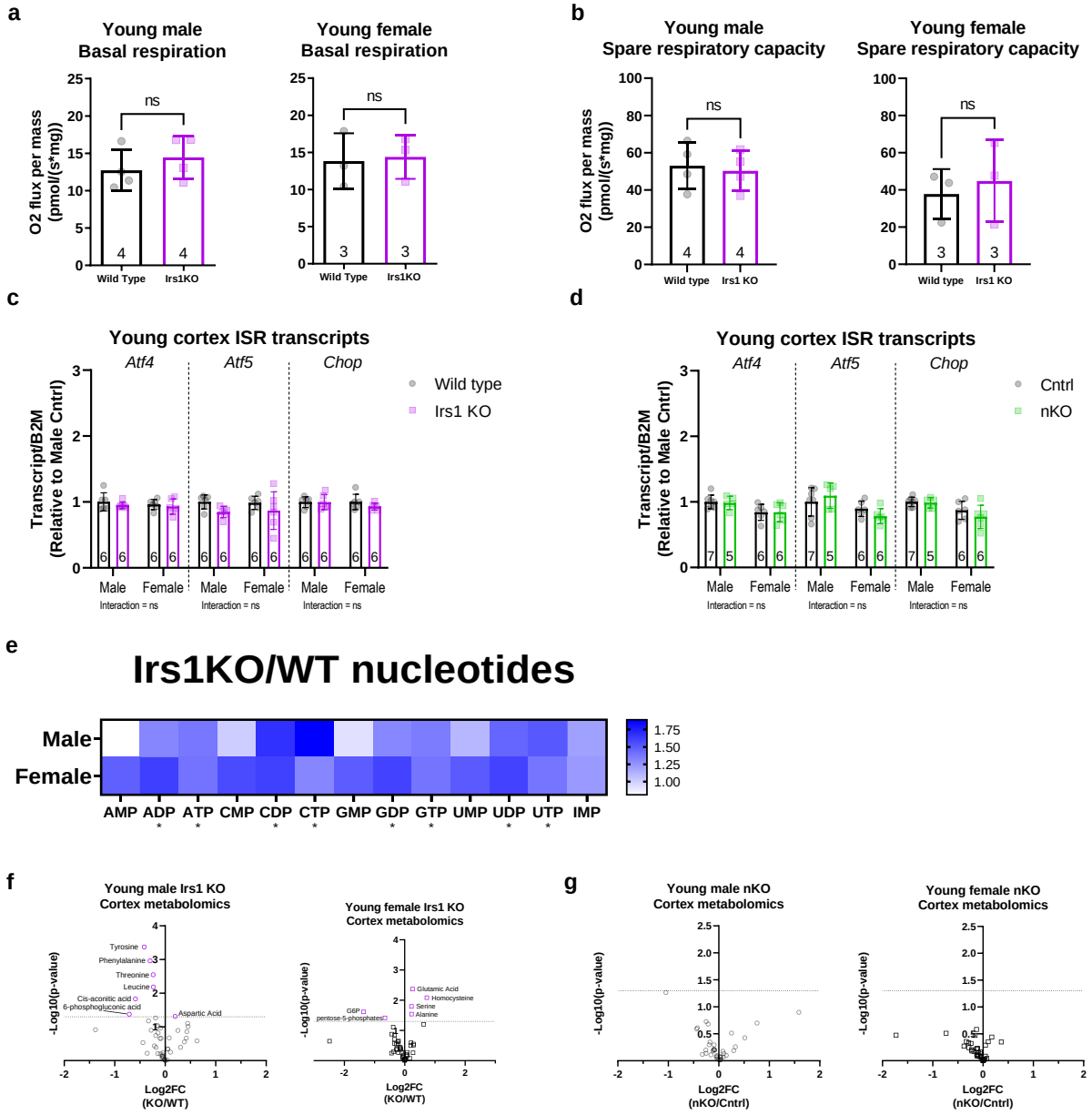

Figure 16: No activation of ISR in brains of young Irs1KO and nKO mice

(A) Basal oxygen consumption of brain tissue showed no difference in the basal respiration of mitochondria of young (6 months) male or female Irs1KO mice. **(B)** Mitochondrial spare respiratory capacity in brain tissue revealed no significant difference in young male or female Irs1KO mitochondrial function. **(C)** Quantitative real-time PCR was performed on brains of young male and female

Irs1KO mice and their wild type littermates to measure transcript levels of several integrated stress response (ISR) markers revealed no significant differences. **(D)** Transcripts of ISR markers were measured in brains of young male and female nKO mice and their control littermates showed no significant differences. **(E)** Purines detected in old Irs1KO brain tissue revealed a genotype-specific upregulation in di- and tri-phosphate purines in male and female cortex. **(F)** Semi-targeted metabolomics revealed down-regulation in metabolites in male Irs1KO mice and up-regulation in metabolites in female Irs1KO mice (male wild type and Irs1KO n=6, female wild type and Irs1KO n=6). **(G)** No significant change in metabolites in either male or female young nKO brain tissue (male control n=7 and nKO n=5, female control and nKO n=6). All error bars correspond to standard deviation. Detailed statistical values found in Table 1. Full metabolites measured in Table 2.

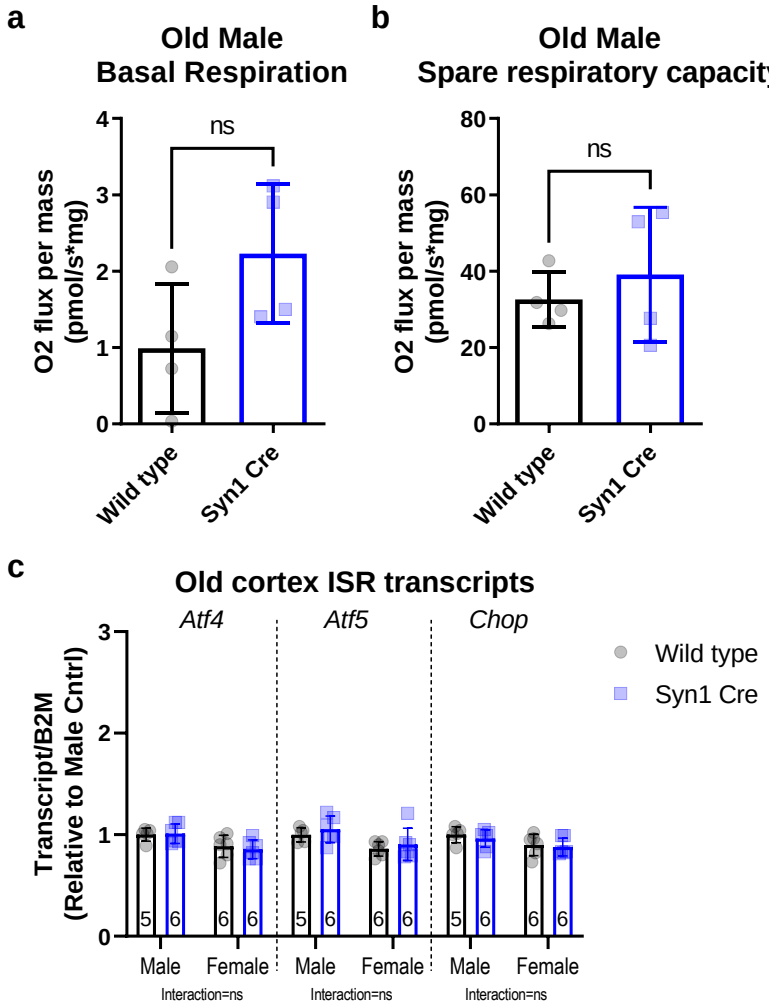

Figure 17: Syn1Cre expression does not lead to brain ISR activation

(A) Basal oxygen consumption of brain tissue showed no difference in the basal respiration of mitochondria of old (22 months) male Syn1Cre mice compared to their wild type littermates. **(B)** Mitochondrial spare respiratory capacity in brain tissue revealed no significant difference in old male Syn1Cre mitochondrial function. **(C)** Quantitative real-time PCR was performed on brains of old male and female Syn1Cre mice and their wild type littermates to measure transcript levels of several integrated stress response (ISR) markers revealed no significant differences. All error bars correspond to standard deviation. Detailed statistical values found in Table 1.

3.2.3.4 IRS1 deletion in peripheral tissues did not activate an ISR signature

To assess if deletion of IRS1 in other tissues than neurons would also trigger a local ISR signature, we measured *Atf4*, *Atf5* and *Chop* transcript levels in the liver, muscle and adipose tissue of the respective tissue-specific *Irs1* knockouts. In contrast to the findings in the nKO males, ISR marker

genes were not up-regulated in the liver, muscle or BAT of old lKO, mKO or fKO mice (Fig. 18 a-c), suggesting that neuronal tissue is particularly susceptible to IRS1-deletion mediated ISR.

In summary, IRS1 deletion led to a male-specific reduction in mitochondrial spare respiratory capacity, associated with a male-specific activation of *Atf4* signalling in brain tissue of old Irs1KO mice. A similar metabolic adaptation was activated in male and female Irs1KO mice with regards to purines, but there were sex differences in the metabolites that were differentially regulated in brain tissue. Finally, neuronal tissue alone among those tested where IRS1 deletion was sufficient to recapitulate the reduction in mitochondrial spare capacity, increase in *Atf4* signalling, and up-regulation of metabolites associated with increased cellular resistance seen in Irs1KO mice.

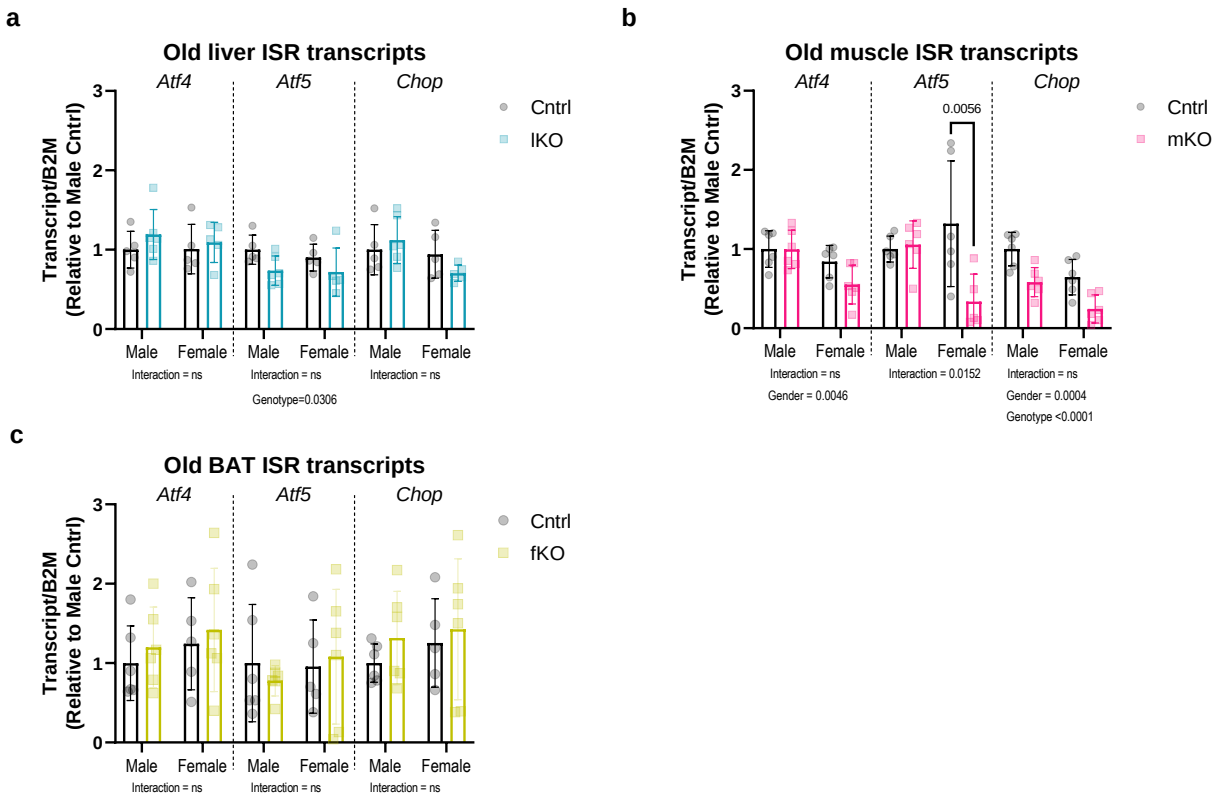

Figure 18: IRS1 deletion in peripheral tissues is insufficient to induce local ISR signature in old mice
Quantitative real-time PCR performed on metabolic organs of Irs1 tissue-specific deletion in old (16 months) mice targeting various integrated stress response (ISR) markers. **(A)** No significant difference in ISR transcripts was detected in the liver of lKO mice (male control n=5 and lKO n=6, female control n=5 and lKO n=5). **(B)** No significant increase in ISR transcript levels in hind limb muscle tissue of mKO mice, however we did detect a sex-specific downregulation of Atf5 transcripts in female mKO mice and genotype specific downregulation of Chop levels in mKO mice (n=6 biologically independent animals for all groups). **(C)** No difference in ISR transcripts was found in supraclavicular brown adipose tissue (BAT) of fKO mice (male control n=6 and fKO n=6, female control n=5 and fKO n=6). Detailed statistical values found in Table 1.

3.2.4 Neuronal ISR in response to IRS1 deletion induces systemic benefits through an FGF21-independent mechanism

Mitochondrial dysfunction in the CNS can cause systemic responses [73,74], and we assessed these in old male Irs1KO and nKO mice. We hypothesised that, based on the broad targets of the signal, that *Fgf21* was a likely candidate given its role in mediating EE[75] and insulin sensitivity[76], as well as being responsive to mitochondrial stress[77]. Moreover, given the role of the mitokine *Fgf21* in the

CNS ISR response [73,74], we tested for up-regulation of *Fgf21* transcript and protein levels in the brains of old nKO and Irs1KO mice, but did not find detectable levels in brain tissue (data not shown). A primary source of circulating FGF21 is the liver [78]. Moreover, reports have linked male-specific lifespan[79] and healthspan improvement [80] with a hepatic *Fgf21* signal[75]. To investigate if IRS1 deletion led to an up-regulation of hepatic *Fgf21*, we first tested for activation of ISR, and found a male-specific up-regulation of *Atf4* transcripts in livers of Irs1KO mice (two-way ANOVA, sex*genotype interaction $P<0.0299$; $F(1,20)=5.464$, Fig. 19a), and a trend in *Atf5* levels. Moreover, we also detected a genotype-dependent up-regulation of *Chop* in both male and female Irs1KOs. Surprisingly, when we measured hepatic *Fgf21* transcript levels we detected a significant reduction in the livers of Irs1KO mice (Fig. 19b), but no difference in nKO mice (Fig. 19c and d). While *Fgf21* is downstream of *Atf4* [81], our data suggests that the *Atf4* regulation of *Fgf21* is context-specific. This down-regulation of hepatic Fgf21 in our Irs1KO mice is consistent with a previous report of IRS1 and IRS2 double knockout mice, where there was a reduction in hepatic *Fgf21* expression in mutant mice during fasted and refed conditions[53].

Given that other organs are also implicated in FGF21 secretion[82], we conducted a FGF21 enzyme-linked immunoassay (ELISA) on plasma samples from old male and female Irs1KO mice to assess if a systemic ISR signature was being transmitted through FGF21 levels from other tissues. Consistent with the data of *Atf4* transcripts from the liver of Irs1KO mice (Fig. 19a), we found a significantly reduced level of circulating FGF21 in the plasma of old Irs1KO mice of either sex (Fig. 19e). A reason could be an increase in nuclear FOXO1 due to the reduction in IIS, as hepatic FOXO1 has been implicated in reducing circulating FGF21 levels[83]. Moreover, given that central action of FGF21 leads to browning of WAT which then increases EE[84,85], we tested whether we saw a signal of increased mitochondrial uncoupling in the WAT of old nKO mice. We found no evidence of increased *Ucp1* or *Pgc1a* expression in old nKO WAT (Fig. 20a and b), suggesting lack of central FGF21 signalling activation. Therefore, our data suggests the existence of a mechanism by which neuronal ISR induces a systemic response independent of FGF21 in both Irs1KO and nKO mice.

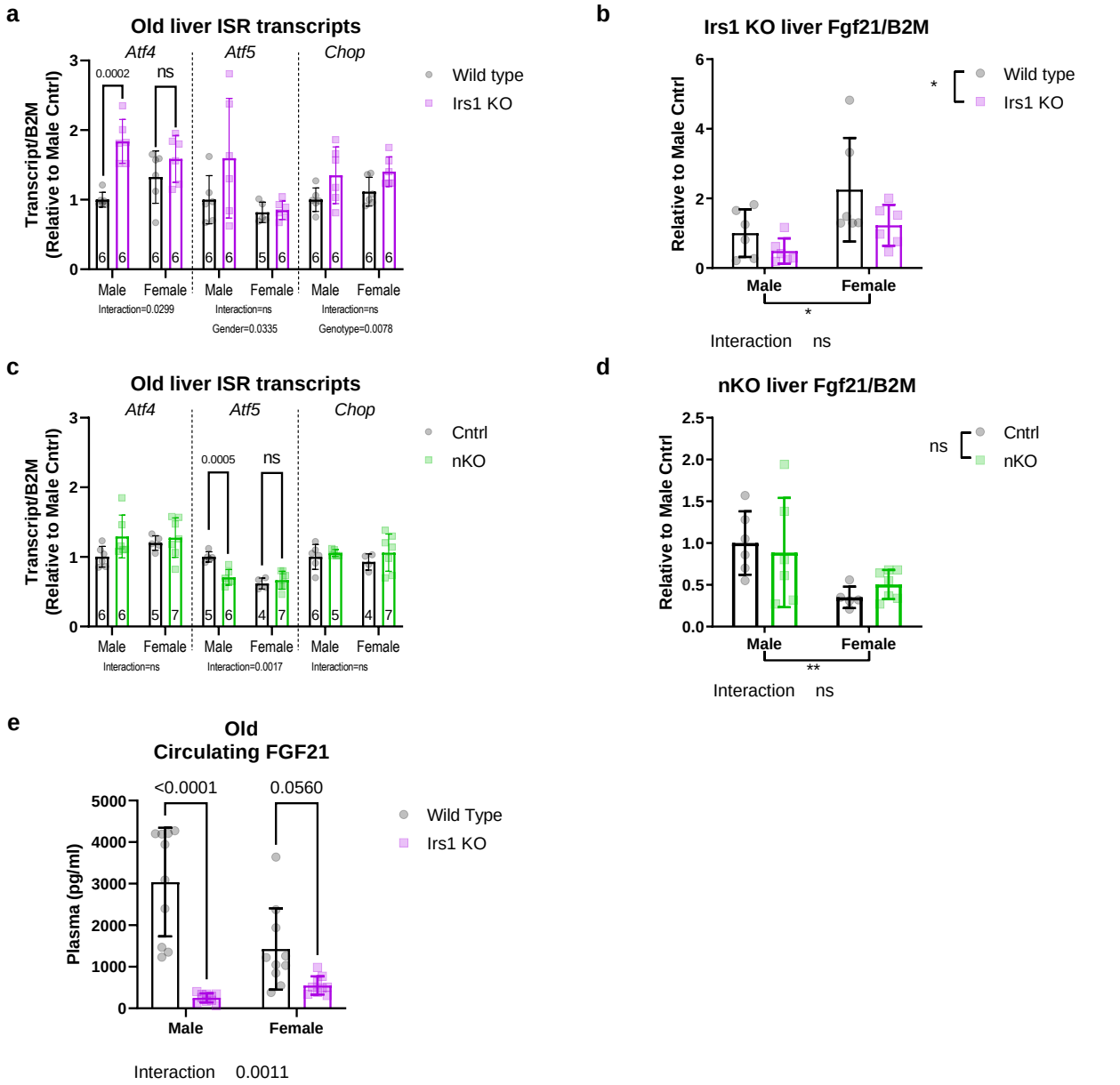

Figure 19: Sex-specific brain ISR signal triggers does not lead to systemic FGF21 signal

(A) Liver integrated stress response (ISR) transcripts of old (18 months) Irs1KO mice and their wild type littermates reveal sex-specific upregulation in male Irs1KO Atf4 levels, as well as a significant difference due to genotype in Chop levels. **(B)** Fgf21 transcript levels performed on liver tissue of old Irs1KO mice and their wild type littermates found a significant reduction of Fgf21 levels (n=6 biologically independent animals for all groups). **(C)** Liver ISR transcripts in old (16 months) nKO mice and their control littermates revealed a sex-specific downregulation in Atf5 levels of male nKO mice. **(D)** Fgf21 transcript levels in liver tissue of old nKO mice was not significantly different from their control littermates (male control and nKO n=6, female control n=5 and nKO n=7). **(E)** ELISA for FGF21 levels on plasma samples of old Irs1KO mice revealed sex-specific significant reduction of plasma FGF21 levels in male Irs1KO mice (male wild type and Irs1KO n=10, female wild type n=10 and Irs1KO n=9). Detailed statistical values found in Table 1.

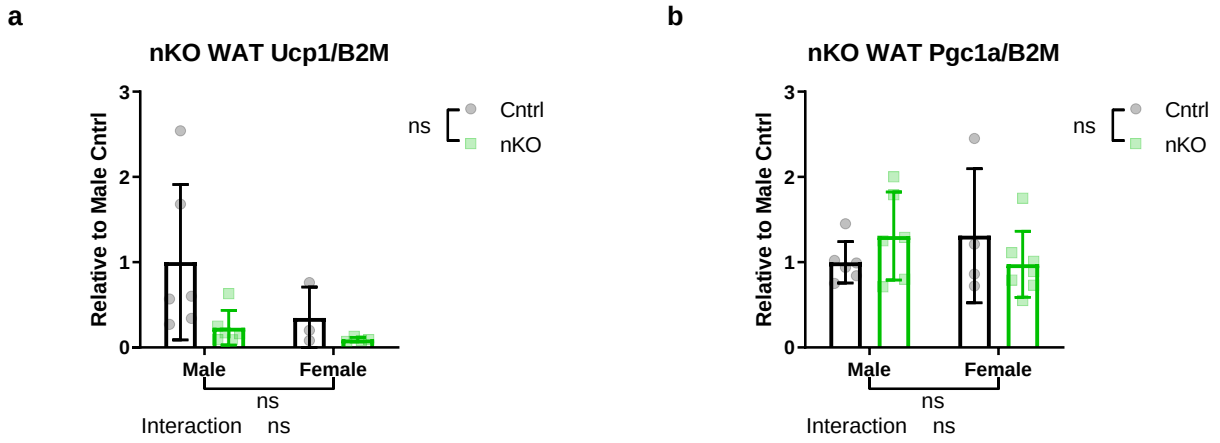

Figure 20: Energy expenditure is acting through an FGF21 independent manner
(A) Quantitative real-time PCR of Ucp1 (male control and nKO n=6, female control n=3 and nKO n=4) and Pgc1a **(B)** (male control and nKO n=6, female control n=4 and nKO n=7) in old nKO mouse white adipose tissue shows no difference. Detailed statistical values found in Table 1.

3.3 Discussion

The contribution of metabolic tissues to IIS mediated lifespan extension is still unknown. In *Drosophila* the causal mechanisms that contribute to extended lifespan are tissue-specific[86]. Here, we assess the effect of IIS reduction by deletion of IRS1 in major metabolic tissues on health and lifespan of mice. We deleted IRS1 in liver, muscle, fat, and brain tissue. The most appropriate control for this tissue-specific knockout approach would be an IRS1 deletion model under the ubiquitous Actin Cre driver. However, there was a depletion of Actin Cre +/T: Irs1 fl/fl pups generated from Actin Cre +/+: Irs1 fl/+ and Actin Cre +/T: Irs1 fl/fl matings, suggesting greatly reduced viability of IRS1 deletion mice. Nor could we successfully breed C57BL/6N Irs1KO mice, because Irs1KO progeny dropped in the third generation of backcrossing to approximately 4%. Therefore, we employed a robust C3B6F1 hybrid mouse strain, where there was no effect on Irs1KO viability, and progeny were born in a Mendelian ratio.

Given the reported effects of mouse genetic background on lifespan extension in response to various interventions[87], and specifically the contradictory effects observed in IIS mutants [88,89], we validated the previously reported C57BL/6J Irs1KO lifespan[25] and health phenotypes[1] in the novel hybrid C3B6F1 mouse background. We find consistent effects among the previously reported female C57BL/6J strain and our C3B6F1 mice with regards to decreased body size, lower adiposity, improved locomotion and insulin resistance. Taken together, this suggests that IRS1 deletion is a reproducible intervention that extends lifespan in different mouse strains.

IIS reduction has been shown to not only extend lifespan, but also improve healthspan in invertebrates [90,91] and mammalian models[1] potentially by slowing down rate of ageing[92]. The role of central IIS in longevity is still controversial in mammals[93]. Previous studies of peripheral tissue-specific reduced IIS mammalian models, using the stronger IR knockout mice, did not lead to lifespan extension[94], potentially suggesting a role for IIS in the CNS on regulating lifespan. In *C. elegans* neuronal IIS reduction can induce longevity [95,96], while in mammalian models of neurodegenerative diseases it improves cellular resilience especially with regards to proteotoxic stress[97]. We found that IRS1 depletion in neurons was unique in bringing about systemic metabolic

changes without any detrimental effects such as reduced body size and fertility observed in whole body C57BL/6J Irs1KO mice. Neuronal IIS reduction led to enhanced insulin sensitivity, increased EE and improved motor activity, specifically in old male mice. The healthspan benefits as a result of neuron-specific IIS intervention are consistent with data obtained from fly models [98,99]. Moreover, similar results were obtained from male mice with IR knockout specifically in the hypothalamus under high fat diet conditions [60]. One possibility for the sex difference is the age-associated and tissue-specific difference in activation of the IIS pathway in male and female mice[100].

Previous reports in *C. elegans* demonstrated that a mild impairment of mitochondrial function in neurons can initiate a non-cell-autonomous stress response which extends lifespan[101]. Moreover, in *Drosophila* mitochondrial stress resulting from whole body RNAi of the different mitochondrial complexes resulted in lifespan extension [102]. Nutrient-stress-induced systemic ISR in mice implicates an endocrine signal leading to a male specific lifespan[79] and healthspan[80] improvement. Moreover, recent reports have shown that brain mitochondrial stress is sufficient to induce systemic ISR[74], but the effect of brain ISR on metabolic health and ageing remains to be elucidated. Previous studies on Irs1KO mice implicate mitochondrial function[1] and specifically mitochondrial electron transport chain activity[33] as potential consequences of the IIS intervention. However, this has not been investigated in brain tissue. Therefore, we asked whether Irs1KO led to mitochondrial dysfunction in the brain, and we found that brain tissue of Irs1KO mice had a male-specific reduction in mitochondrial spare respiratory capacity. Although we observed similar systemic metabolic phenotypes in female Irs1KO mice, we could not detect a mitochondrial dysfunction or the same ISR response in their brain tissue. This suggests that the female phenotypes may be mediated through a different mechanism, or that the ISR in females functions in a different way. Alternatively, male neurons may be particularly sensitive or the female neuronal population resilient to this type of mitochondrial stress. Indeed, in a previous report of mitochondrial DNA damage induced mitochondrial stress in muscle tissue revealed sex difference in muscle free amino acids in aged mice[103]. Moreover, neuronal IRS1 deletion was sufficient to induce this effect and in neurons of mice, activation of a mitochondrial stress response caused by impairment of IIS may also elicit beneficial systemic effects such as enhanced insulin sensitivity and reduced age-associated loss of locomotion.

There are many potential proteins that can play a role in inter-organ communication in mammalian systems to mediate metabolic health and integrity[104]. However, one of the most likely candidates is FGF21, an endocrine and paracrine signal. ATF4 induces *Fgf21* expression and is up-regulated upon ISR activation [81]. Overexpression of FGF21 in mice can extend lifespan[38], and has been implicated in male-specific extension of lifespan and healthspan due to protein restriction[75]. Moreover, neuron-specific mitochondrial stress has been shown to lead to an increase in brain *Fgf21* transcript levels and circulating FGF21[74]. However, we could not detect any evidence of an increase in *Fgf21* transcript levels in the brain, or in circulating FGF21 levels in Irs1KO mice. Therefore, we provide evidence that, in neurons of mice, activation of a mitochondrial stress response caused by impairment of IIS may also elicit beneficial systemic effects such as enhanced insulin sensitivity, increase in EE and reduced age-associated loss of locomotion through an FGF21 independent mechanism. Consistent with our findings, another recent study has found that FGF21 signalling is not necessary for mitochondrial ISR in a severe mitochondrial stress mutant [105]. Together, these results imply different mitochondrial ISR programs that regulate metabolic adaptation may depend on the tissue, type or extent of mitochondrial stress.

Limitations

We acknowledge several limitations in this study. First, given that all our interventions are constitutive we can not be certain to what extent the developmental effect of reduced IIS induces the observed phenotypes. Although we could not detect EE, locomotor activity changes, ISR transcripts or mitochondrial function disruption in young age, developmental effects generated early in life can have late-life consequences. Using time-specific genetic tools can target the IIS intervention to an adult age and help eliminate any developmental confounds. Second, Irs1KO EE is confounded by the reduced body size. Therefore, we can not conclude whether EE increase is due to our intervention or the body size difference even if normalising to lean mass or body mass, since we can not adjust for it by ANCOVA with such a difference in the range of values between wild type and mutant mice. However, what we see in nKO mice can give some confidence that reduced IIS can increase EE as the body weight of those mice allow proper and robust analysis using an ANCOVA. Finally, when determining the sex differences in our study, we did not characterise or distinguish between females in different stages of their oestrous cycle. Given the influence of ovarian hormones on mitochondrial oxidative rate[106], we can not be confident in how the female sex hormones are affecting the phenotypes we are measuring. Moreover, the variability among individuals in old post cyclic female mice (>18 months) did not allow us to feasibly synchronise the cycle of these animals[107].

In conclusion, we find evidence for a unique and causal role of neuronal IRS1 deletion in triggering systemic health benefits that recapitulate those found in Irs1KO mice in a sex-specific manner. Moreover, this data suggests that males and females respond differently to ISR in response to IRS1 deletion, evidence for sex-specific ISR activation due to nutrient stress has been reported previously[80]. However, it is currently unclear to what extent is ISR sex-specific in mammals and how different tissues react to the induction of ISR. We suggest that future research should investigate both sexes when studying the ISR pathway in response to various stressors and in a tissue-specific manner.

4. Cognitive effects of whole body Irs1 knockout

Author contributions:

Conception of the study predominantly by Maarouf Baghdadi and Linda Partridge

Execution of experiments by Maarouf Baghdadi

Evaluation of data by Maarouf Baghdadi

Graphical representation by Maarouf Baghdadi

Writing of the manuscript by Maarouf Baghdadi

Editing and correction of manuscript proportionally by Maarouf Baghdadi and Linda Partridge

Cognitive effects of whole body Irs1 knockout

Authors:

Maarouf Baghdadi [1], Dominic Withers [2], Linda Partridge [1 3]

Affiliations:

1. Max-Planck Institute for Biology of Ageing, Cologne, Germany
2. Institute of Clinical Sciences (ICS), Faculty of Medicine, Imperial College London, London, UK
3. Institute of Healthy Ageing, and GEE, UCL, London, UK

4.1 Introduction

As life expectancy at birth continues to increase and birth rates decline, the proportion of elderly people is expected to increase in many populations worldwide [108,109]. Recent reports have estimated that dementia is the leading cause of disability in people over 60, surpassing cardiovascular disease, cancer, and stroke [110]. The hallmark symptoms of dementia, and a leading cause of elderly dependence [111], are age-associated cognitive decline and memory impairment [112].The personal, societal, and financial burden incurred by cognitive decline will soon become unmanageable [113,114].

Recently, researchers have exploited decreased insulin/insulin-like growth factor 1 (IGF1) signalling (IIS) as a method to promote longevity in model organisms and healthspan in humans through its role in regulating metabolism, proteostasis, and oxidative stress-resistance [115–118]. Moreover, recent studies have found that a reduction in whole body insulin substrate receptor 1 (IRS1) signalling can increase life span in nematodes, fruit flies and mice [1,119,120]. Unsurprisingly, IRS1 deficiency results in a 70-80% reduction in IGF1 signalling [121], which has been associated with increased longevity [122]. IRS1 deficiency is a robust intervention to extend lifespan and health parameters in different mouse strains (Chapter 3).

IIS signalling mediates a variety of cellular effects such as promoting DNA repair, oxidative stress resistance, and protein recycling, all of which could promote healthy ageing in post-mitotic neurons [123]. Microglial-specific genes have been shown to increase globally in the human brain upon ageing [124]. Inflammation in the hippocampus due to insulin resistance has been linked to impaired cognitive function and spatial learning deficits [125]. Inflammatory factors can also be generated throughout the brain by microglia, astroglia, and neurons [126,127], resulting in systemic inflammation of the brain. Inhibitors of the IIS pathway are currently being developed as anti-inflammatory drugs [128]. The changes associated with cognitive decline are difficult to quantify, as they can often occur in the absence of macroscopic neuropathology, unlike Alzheimer's Disease. Cognitive decline can be measured by assessing hippocampal function, as this brain region plays a central role in mammalian learning and memory. Moreover, impaired excitability of neurons and loss of functional synapses in the hippocampus have been linked to the age-related impairments in memory and cognition observed in ageing mammals [129,130].

To further investigate the relationship between decreased IIS and age-associated cognitive decline, we characterised the behaviour of whole body Irs1 knockout mice (Irs1KO). Young (4 months) and old (18 months) male and female Irs1KO mice were assessed for their motor learning and coordination, anxiety-like behaviour, exploratory drive, short-term spatial learning and memory capacity. Our cross-sectional experiments were designed to assess sex differences in Irs1KO mice

by measuring male and female mice on subsequent days, while different ages were performed many months apart. The sensitivity of behavioural assays to experimental conditions prohibits the direct ageing comparisons of young versus old mice of the same genotype. Therefore, we assessed the difference in the effect of IRS1 deletion compared to wild type littermates between young and old age. We found no significant deficits in motor or cognitive performance of young and old Irs1KO mice other than in assays where their reduced body size was detrimental to performance. We found no sex differences in any of the parameters we assessed. However, we detected a significant improvement in short-term memory at old age in Irs1KO mice which we did not observe at young age, suggesting a protection of old Irs1KO mice from age-associated cognitive decline.

4.2 Results

4.2.1 Locomotor learning, neuromuscular strength, and non-aversive exploratory behaviour of Irs1KO mice

We performed a series of complementary tasks designed to assess overall neuromuscular function of young and old, male and female, Irs1KO mice and controls, to assess the effects of IRS1 deficiency.

We assessed motor coordination and balance using the rotarod. Irs1KO mice were placed on an accelerating rotating rod to determine the average latency to fall across four trials. We administered the rotarod experiment through repeated training sessions across four days to evaluate the improvement in motor performance across time as a measure of motor learning. We detected a significant increase in average latency to fall across training days for both young Irs1KO male mice and their wild type littermates (Fig. 21a), suggesting that deletion of IRS1 did not lead to any deficit in motor learning at young age in male mice. However, we observed a significant interaction in the genotype*time term for young females (Fig. 21b). Post-hoc tests revealed a significant difference in female wild type mice between day 1 and remaining days. While no significant difference was detected in female Irs1KO mice between day 1 and other days, suggesting that they did not successfully achieve significant motor learning across the four days of training. No deficit in overall motor coordination was detected in analysis of area under the curve (AUC) of either male (Fig. 21a) or female (Fig. 21b) young Irs1KO mice. In contrast, in old Irs1KO mice there was no sex difference, with both males (Fig. 22a) and females (Fig. 22b) increasing their average latency to fall, indicating intact motor learning capacity. Analysis of rotarod AUC revealed no significant difference in overall motor coordination of either male (Fig. 22a) or female (Fig. 22b) old Irs1KO mice. In summary, we observed the expected age-associated decrease in motor coordination equally in both Irs1KO mice and their wild type littermates. A previous report of female Irs1KO mice found a delay in age-associated decrease in motor coordination [1], however, whether it was the difference in age or genetic background across studies we could not replicate their results.

We performed a grip strength assay to assess neuromuscular strength. Mice were allowed to grip a metal bar or grid to assess front paw or four paw strength respectively. We detected a significant reduction in front and four paw grip strength of young (Fig. 21c and d) and old (Fig. 22c and d) Irs1KO mice of both sexes. However, the difference was most likely due to the dwarf phenotype in Irs1KO mice (Section 3.2.1). We did not detect any significant difference due to age as our time point was earlier than the 24-month time point in which grip strength begins to deteriorate in mice

[131]. Moreover, as muscle size or body weight is a mediator of muscle strength, a difference in body weight must be adjusted for across groups using an analysis of covariance (ANCOVA) [132]. However, body weight, or the covariate in the ANCOVA, is affected by the Irs1KO treatment leading to a complete separation of the groups prohibiting the use of an ANCOVA [133]. Therefore, we conclude that Irs1KO mice are weaker in absolute grip strength, but the effect of reduced body weight on this weakness can not be delineated in our study.

Finally, we assessed locomotion and general exploration in a non-aversive 50cm-by-50cm arena for 10 minutes. We did not detect any significant difference in total distance travelled in young (Fig. 21e) or old (Fig. 22e) Irs1KO mice. Similarly, we also did not detect any significant difference in average locomotion speed in young (Fig. 21f) or old (Fig. 22f) Irs1KO mice. Taken together, data from the non-aversive arena suggests that in the absence of anxiogenic stimuli there is no deficit in the motivation and capacity of young or old Irs1KO mice to explore.

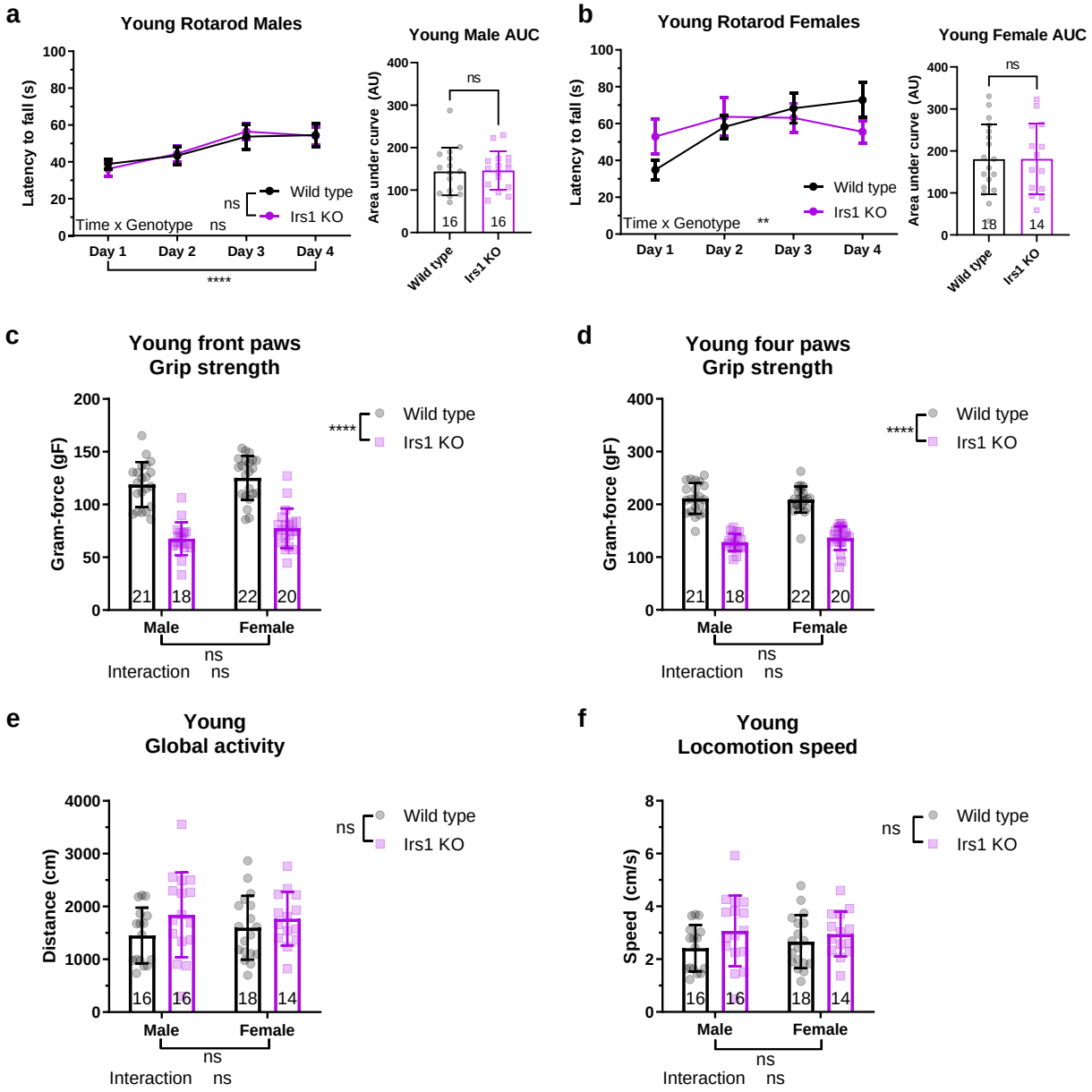

Figure 21: No deficit in locomotor coordination or capacity in young Irs1KO mice (below)

Average latency to fall during four days of training in the Rotarod revealed no significant defect in motor learning over time in young male **(A)** or female **(B)** Irs1KO mice. **(C)** Analysis of front-paw grip strength revealed significant reduction in strength of young male and female Irs1KO mice. **(D)** Analysis of all four paws revealed a significant reduction in strength of young male and female Irs1KO mice. **(E)** Exploration and locomotion in a non-aversive arena were not significantly affected in young Irs1KO mice. **(F)** No significant difference was detected in locomotion speed during exploration in a non-aversive arena of young Irs1KO mice. Number of animals reported at the bottom of the bars for each condition or in figure legends. All error bars correspond to standard deviation of the mean except for longitudinal Rotarod where standard error of the mean is reported. Detailed statistical values found in Table 3.

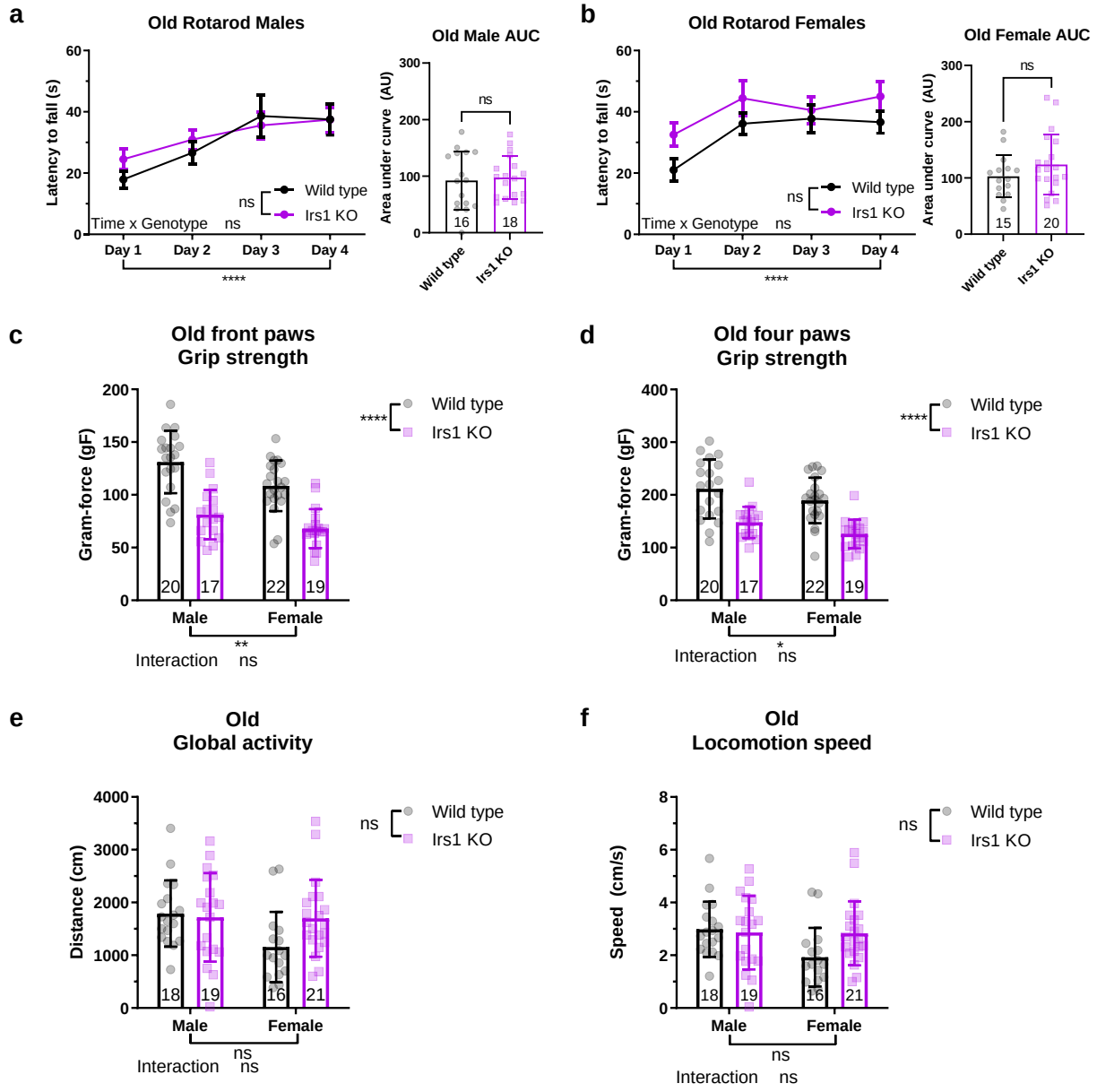

Figure 22: No deficit in locomotor coordination or capacity of old Irs1KO mice

Average latency to fall during four days of training in the Rotarod revealed no significant defect in motor learning over time in old male **(A)** or female **(B)** Irs1KO mice. **(C)** Analysis of front-paw grip strength revealed significant reduction in strength of old male and female Irs1KO mice. **(D)** Analysis of all four paws revealed a significant reduction in strength of old male and female Irs1KO mice. **(E)** Exploration and locomotion in a non-aversive arena were not significantly affected in old Irs1KO mice. **(F)** No significant difference was detected in locomotion speed during exploration in a non-aversive arena of old Irs1KO mice. Number of animals

reported at the bottom of the bars for each condition or in figure legends. All error bars correspond to standard deviation of the mean except for longitudinal Rotarod where standard error of the mean is reported. Detailed statistical values found in Table 3.

4.2.2 Irs1KO mice have reduced exploration and anxiety-like behaviour

In mice, anxiety-related behaviour can be assessed to determine a mouse's proclivity to approach or avoid a certain anxiogenic stimulus. We used the open field assay, which measures exploratory behaviour in a 50cm-by-50cm open arena in the presence of a strong light (~220 lux) in the centre to stimulate an anxiogenic response in the animal. We allowed the mice to explore the arena for 10 minutes to give the opportunity to explore the arena thoroughly.

Interestingly, we saw an age-independent, significant reduction in distance travelled of young (Fig. 23a) and old (Fig. 24a) Irs1KO mice of both sexes during 10 minutes of exploration. Furthermore, we saw a significant reduction in locomotion speed of young (Fig. 23b) male and female Irs1KO mice in the open field. However, we detected a male-specific reduction in locomotion speed in old Irs1KO mice (two-way ANOVA, sex*genotype interaction P=0.0492; F (1,70) =4.005, Fig. 24b). We measured the number of rearing counts in the open field arena as a further measure of exploratory behaviour, and detected a significant reduction in rearing counts in young (Fig. 23c) and old (Fig. 24c) Irs1KO mice. Finally, we measured the time spent in the centre of the open field as a percentage of total time spent in the arena, as a proxy for the animals' proclivity to avoid the highly illuminated and exposed centre. The longer an animal spends in the centre the less anxiety-like behaviour the animal expresses. We did not detect any significant difference in the centre occupancy of young male and female Irs1KO mice (Fig. 23d). In contrast, we detected an age-dependent decrease in anxiety-like behaviour in male and female old Irs1KO mice (Fig. 24d). All together, we find that the reduced IIS longevity intervention leads to an age-associated reduction in anxiety-like behaviour.

4.2.3 Elimination of age-dependent anxiety-like behaviour in old Irs1KO mice by low-light conditions

To test whether the increase in centre occupancy observed in old Irs1KO mice was due to reduced avoidance of the highly lit centre (~220 lux), we measured centre occupancy using a dark non-aversive arena (~20 lux). We did not detect a significant difference in centre occupancy in the dark arena in young Irs1KO mice (Fig. 23e), and there was no change in centre occupancy in response to light intensity changes (Fig. 23f). This data suggests that reduction in light intensity is insufficient to reduce the anxiogenic stimuli that young mice encounter in an open space. Interestingly, the non-aversive arena eliminated any significant difference between old Irs1KO mice and their wild type littermates (Fig. 24e). A paired two-way ANOVA analysis of combined data from male and female mice revealed a similar significant increase in centre occupancy due to the reduced illumination of the centre of the arena (Fig. 24f). Therefore, the presence of the anxiogenic light source in the open field and not the novel environment led to the centre avoidance by old wild type, suggesting an increased resilience of old Irs1KO mice to illuminated areas.

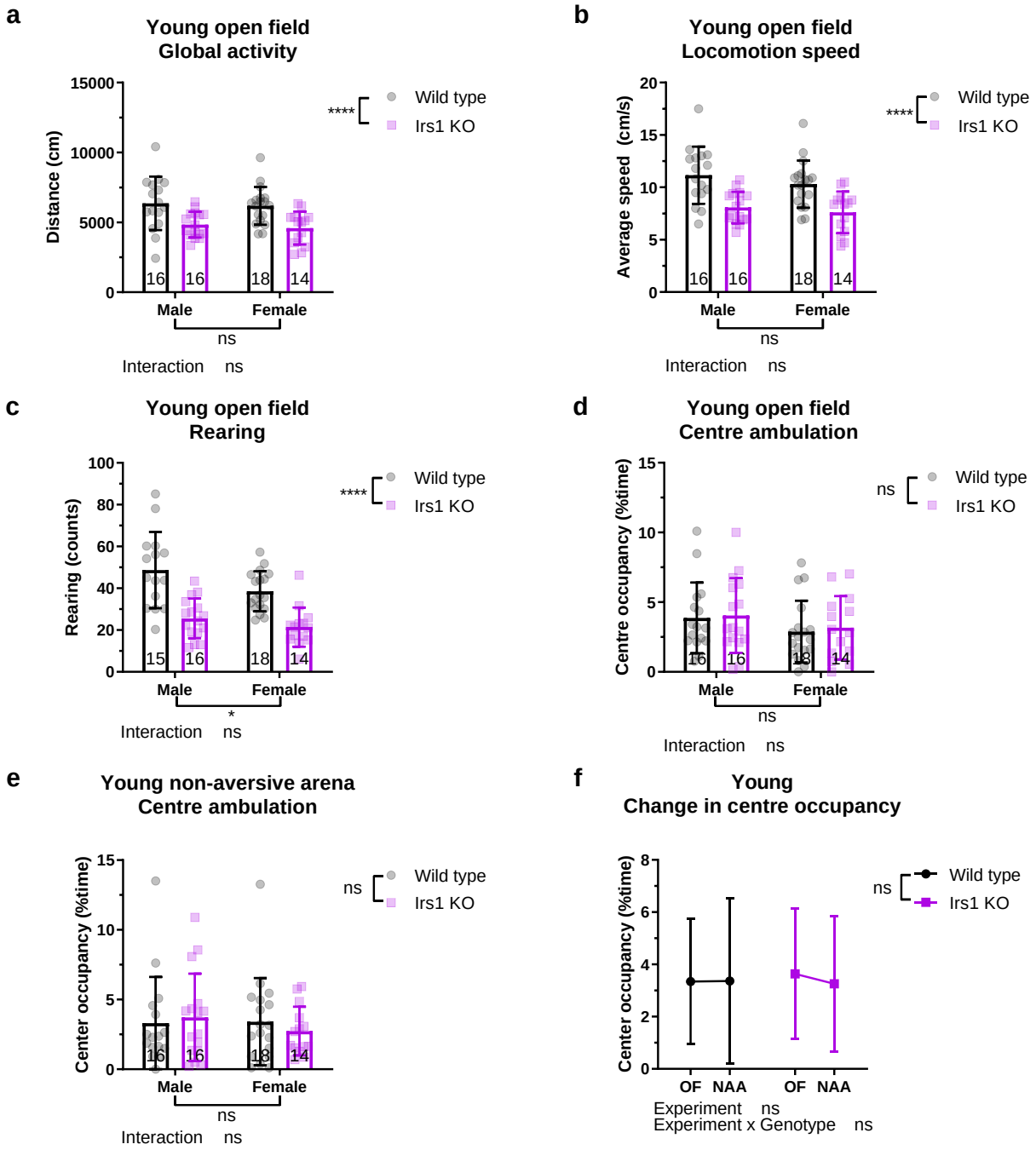

Figure 23: Reduced exploratory behaviour in young Irs1KO mice

(A) Locomotor activity measured during the aversive open field experiment revealed significant reduction in young Irs1KO mice. **(B)** Locomotor speed was also significantly reduced in the open field arena in young Irs1KO mice. **(C)** Rearing behaviour measurement revealed significant reduction in rearing of young Irs1KO mice. **(D)** Centre occupancy normalised to total time was analysed and revealed no significant difference in centre occupancy of young Irs1KO mice. **(E)** Centre occupancy normalised to total time measured in the non-aversive arena revealed no significant difference in young Irs1KO mice. **(F)** Paired comparison of centre occupancy in the open field (OF) compared to non-aversive arena (NAA), revealed no significant difference in centre occupancy of young Irs1KO mice between OF and NAA. Number of animals reported at the bottom of the bars where possible, otherwise in the figure legend. All error bars correspond to standard deviation of the mean. Detailed statistical values found in Table 3.

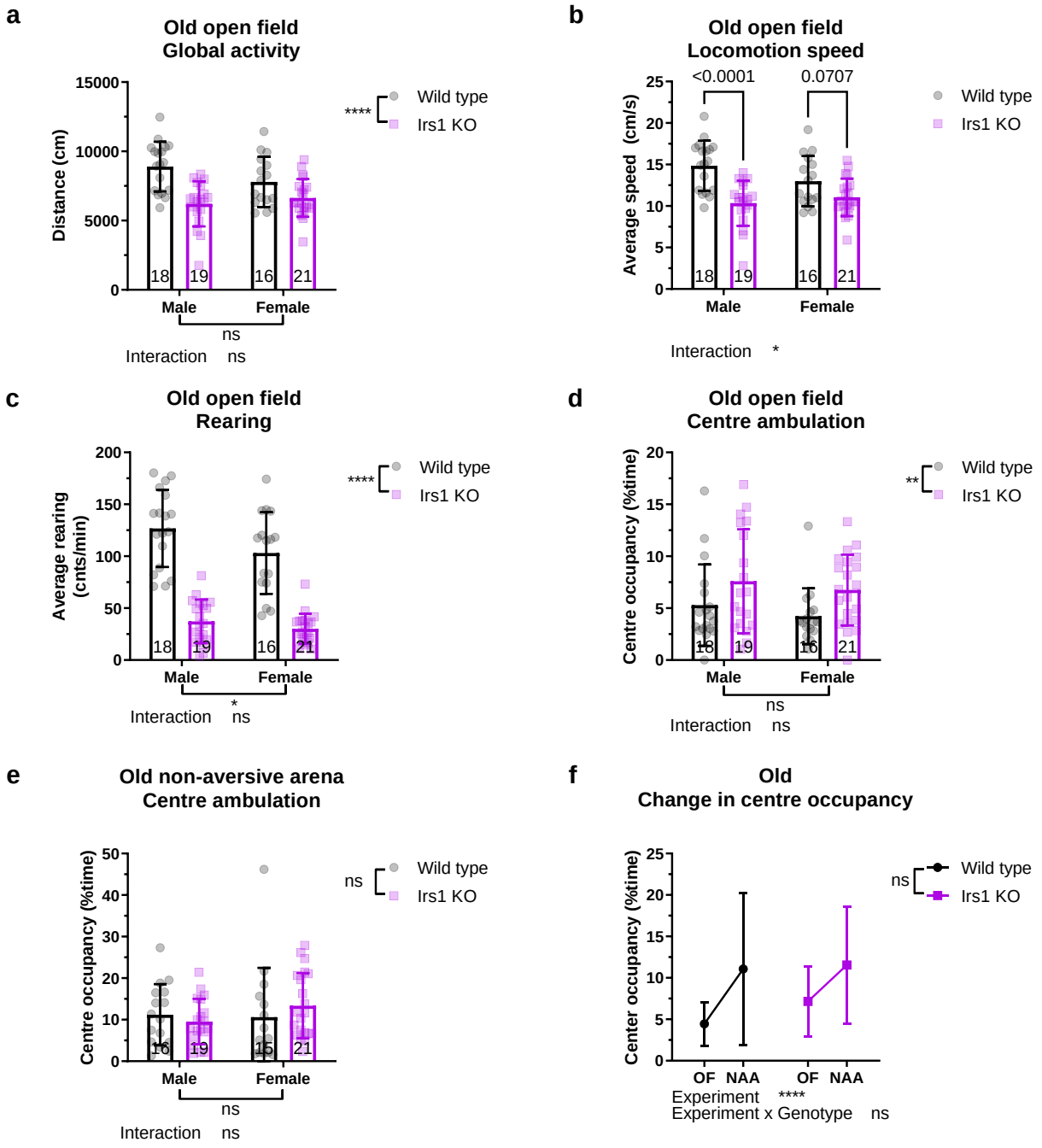

Figure 24: Reduced exploration and anxiety-like behaviour in old Irs1KO mice

(A) Locomotor activity measured during the aversive open field experiment revealed significant reduction in old Irs1KO mice. **(B)** Locomotor speed was also significantly reduced in the open field arena in old Irs1KO mice. **(C)** Rearing behaviour measurement revealed significant reduction in rearing of old Irs1KO mice. **(D)** Centre occupancy normalised to total time was analysed and revealed a significant increase in centre occupancy of old Irs1KO mice. **(E)** Centre occupancy normalised to total time measured in the non-aversive arena revealed no significant difference in old Irs1KO mice. **(F)** Paired comparison of centre occupancy in the open field (OF) compared to non-aversive arena (NAA), revealed no significant difference between the significant increase in centre occupancy of old Irs1KO mice and wild type littermates. Number of animals reported at the bottom of the bars where possible, otherwise in the figure legend. All error bars correspond to standard deviation of the mean. Detailed statistical values found in Table 3.

4.2.4 Intact long-term reference memory in Irs1KO mice

Hippocampus-dependent long term memory formation deteriorates with age and is a primary cognitive health parameter in mammals [134]. We tested the ability of old Irs1KO mice to learn the location of a hidden platform using distal spatial cues. Learning was assessed by measuring the latency to escape the water in Irs1KO mice. Male and female Irs1KO mice learned the location of the hidden platform equally well compared to their respective wild type littermates (Fig. 25a-b). However, male mice needed more training days to reach criterion due to the high variability (30 sec escape latency) compared to female mice (Fig. 25a-b). Long-term memory was assessed 24 hours following the last training trial by measuring the preference of Irs1KO mice to swim in the target quadrant previously containing the hidden platform. Indeed, after five training days wild type male mice were able to remember the location of the hidden platform in the probe trial (Fig. 26a). Male Irs1KO mice also showed a significant preference for the target quadrant (Fig. 26b). However, male Irs1KO mice long-term spatial memory was not significantly different from wild type littermates (Fig. 25c). In contrast, old female wild type and Irs1KO mice showed no preference for any quadrant (Fig. 25d), as reported previously in other strains of old female wild type mice [135]. One potential explanation for the female-specific impairment in memory could be the low number of training days.

Finally, the motivation and capability of Irs1KO mice to escape the water was assessed by performing a visual cued water maze trial, where we detected a significant reduction in cued trial latency to the cued platform in old Irs1KO mice (Fig. 25e). While we detected a significant reduction in swim path during the probe trial (Fig. 26c), we did not detect a significant difference in the swim path during the cued trial, suggesting no deficits in visual acuity (Fig. 26d). However, we detected a significant reduction in swim speed in the probe and cued trial (Fig. 26e and f), which may have been due to the reduced size of Irs1KO mice and explains the reduced swim path during the probe trial (Fig. 26c).

Taken together, our data suggests that despite the size difference, Irs1KO mice do not display significant differences in learning or memory.

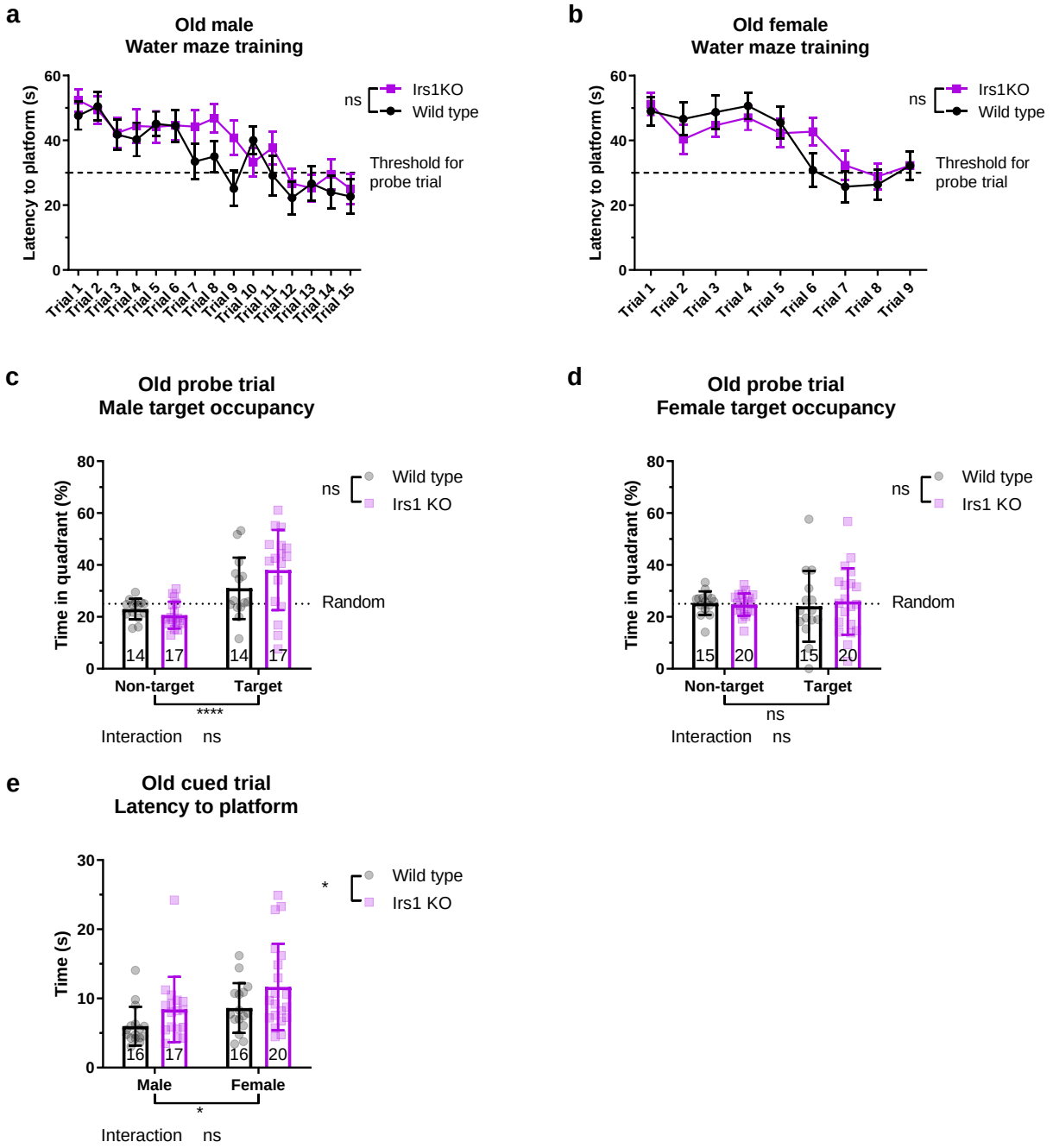

Figure 25: No deficit in learning or long-term memory in old Irs1KO mice

Assessment of escape latency across trials of water maze training showed significant learning of both old male **(A)** and female **(B)** Irs1KO mice (male wild type n=14 and Irs1KO n=17, female wild type n=15 and Irs1KO n=20). **(C)** Probe trial quadrant occupancy showed no significant difference in target quadrant occupancy in old male Irs1KO mice, revealed similar levels of memory in Irs1KO mice and wild type littermates. **(D)** Probe trial quadrant occupancy revealed no memory in old female wild type or Irs1KO mice. **(E)** Latency to escape in the cued water maze revealed a significant increase of time needed to reach the platform in male and female Irs1KO mice. Number of animals reported at the bottom of the bars where possible, otherwise in the figure legend. All error bars correspond to standard deviation of the mean except water maze training where standard error of the mean was plotted. Detailed statistical values found in Table 3.

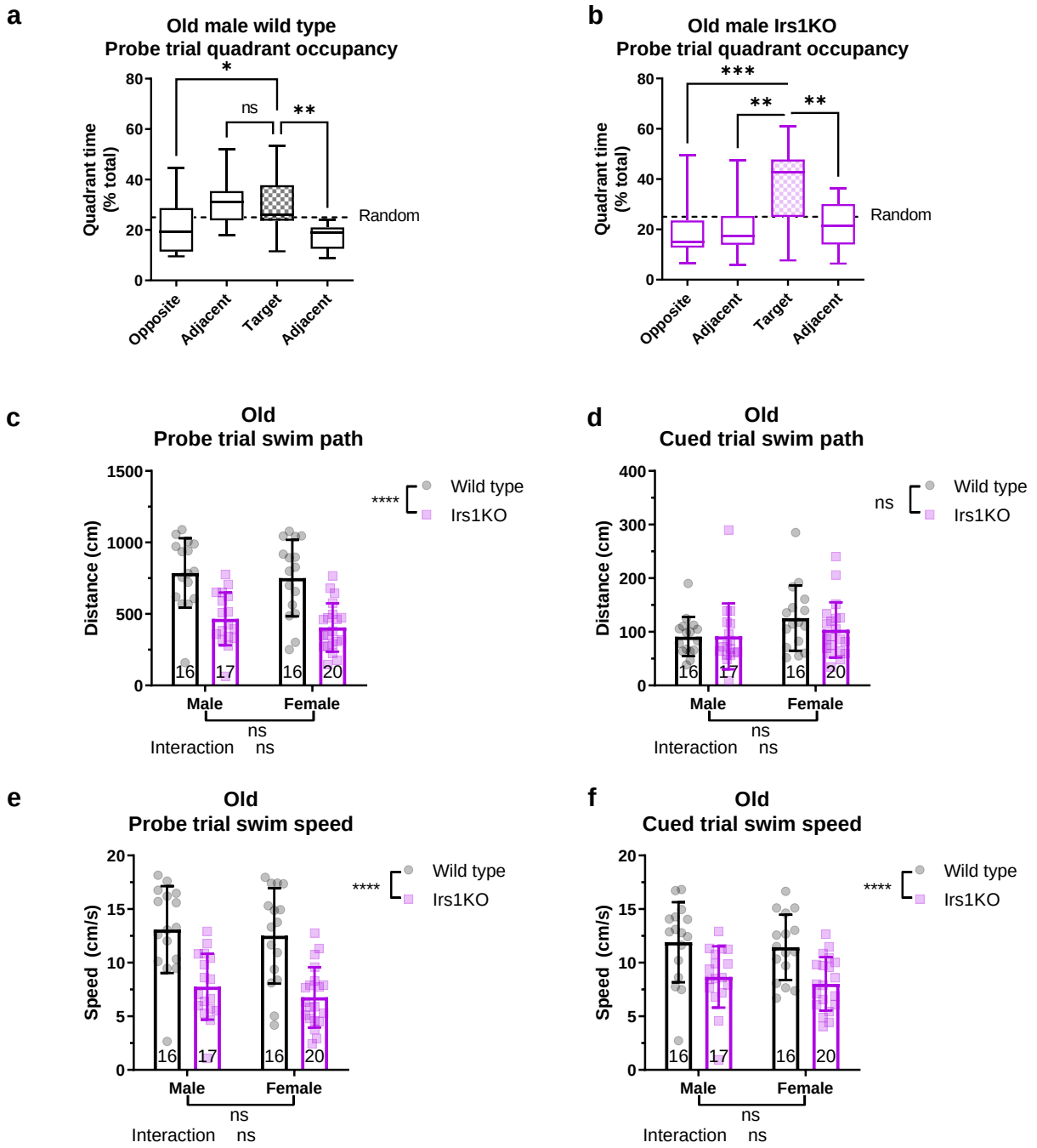

Figure 26: No deficiency in motivation or visual acuity of old Irs1KO mice

(A) Old male wild type quadrant occupancy during probe trial revealed significant increase in mouse occupancy in the target quadrant reflecting long term memory formation. **(B)** Old male Irs1KO quadrant occupancy during probe trial revealed significant increase in mouse occupancy in the target quadrant reflecting long term memory formation. **(C)** Total swim path during the probe trial revealed significant reduction in old Irs1KO mice. **(D)** Total swim path in the cued variation of the water maze showed no significant change in old Irs1KO mice. **(E)** Assessment of swim speed during the probe trial revealed significant reduction in old Irs1KO mice. **(F)** Swim speed in the cued water maze variant revealed significant reduction in old Irs1KO mice. Number of animals reported at the bottom of the bars where possible, otherwise in the figure legend. All error bars correspond to standard deviation of the mean. Detailed statistical values found in Table 3.

4.2.5 Improved short-term contextual memory in Irs1KO mice

Hippocampus-dependent working memory is used to orient the animal in the environment and explore novel areas for foraging. Previous studies have reported that working memory deteriorates with age in mice [134] and humans [136]. The effect of IRS1 deletion on working memory has not been assessed. We performed a novel object recognition (NOR) task to test working memory. The NOR exploits the natural proclivity of mice to explore novel objects without any positive or negative reinforcing stimuli. In the NOR task mice are allowed to explore two identical familiar objects, then one object is replaced by a novel object. The percentage of time a mouse explores the novel object relative to total time spent exploring both objects was then scored, and is a measure of their capacity to form a memory of the familiar object. We found no significant difference in the locomotor performance of young or old Irs1KO mice in the NOR (Fig. 27a-b and Fig. 28a-b). Due to the limited number of animals that reached the exploratory criteria in the old time point (over 5% of object exploration time), and the lack of genotype*sex interaction in the NOR, we decided to combine both sexes for subsequent analysis. We analysed the change in exploration when an identical object was replaced by a novel object and found that both young wild type and Irs1KO mice displayed a significant increase in object exploration (Fig. 27c). However, we detected a significant interaction between genotype*object using a repeated measures two-way ANOVA, revealing a significant increase of novel object interaction time in old Irs1KO mice but not in wild type mice (Fig. 28c). When novel object preference was calculated, we detected a significant increase in old Irs1KO mice (Fig. 28d) but no significant difference in young Irs1KO mice (Fig. 27d). This data suggests that we observed a protection from age-associated decline in working memory in Irs1KO mice.

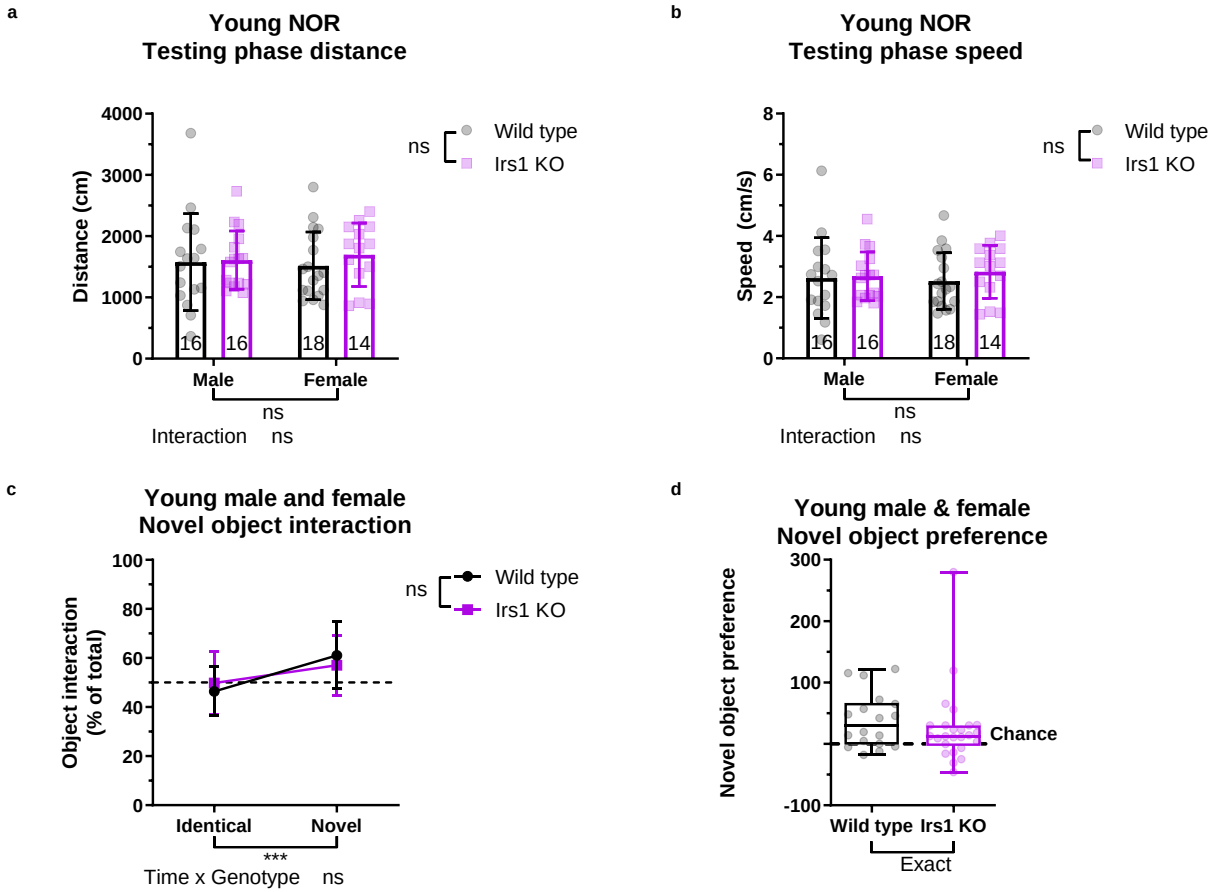

Figure 27: No significant difference in working memory of young Irs1KO mice

(A) Locomotor activity measured during the testing phase of the novel object recognition experiment revealed no difference in activity of young Irs1KO mice. **(B)** No significant difference in locomotor speed between young Irs1KO and wild type littermates. **(C)** Time interacted with an object as a percentage of total time interacting with both objects revealed a significantly increased preference to the novel object in young Irs1KO and wild type littermates. **(D)** Novel object preference revealed no significant difference in novel object preference between young Irs1KO and wild type mice. Number of animals reported at the bottom of the bars where possible, otherwise in the figure legend. All error bars correspond to standard deviation of the mean. Detailed statistical values found in Table 3.

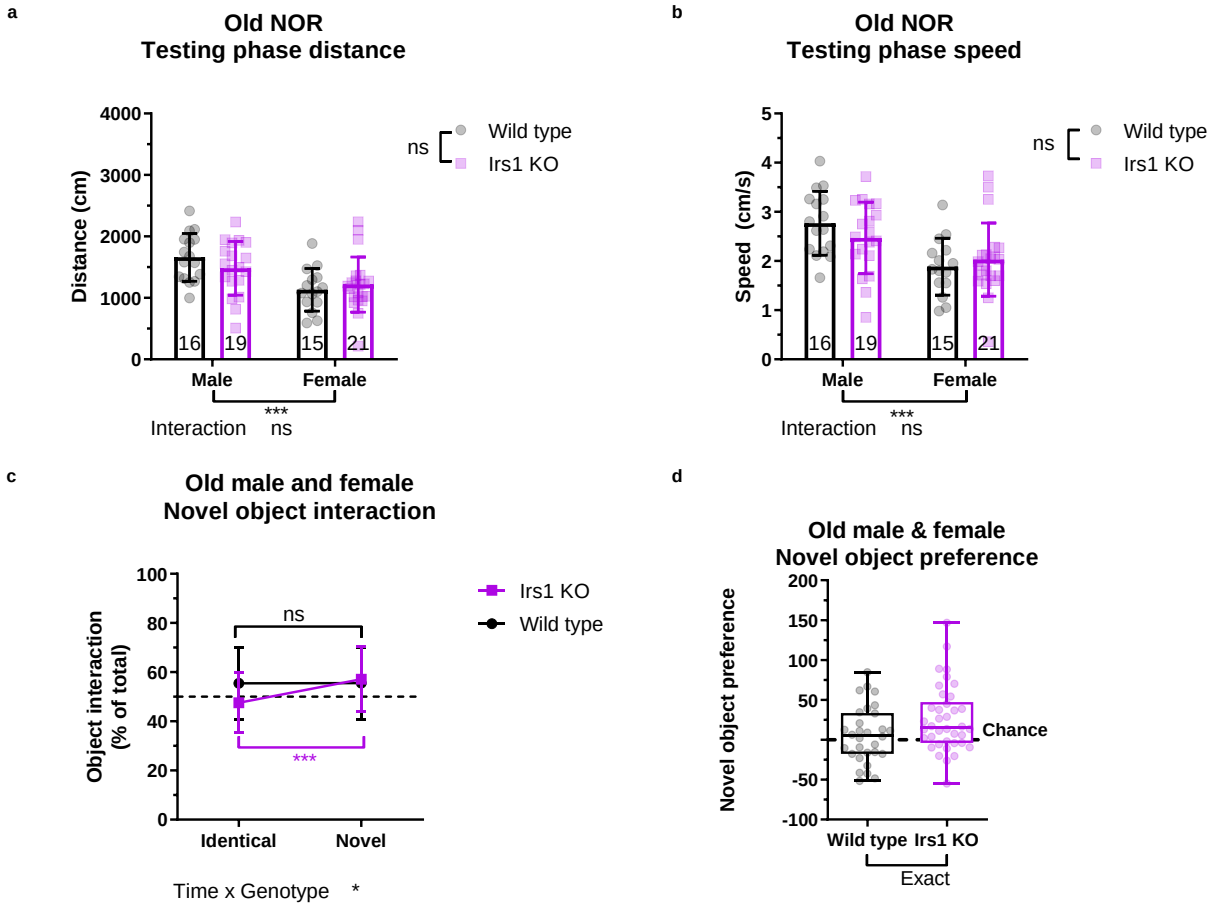

Figure 28: Reduced age-associated decline in working memory of old Irs1KO mice
(A) Locomotor activity measured during the testing phase of the novel object recognition experiment revealed no difference in activity of old Irs1KO mice. **(B)** No significant difference in locomotor speed between old Irs1KO and wild type littermates. **(C)** Time interacted with an object as a percentage of total time interacting with both objects revealed a significantly increased preference to the novel object in old Irs1KO. **(D)** Novel object preference revealed significantly higher preference to the novel object in old Irs1KO mice compared to wild type mice. Number of animals reported at the bottom of the bars where possible, otherwise in the figure legend. All error bars correspond to standard deviation of the mean. Detailed statistical values found in Table 3.

4.3 Discussion

Increasing age is one of the primary risk factors for cognitive decline and dementia, a leading cause of morbidity and elderly dependence [111]. The geroscience approach proposes that ageing is a common risk factor of many debilitating disorders and an intervention in the ageing process would lead to a delay or prevention of multiple age-dependent diseases. Therefore, we asked whether Irs1KO mice which show a robust extension in lifespan and an improvement in metabolic health also possess benefits in cognitive performance. We tested young and old Irs1KO mice for behavioural parameters with evidence of an age-associated decline such as motor performance, anxiety-like behaviour, learning and memory [137].

We assessed motor performance using different complementary assays that test motor coordination, neuromuscular function and exploratory behaviour. We found no significant deficits in motor performance in young or old Irs1KO mice of either sex. However, it is important to note that performance in the rotarod and grip strength assay is modulated by the body weight of an

animal. Irs1KO mice are dwarfs (Section 3.2.1), which may lead to an easier time staying on the rotating rod compared to wild type littermates. Moreover, the reduced muscle mass in Irs1KO mice may contribute to the reduction in grip strength observed. However, the body weights of Irs1KO and their wild type littermates do not overlap and prevents the application of an analysis of covariance (ANCOVA) to adjust for body weight while comparing assay performance.

Generalised anxiety disorder is the hyperactivation of an adaptive response to a perceived threat that can lead to pathological outcomes in humans. Mouse models can be used to assay anxiety-like behaviour to understand how a scientific intervention can modulate neuropsychiatric disease [138]. We investigated whether Irs1KO mice displayed an increase in anxiety-like behaviour with age as reported in previous studies [137]. Interestingly, we found a significant reduction in anxiety-like behaviour in male and female old Irs1KO mice as measured by comparing centre occupancy in the open field. However, there was no significant difference in centre occupancy in young Irs1KO mice which may suggest that there was an age-associated reduction in anxiety in old Irs1KO mice. Models of neurodegenerative diseases have found a significant reduction in centre occupancy or an increase in anxiety-like behaviour in contrast to our results in old Irs1KO mice [139]. Irs1KO mice may offer new opportunities for the neuropsychiatric field to investigate some of the biological underpinnings of the increase in age-associated anxiety [137].

We tested the spatial learning and memory capabilities of old Irs1KO mice, a phenotype with evidence of age-associated decline [140]. Previous reports have associated reduction of IIS with deficits in forming long term memory fear [141]. Additionally, constitutively activating Ras, a downstream member of IIS [142], has been associated with cognitive enhancement in mice [143]. S6K mutant mice show reduced memory and one explanation could be the link between reduced IIS and protein translation [144], given the relationship between memory formation and protein translation [145]. On the other hand, the reduction of memory could be due to reduced activation of *CREB*, a transcription factor downstream of the IIS [146], that has been associated with neuronal excitability and memory formation [147]. Therefore, we asked whether reduced IIS in the brains of Irs1KO mice would lead to deficits in learning or long-term memory formation. Surprisingly, we find no deficits in the use of distal spatial cues by male and female Irs1KO mice to learn the location of the hidden platform (Section 4.2.4). Moreover, old male Irs1KO mice could recall the location of the hidden platform during the probe trial similar to male S6K deficient mice (Section 4.2.4). However, both old wild type and Irs1KO female mice did not form or could not recall the location of the hidden platform during the probe trial. This was not due to deficits in visual acuity, motivation or swimming capability as wild type males and females behaved equally well in the cued version of the water maze. The significant reduction in swim speed of male and female Irs1KO mice could be due to their smaller size, as reduced swim speed is consistent with findings in S6K mutant mice which were also significantly smaller than their control littermates (~85% of controls)[141]. One potential cause for the lack of memory deficit is that out intervention only slightly reduces pathway activity.

In an attempt to circumvent potential confounds due to the diminished swimming capability of Irs1KO mice, we used an object recognition task to investigate whether hippocampus-dependent memory is impaired in aged Irs1KO mice. Indeed, we found no significant reduction in locomotion speed or total distance travelled in young or old Irs1KO mice (Section 4.2.5). We found no significant difference in the novelty preference of young Irs1KO mice. However, we detected a significant increase in novelty preference in old Irs1KO mice. Previous reports have found that novel object recognition deteriorates with age [148], suggesting that the difference detected in old Irs1KO mice may indicate a reduction of age-associated decline in hippocampus dependent

memory. Indeed, a chronic pharmaceutical inhibitor of the mTOR pathway, downstream of IIS, has revealed an association between reduced IIS and a decrease in age-associated cognitive decline [149].

In summary, we find improvements in some cognitive parameters of old Irs1KO mice in a sex-independent manner consistent with the improvement of metabolic parameters.

5. Sex-specific effects of Cre expression in Syn1Cre mice

Author contributions:

Conception of the study predominantly by Maarouf Baghdadi and Linda Partridge

Execution of experiments predominantly by Maarouf Baghdadi. Maarouf Baghdadi, Andrea Mesaros and Martin Purrio performed metabolic phenotyping

Evaluation of data by Maarouf Baghdadi

Graphical representation by Maarouf Baghdadi

Writing of the manuscript by Maarouf Baghdadi

Editing and correction of manuscript proportionally by Maarouf Baghdadi and Linda Partridge

Sex-specific effects of Cre expression in Syn1Cre mice

Authors:

Maarouf Baghdadi [1], Andrea Mesaros [1], Martin Purrio [1], Linda Partridge [1 2]

Affiliations:

1. Max-Planck Institute for Biology of Ageing, Cologne, Germany
2. Institute of Healthy Ageing, and GEE, UCL, London, UK

5.1 Introduction

Genetically engineered mice are commonly used to model certain aspects of human disease and probe specific gene function. One method is the use of transgenic mouse lines in which Cre-recombinase (Cre) is expressed under the control of specific gene promoters. The Cre then excises a section of DNA flanked by loxP sites creating a knockout mouse line. The Cre-loxP system has been developed as a critical experimental tool to achieve spatial control when investigating genotypes of interest in a tissue- or cell-specific manner. Many tissue-specific Cre-driver mouse lines have been generated to target specific cell types within a heterogeneous tissue.

The brain is a complex and heterogeneous tissue analysis of which has benefited tremendously from the genetic access provided by Cre-drivers to specific brain areas through enriched or restricted gene expression patterns [150]. The brain not only mediates behaviour in an animal but is also a central mediator of peripheral metabolism, largely but not solely through the action of the hypothalamus [54]. Therefore, Cre drivers with widespread expression have been used to understand the role of neuronal function on systemic metabolism. Seminal studies have implemented the Nestin-Cre mouse model as a tool to target a relatively wide range of neuron subtypes and assess the effect of insulin receptor deficiency in neurons on peripheral metabolism [151]. While originally thought to be uniquely driving recombinase expression in neurons, the tool is now widely recognized to affect radial glia as well as their astrocyte progeny [152]. Moreover, the Nestin-Cre tool has a number of pitfalls for conducting metabolism and behavioural research due to the off-target effects of Cre recombinase expression in other organs [56].

An alternative pan-neuronal Cre-driver to test the role of neuronal function on metabolic parameters is Cre driven from rat-Synapsin I promoter (Syn1Cre), which has been shown to drive transgene expression widely in neuronal cells, with the exception of the cerebellum [8]. In this study we characterised the pan-neuronal Syn1Cre line for applications in behavioural and metabolic studies. We implemented a phenotyping pipeline that assessed a variety of behavioural parameters such as motor performance, anxiety-like behaviour, working memory, and spatial reference memory. We found significant sex-specific effects of Syn1Cre on anxiety-like behaviour and spatial reference memory. We then characterised metabolic parameters and found a significant reduction in body weight of Syn1Cre mice. However, no significant changes were detected in peripheral metabolic phenotypes such as glucose tolerance, insulin sensitivity, energy expenditure, and locomotor activity.

Taken together we find that behavioural assays may be confounded by Syn1Cre expression but that metabolic parameters are less affected.

5.2 Results

5.2.1 No deficit in motor learning, neuromuscular strength and non-aversive exploratory behaviour in Syn1Cre mice

Cre endonuclease can have deleterious effects when over expressed in neurons [153]. Syn1Cre mice express the Cre recombinase across the brain in areas that coordinate motor functions[154]. Therefore, we assessed neuromuscular function in male and female Syn1Cre mice using complementary assays measuring different aspects of neuromuscular function, to ensure that neuronal Cre expression did not produce any deficits that could confound subsequent behavioural phenotyping.

We performed the rotarod experiment to assess if Syn1Cre mice show symptoms similar to ataxia [155]. We measured the average latency of a mouse to fall from an accelerating rotating rod across four training days. This assay not only evaluated motor coordination and balance as the mouse adjusts to the increasing speed of rotation to avoid falling, but also determined the motor learning capacity by measuring the increase in performance across training days. The increase in average latency to fall across time was analysed by repeated measures ANOVA, and revealed no motor learning deficits in either male (Fig 29a) or female (Fig 29b) Syn1Cre mice. Moreover, no deficit in motor performance was detected by analysing the rotarod area under the curve (AUC) of either male (Fig 29a) or female (Fig 29b) Syn1Cre mice.

For the evaluation of neuromuscular strength, we performed a grip strength assay. We measured muscle strength by gently pulling a mouse after it has gripped a bar assembly until the grip is released. The average gram-force required to release the animal's grip was measured across five trials (separately for front paws or all four paws). Given the influence of body weight on the results, we used analysis of covariance (ANCOVA) using body weight as a covariate to rigorously assess if grip strength is affected in Syn1Cre mice [132]. Front paw grip strength of male (Fig 29c) and female (Fig 29d) Syn1Cre mice did not show any significant deficits in muscular strength. Four paw grip strength of male (Fig 29e) Syn1Cre mice also did not show any significant difference. However, a small but significant reduction in female (Fig 29f) four paw grip strength was detected.

Finally, we measured locomotor and exploratory activity in free behaving Syn1Cre mice in a 50cm-by-50cm arena for 5 minutes. This experiment allows the determination of activity without the presence of any anxiety-provoking stimulus. We observed no significant difference in the distance travelled (Fig 29g) or locomotion speed (Fig 29h) of male and female Syn1Cre mice. This data suggests that in the absence of anxiety-provoking stimuli there is no deficit in the motivation and capacity of Syn1Cre mice to explore an area.

Taken together, our data suggests that neuromuscular function is unaffected in male or female Syn1Cre mice.

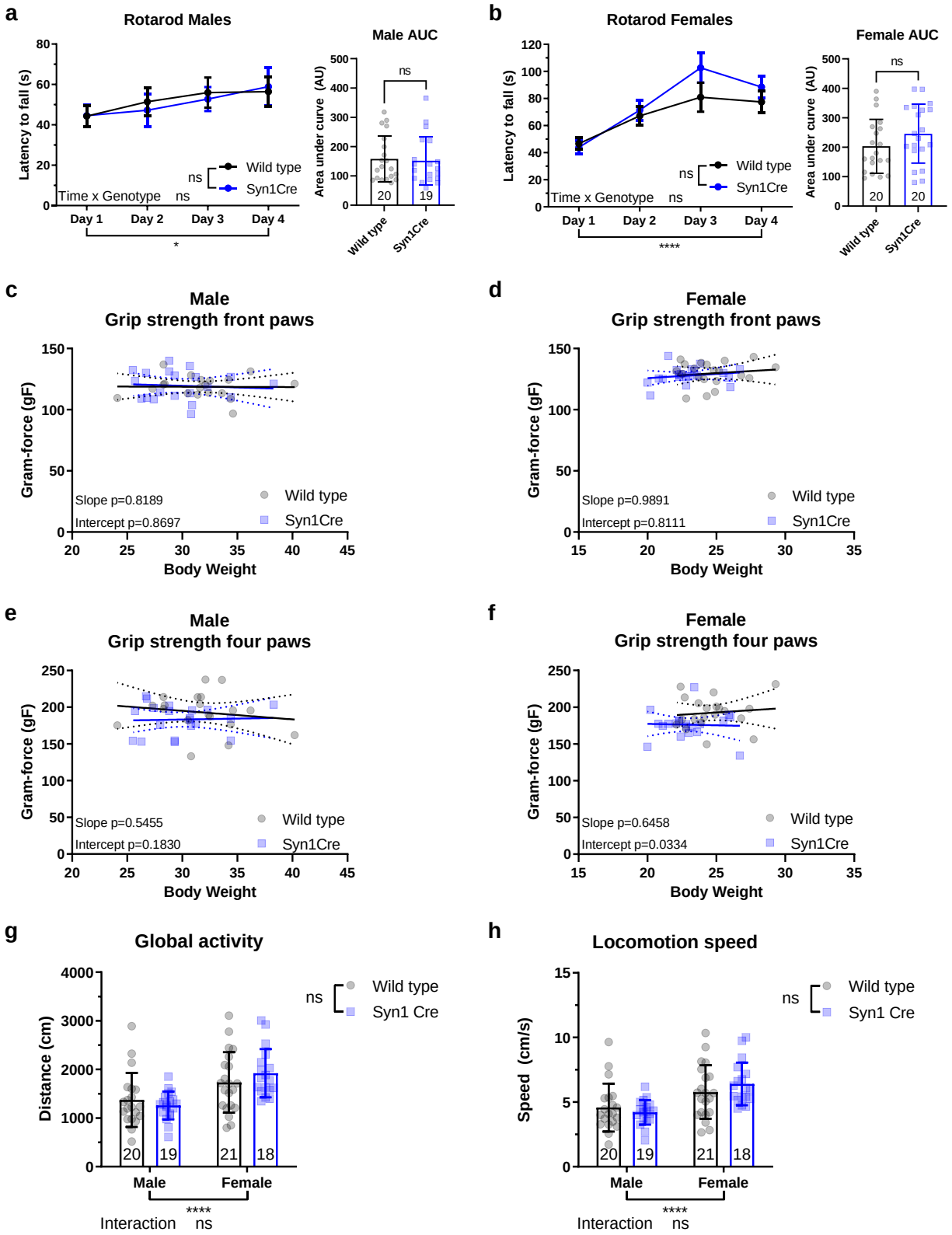

Figure 29: Characterisation of neuromuscular function in Syn1Cre mice

Average latency to fall during four days of training in the Rotarod revealed no significant defect in motor learning over time in male **(A)** or female **(B)** Syn1Cre mice. Analysis of body weight adjusted front-paw grip strength revealed no significant difference in strength of male **(C)** or female **(D)** Syn1Cre mice. Analysis of all four paws showed no significant difference in male Syn1Cre mice **(E)**, but a significant reduction in body weight-adjusted strength of all four paws in female Syn1Cre mice was detected **(F)** (male wild type n=19 and Syn1Cre n=20, female wild type and Syn1Cre n=20). Exploration and locomotion in a non-aversive arena were

not significantly affected in Syn1Cre mice **(G)**. No significant difference was detected in locomotion speed during exploration of a non-aversive arena in Syn1Cre mice. Number of animals reported at the bottom of the bars for each condition or in figure legends. All error bars correspond to standard deviation of the mean except for longitudinal Rotarod where standard error of the mean is reported. For ANCOVA analysis the 95% confidence interval is plotted. Detailed statistical values found in Table 4.

5.2.2 Reduced exploration and sex-specific increase in anxiety-like behaviour in Syn1Cre mice

In the absence of any baseline deficits in locomotor capabilities in Syn1Cre mice, we assessed exploration and anxiety-like behaviour in the open field. Mice were placed in an anxiety provoking open field arena with a highly illuminated centre (~220 lux) for five minutes. The total distance covered was measured using an automated system and revealed a significant reduction in total locomotion of both male and female Syn1Cre mice (Fig 30a). Moreover, average locomotion speed during exploration of the open field was also significantly lower in male and female Syn1Cre mice (Fig 30b). Rearing counts were assessed as another measure of exploratory behaviour. We found consistent results that male and female Syn1Cre mice had a significantly lower number of rearing counts (Fig 30c). This data suggests that the presence of anxiogenic stimuli, such as the bright lights, leads to reduced motivation of Syn1Cre mice to explore an illuminated arena compared to a darker (~20 lux) arena (Fig 29g and h).

Next, to assess anxiety-like behaviour in Syn1Cre mice, we measured the distance travelled in the centre of the highly illuminated arena [156]. However, given the difference in total distance travelled in the open field, we normalised distance travelled in the centre by total distance travelled in the five minutes. Interestingly, we detected a significant sex-specific decrease in centre occupancy (two-way ANOVA, sex*genotype interaction P=0.0211; F (1,75) =5.553, Fig. 30d). Male Syn1Cre mice had significantly lower distance travelled in the centre of the arena suggesting that Syn1Cre expression leads to a male-specific increase in anxiety (Fig. 30d). To confirm the reduction in centre occupancy was due to anxiety-like behaviour, we measured centre occupancy in the darker arena where mice were not exposed to anxiogenic stimuli. We found no significant difference in male or female Syn1Cre distance travelled in the centre of the darker arena (Fig 30e), suggesting that the phenotype observed in the open field was due to anxiety-like behaviour.

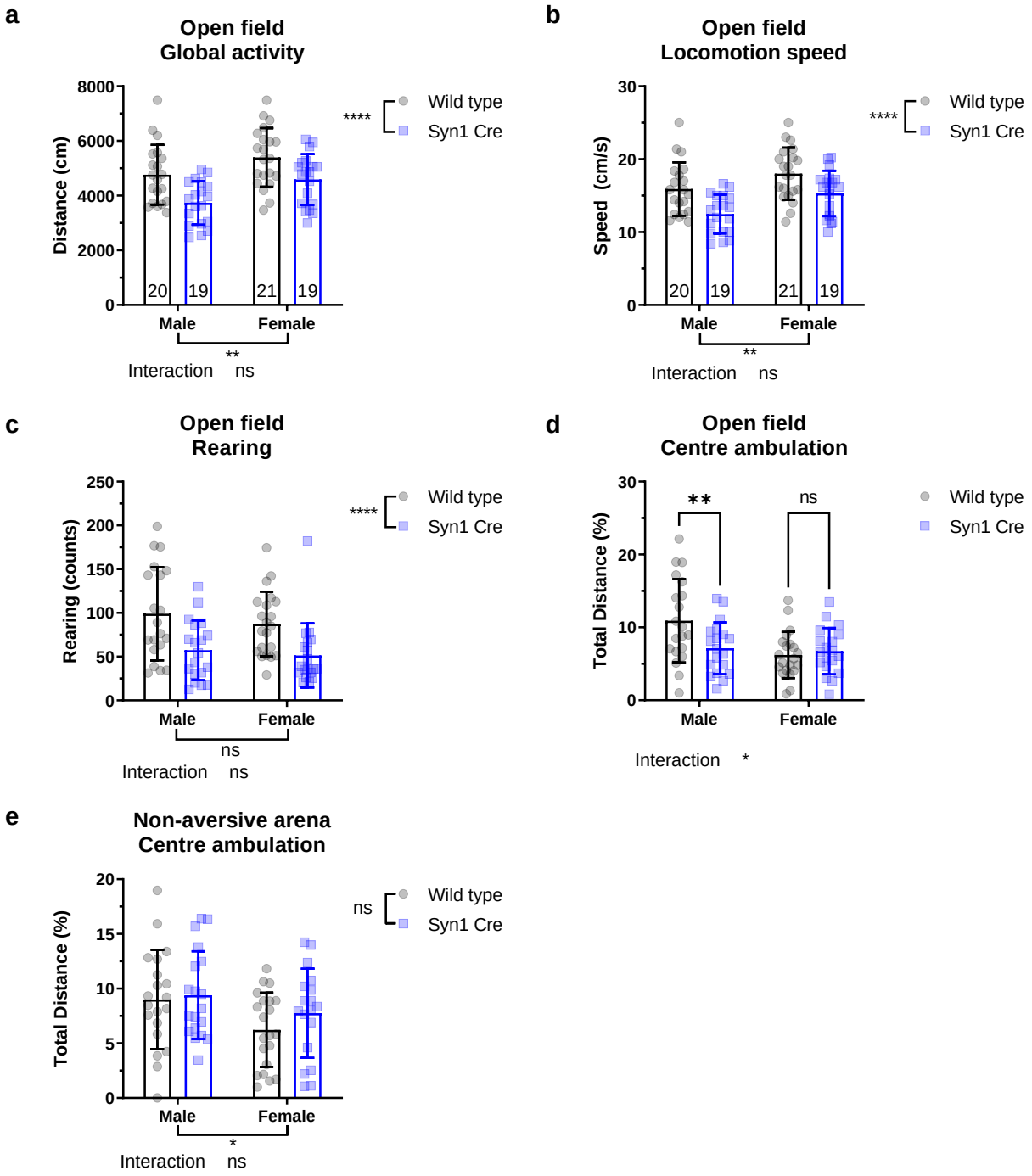

Figure 30: Exploratory and anxiety-like behaviour in Syn1Cre mice

(A) Locomotor activity measured during the aversive open field experiment revealed significant reduction in Syn1Cre mice. **(B)** Locomotor speed was also significantly reduced in the open field arena in Syn1Cre mice. **(C)** Rearing behaviour measurement revealed significant reduction in rearing of Syn1Cre mice (male wild type n=20 and Syn1Cre n=19, female wild type n=21 and Syn1Cre n=19). **(D)** Centre occupancy normalised to total time was analysed by two-way ANOVA and revealed sex-specific reduction in centre occupancy of male Syn1Cre mice (male wild type n=20 and Syn1Cre n=19, female wild type n=21 and Syn1Cre n=19). **(E)** Centre ambulation normalised to total distance measured in the non-aversive arena revealed no significant difference in Syn1Cre mice (male wild type n=20 and Syn1Cre n=19, female wild type n=21 and Syn1Cre n=18). Number of animals reported at the bottom of the bars where possible, otherwise in the figure legend. All error bars correspond to standard deviation of the mean. Detailed statistical values found in Table 4.

5.2.3 Impairment in learning and long-term spatial reference memory in Syn1Cre mice

An important function of the brain is hippocampus-dependent learning and memory which can be assessed using the water maze task [15,157]. The water maze, a test of spatial reference memory, is split into two major components which allows the experimenter to detect deficits in learning as well as memory impairment.

First, a learning stage was administered, where mice were placed in a water arena with a hidden platform. The average latency to escape the water by using the distal spatial cues to find the hidden platform was recorded. Male Syn1Cre mice were trained in the water maze task for three days until the wild type mice reached the threshold indicating adequate learning. However, during that time a significant difference was detected between the average escape latency between male Syn1Cre and their wild type littermates (Fig. 31a). This data suggests that Syn1Cre mice could not reliably find the hidden platform in the same amount of time as wild type mice, indicating a learning deficit in the Syn1Cre mice. Female Syn1Cre mice learned the location of the hidden platform equally well compared to the wild type littermates but took four days to reach the threshold (Fig. 31b).

Second, a probe trial was administered 24 hours after the last training session where the hidden platform was removed and the animal was allowed to search for the platform for 60 seconds. During the probe trial we detected a significant reduction in total swim path (Fig. 32a) and locomotion speed (Fig. 32c) of Syn1Cre mice, similar to the results we observed in the open field task (Fig 30a and b). Long-term memory formation was measured by occupancy of the target quadrant previously containing the hidden platform and the number of platform crossings. We measured the percentage time that male Syn1Cre mice swam in the target quadrant (quadrant containing hidden platform during training) and found a significant reduction of target quadrant occupancy in male Syn1Cre mice (Fig. 31c). Moreover, the number of platform crossings in male Syn1Cre mice was significantly lower than wild type littermates (Fig. 31e). This data suggests that, unlike wild type mice, male Irs1KO mice failed to form a memory of the hidden platform location in three days of training. Although we saw significant learning in female wild type and Syn1Cre mice (Fig. 31b), we could not detect evidence of memory formation 24 hours later neither in quadrant occupancy (Fig 31d) nor in platform crossing (Fig. 31e).

Additionally, we administered a visually cued variant of the water maze to assess the visual ability of Syn1Cre mice, as the water maze task depends on intact visual acuity. The cued water maze was administered 24 hours after the probe trial. The platform location was changed, and the distal spatial cues were covered using a curtain around the maze to motivate the animals to use the new proximal cue on the platform to escape. Three training trials were administered from different start locations and the average of the three trials was used to assess visual acuity. We detected no significant difference in swim path (Fig. 32b) but a significant reduction in swim speed (Fig. 32d) of Syn1Cre mice in the cued variant of the water maze. The reduction in swim speed may suggest impaired swimming performance in Syn1Cre mice. The latency to the escape platform in the cued water maze was measured and we detected a significant, sex-specific difference (two-way ANOVA, sex*genotype interaction $P=0.0327$; $F(1,75)=4.733$, Fig. 31f). Male Syn1Cre mice took significantly longer to escape the water maze even when a proximal visual cue was placed on the platform (Fig. 31f). This suggests that male Syn1Cre mice may have visual deficits preventing them from using proximal or distal cues to locate the platform (Fig. 31a). Therefore, the impairment in

learning and memory deficits we observed in male Syn1Cre mice (Fig. 31a and c) may in fact be due to deficits in visual acuity. Moreover, the data suggests that the memory deficit in female mice may be due to insufficient training trials as they possessed the motivation and visual acuity to escape during the cued variation of the water maze.

Next, we used the spontaneous alternation version of the Y-maze to assess spatial working memory as visual acuity is not required for this task. Mice were placed in the centre of the maze with three arms at 120 degrees from each other. The mouse was allowed to freely explore and then the number of full ABC alternations were calculated as a percentage of total arm entries. If mice score around 50% ABC alternations, or chance level, that means mice were equally likely to enter the previously visited arm or the novel arm suggesting that there are deficits to working memory formation. We measured total locomotor activity (Fig. 32e) and locomotor speed (Fig. 32f) in the Y-maze and could not detect any significant difference in Syn1Cre mice. When we measured the number of total arm entries in male and female Syn1Cre mice, we could not detect any significant difference, suggesting that both genotypes were equally likely to explore the maze (Fig. 31g). When we measured the number of alternations where the mouse favoured novel arms over previously visited arms (so called ABC alternations), we found no significant deficits in male or female Syn1Cre mice (Fig. 31h). This data suggests that short-term memory formation is still functional in male and female Syn1Cre mice.

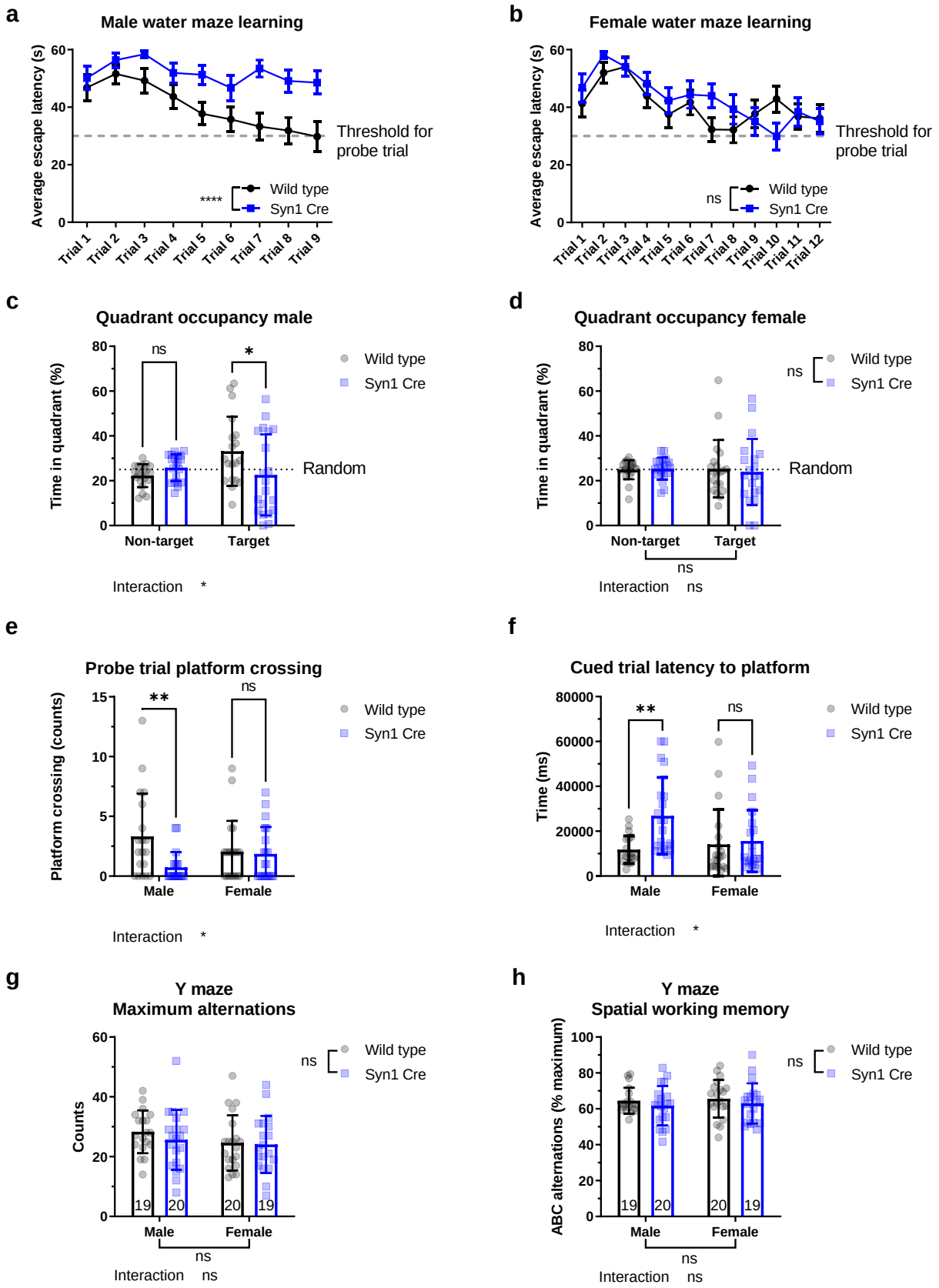

Figure 31: Spatial reference memory and working memory of Syn1Cre mice

(A) Assessment of escape latency across nine trials of water maze training showed significant reduction in learning of male Syn1Cre mice (male wild type n=19 and Syn1Cre n=20). **(B)** Assessment of escape latency across 12 trials of water maze training showed no

significant difference in female Syn1Cre mice (female wild type n=19 and Syn1Cre n=20). **(C)** Probe trial quadrant occupancy revealed a significant reduction in target quadrant occupancy in male Syn1Cre mice compared to wild type littermates (male wild type n=19 and Syn1Cre n=20). **(D)** Probe trial quadrant occupancy revealed no memory in female wild type or Syn1Cre mice (female wild type n=19 and Syn1Cre n=20). **(E)** Platform crossings during probe trial revealed presence of long-term memory exclusively in male wild type mice. **(F)** Latency to escape in the cued water maze revealed significant sex-specific increase of time in male Syn1Cre mice. **(G)** Number of alternations during the spontaneous Y-maze assay revealed no significant difference in Syn1Cre mice. **(H)** Number of correct A>B>C alternations as a percentage of total alternations did not show any significant difference in Syn1Cre mice. Number of animals reported at the bottom of the bars where possible, otherwise in the figure legend. All error bars correspond to standard deviation of the mean except water maze training where standard error of the mean was plotted. Detailed statistical values found in Table 4.

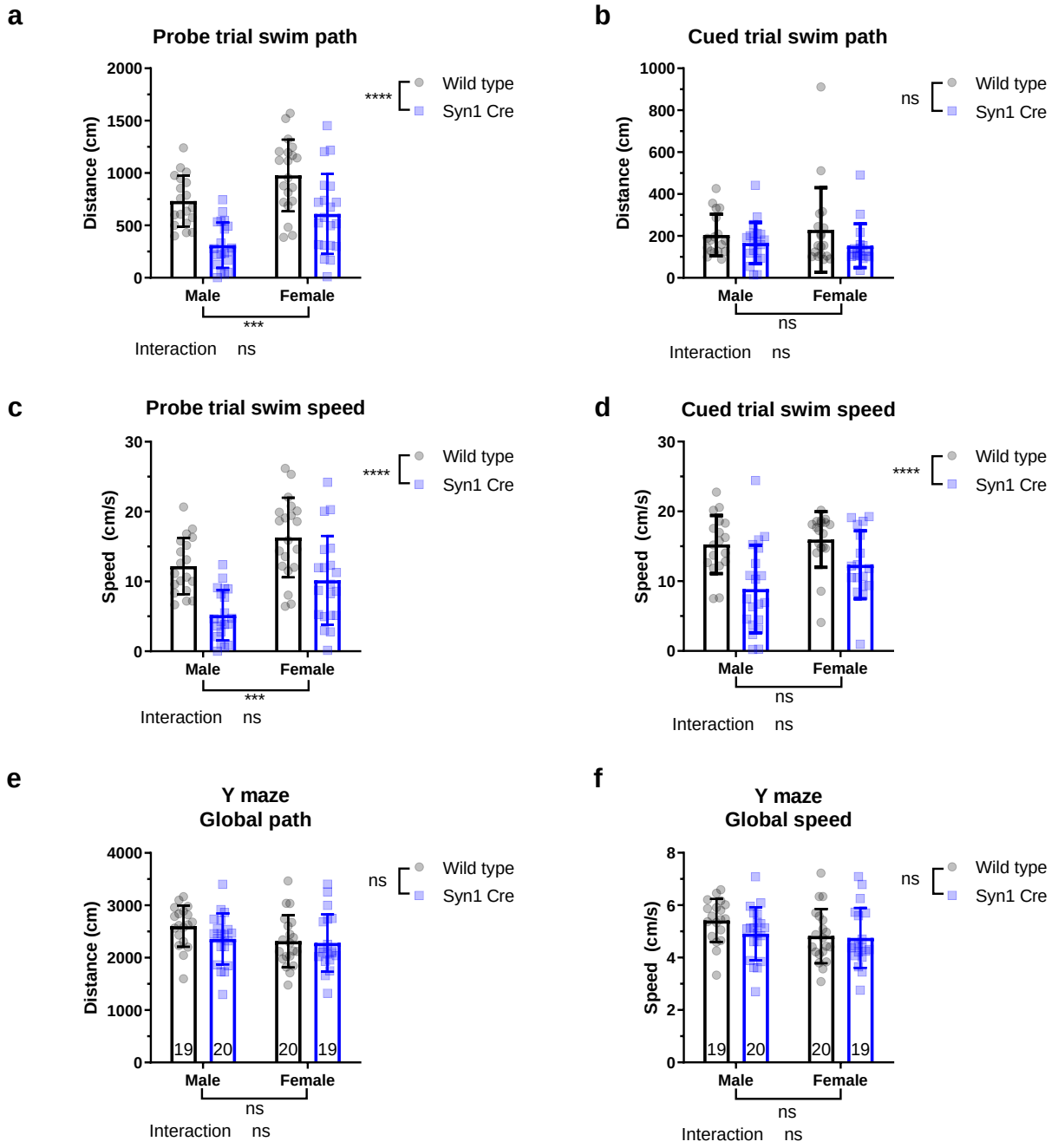

Figure 32: Additional outcome measures from memory tasks

(A) Total swim path during the 60 second probe trial revealed significant reduction in Syn1Cre mice (male wild type n=19 and Syn1Cre n=20, female wild type n=19 and Syn1Cre n=20). **(B)** Total swim path in the cued variation of the water maze showed no significant change in Syn1Cre mice (male wild type n=18 and Syn1Cre n=20, female wild type n=18 and Syn1Cre n=17). **(C)**

Assessment of swim speed during the probe trial revealed significant reduction in Syn1Cre mice. **(D)** Swim speed in the cued water maze variant revealed significant reduction in Syn1Cre mice. **(E)** Measurement of total distance covered in the Y-maze did not detect any significant difference in Syn1Cre mice. **(F)** Locomotion speed in the Y-maze was not significantly different in Syn1Cre mice. Number of animals reported at the bottom of the bars where possible, otherwise in the figure legend. All error bars correspond to standard deviation of the mean. Detailed statistical values found in Table 4.

5.2.4 Increased hypothalamic hGH expression leads to sex-specific decrease in Syn1Cre growth

The brain is a primary site for the control of feeding and satiety through the action of the hypothalamic-pituitary axis [158].

Syn1Cre mice showed a significant decrease in body weight compared to wild type littermates (Fig. 33a). We assessed whether the reduction in body weight was due to a reduction in adiposity, but no significant difference was detected in fat mass as a percentage of total body weight (Fig. 33b). In order to assess whether the difference in body weight was due to feeding, we measured body weight adjusted food consumption but did not detect any significant difference (Fig. 34a). Previous reports in the Nestin-Cre mouse model have reported similar findings of a reduction in body weight due to Cre recombination under a neuronal promoter [159]. They attributed the reduction to the human growth hormone (hGH) minigene that was inserted downstream of the Cre recombinase, to achieve a higher expression level of the Cre transgene [160]. The original report of the Syn1Cre mouse model also indicated that they used a similar strategy of placing the hGH gene 3' of the Cre transgene [8].

Therefore, we asked whether the hypothalamus of Syn1Cre mice had increased expression of hGH. We tested hGH transcript levels by quantitative real-time PCR (Q-RT-PCR) and observed a significant increase in hGH transcript levels in Syn1Cre mice (Fig. 33c). Furthermore, to test whether the hGH signal we observed was due to the hGH bound to Cre on a single mRNA molecule and not endogenous mouse growth hormone, we used a forward annealing primer to the Cre fragment and a reverse primer annealing to the hGH minigene. Indeed, we found a similar fold change between the CT value of the Cre transgene and the B2M housekeeping gene (Fig. 34b), and the Cre-hGH transgene and B2M (Fig. 34c). The hGH results were not due to primer binding to the endogenous mouse genome as we either could not detect or only detected a signal at 34 cycles in wild type mice hypothalamus relative to detection at 18 cycles of B2M. In summary, Syn1Cre mice have an increased expression of exogenous growth hormone due to the Cre-hGH transgene.

Next, we asked whether the expression of hGH led to an activation of the downstream STAT5 pathway also implicated in Nestin-Cre mice [159]. Therefore, we measured the expression of cytokine inducible SH2-containing protein (*Cish*), which is up-regulated after phosphorylation of STAT5. As expected, we saw a small but significant increase in expression of *Cish* in Syn1Cre mice (1.149±0.09750-fold change) (Fig. 33d). Moreover, the previous report looking at the effect of hGH expression in Nestin-Cre mice also detected elevated phosphorylation of STAT5 in liver, resulting in elevated *CD36* transcript levels due to the role of STAT5 in hepatic lipid metabolism [161]. However, we detected no significant difference in transcript levels of CD36 in livers of Syn1Cre mice (Fig. 33e). One potential explanation for the inconsistent finding is that the Nestin promoter is additionally expressed in a wide variety of peripheral organs, while the Synapsin-1 promoter is confined to the nervous system and testis [56].

Previous reports have found that expression of *hGH* in the hypothalamus leads to the reduction of hypothalamic GH releasing hormone (*Ghrh*) leading to growth hormone deficiency [162]. Surprisingly, when we tested the levels of *Ghrh* in the hypothalamus, we detected no significant difference in Syn1Cre mice (Fig. 33f). However, when we tested the levels of hepatic *Igf1* expression, we did detect a sex-specific reduction in Syn1Cre mice (two-way ANOVA, sex*genotype interaction P=0.0114; F (1,11) =9.193, Fig. 33g). We found that male Syn1Cre mice have a reduced expression of hepatic *Igf1*, suggesting a negative feedback loop is triggered indirectly in male, but not female, Syn1Cre mice. The previous report on Nestin-Cre mice saw a similar reduction in male hepatic *Igf1* transcripts [159]. To confirm whether this reduction in the growth axis in Syn1Cre mice was functionally leading to the size difference in body weight (Fig. 33a), we used the length of the femur to get an accurate body size comparison. Indeed, we found a consistent sex-specific difference in the femur length of Syn1Cre mice (two-way ANOVA, sex*genotype interaction P=0.0448; F (1,11) =5.127, Fig. 33h). Male Syn1Cre mice had shorter femurs compared to wild type littermates, suggesting that the reduction in body weight (Fig. 33a) could be due to reduced body size as a result of reduced systemic growth hormone signalling.

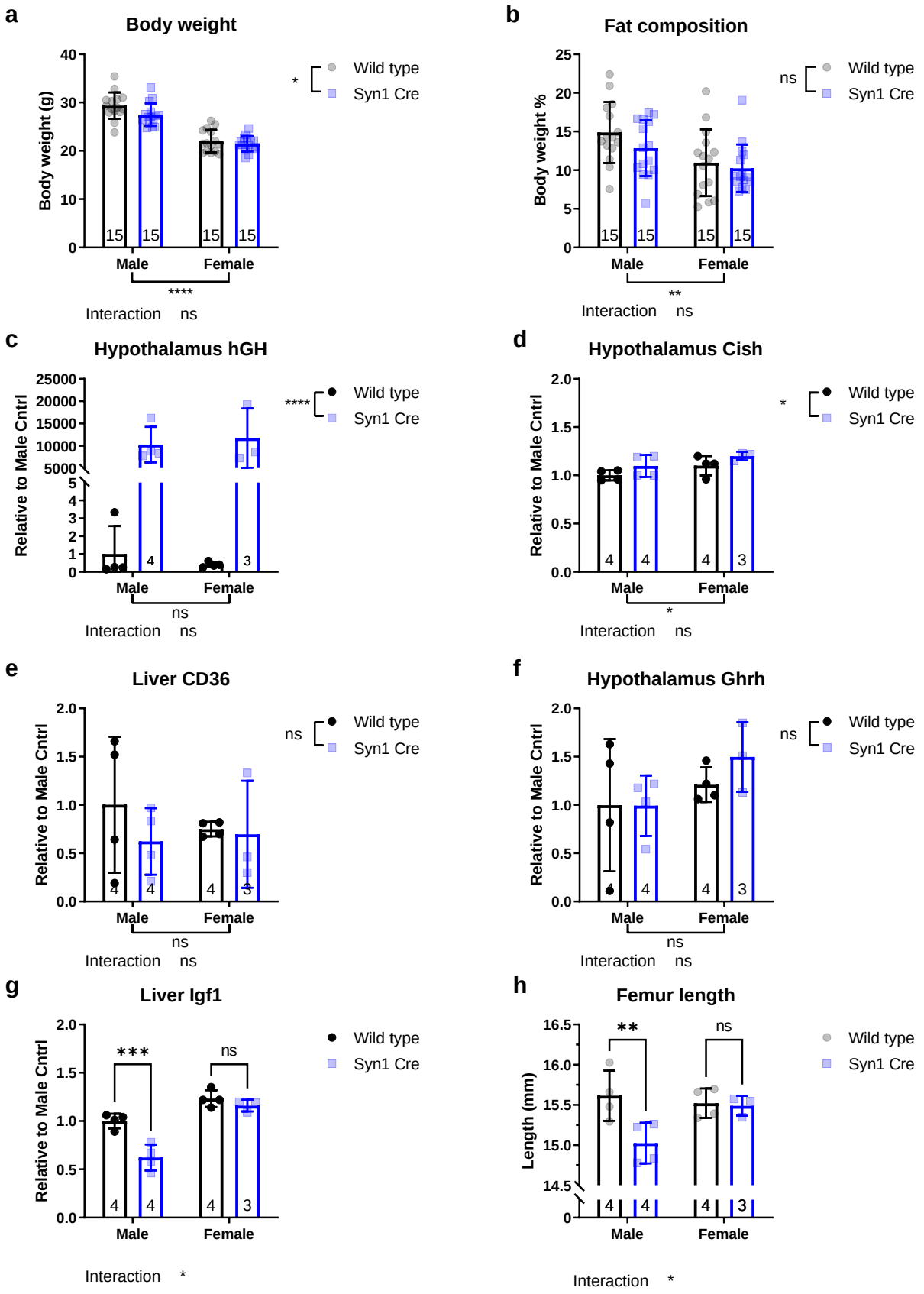

Figure 33: Cre transgene triggers increased hGH expression leading to a sex-specific reduction in body size of male Syn1Cre mice (below)

(A) Measurement of body weight of Syn1Cre mice revealed a small but significant reduction in body weight of Syn1Cre mice. **(B)** Assessment of fat mass as a percentage of body weight did not reveal any difference in body composition of Syn1Cre mice. **(C)** Measurement of hGH transcript levels using quantitative real-time PCR (qPCR) in the hypothalamus revealed significant increase in hGH expression in Syn1Cre mice (Male wild type n=4 and female wild type n=4). **(D)** Significant increase in Cish transcript levels in the hypothalamus of Syn1Cre mice. **(F)** Measurement of CD36 transcripts by qPCR in liver tissue revealed no significant difference between Syn1Cre mice and wild type littermates. **(F)** No significant difference in Ghrh levels in hypothalamus extracts between Syn1Cre mice and wild type littermates. **(G)** Two-way Anova of Igf1 transcript levels in Syn1Cre mice revealed a sex-specific reduction of hepatic Igf1 expression in male Syn1Cre mice. **(H)** Two-way Anova analysis of femur length revealed a sex-specific reduction in male Syn1Cre femur size. Number of animals reported at the bottom of the bars. All error bars correspond to standard deviation of the mean. Detailed statistical values found in Table 4.

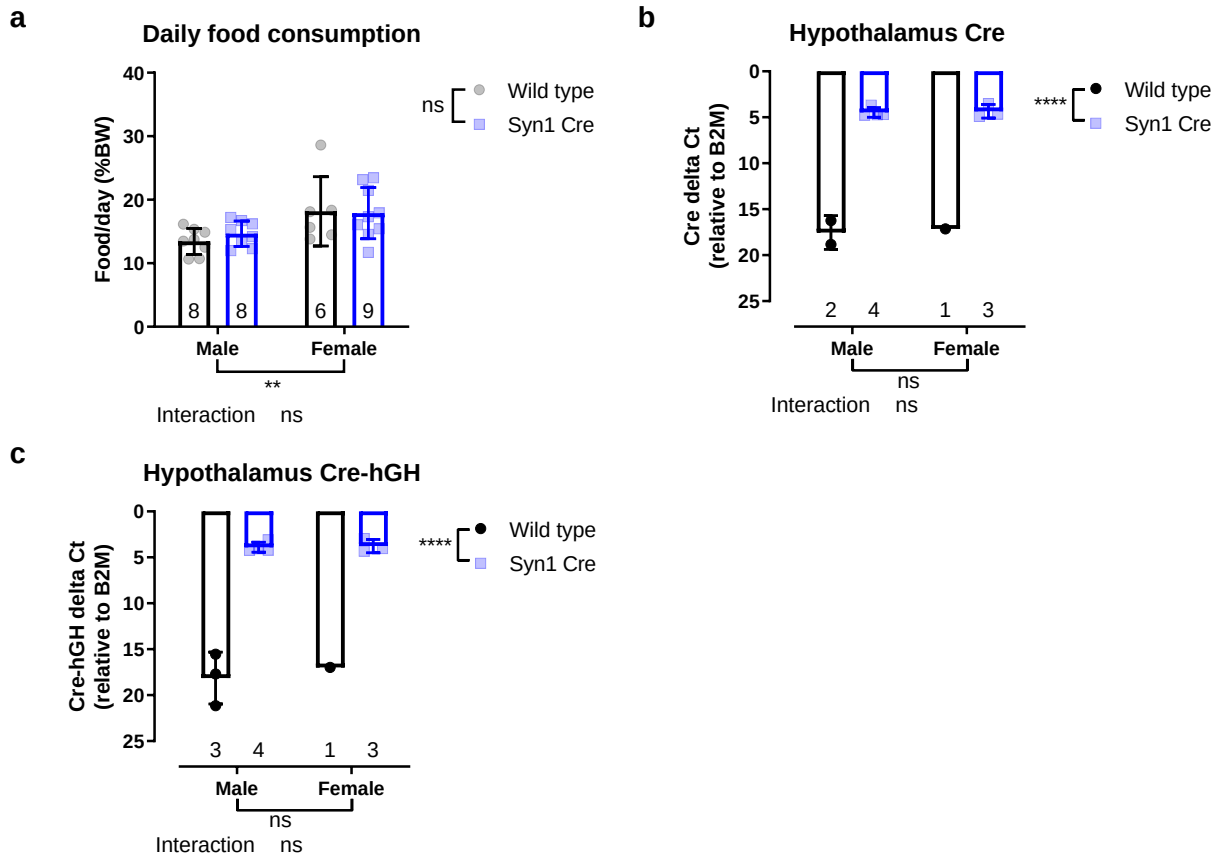

Figure 34: Daily food consumption and Cre expression in Syn1Cre mice
(A) Measurement of body weight adjusted food consumption of Syn1Cre mice did not detect any significant difference between Syn1Cre mice and wild type littermates. **(B)** Measuring level of Cre transcripts in the hypothalamus of Syn1Cre mice revealed a genotype specific expression of Cre recombinase. **(C)** Measurement of Cre-hGH transcripts in the hypothalamus of Syn1Cre mice detected expression only in Syn1Cre mice and not wild type littermates. All error bars correspond to standard deviation of the mean. Detailed statistical values found in Table 4.

5.2.5 Intact systemic metabolic parameters in Syn1Cre mice

The hypothalamus in the brain is a central mediator for peripheral insulin sensitivity and glucose metabolism [54]. We assessed whether Cre recombinase expression in the brain was leading to any effects on peripheral metabolism in Syn1Cre mice.

We assessed glucose tolerance by administration of a glucose tolerance test (GTT) after an overnight fast. This gives insight into pancreatic beta cell function as well as the capability of an animal to suppress hepatic gluconeogenesis in response to a body-weight-adjusted glucose challenge. Area under the curve (AUC) analysis of GTT revealed no significant difference in the glucose sensitivity of male (Fig. 35a) and female (Fig. 35b) Syn1Cre mice. Insulin sensitivity is a cornerstone of metabolic health, since it reflects the ability for insulin to activate peripheral tissue absorption of blood glucose. To assess systemic insulin sensitivity, we administered an insulin tolerance test (ITT) which measures changes in blood glucose levels in response to a body weight-adjusted bolus of insulin injected intraperitoneally. AUC analysis of ITT revealed no significant difference in the insulin sensitivity of male (Fig. 35c) and female (Fig. 35d) Syn1Cre mice.

The hypothalamus in the brain is a mediator of energy expenditure, circadian rhythm and locomotor activity in an animal [14]. Therefore, we assessed energy expenditure and circadian rhythm, given the effects we observed in the hypothalamus. We placed single-housed mice in special metabolic cages that allow measurement of indirect calorimetry over multiple days. We used ANCOVA analysis using body weight as a covariate to analyse if there are differences in energy expenditure between Syn1Cre mice and their wild type littermates. We did not detect any significant differences in day-time or night-time energy expenditure in male (Fig. 35e and Fig. 36a) or female (Fig. 35f and Fig. 36b) Syn1Cre mice. We used beam breaks during the animal's time in the metabolic cages to infer average homecage activity levels across a 24-hour period. We found no significant difference in the amount or phase of activity in male (Fig. 35g) or female (Fig. 35h) Syn1Cre mice. Finally, we used respiratory exchange ratio (RER) measurements in the metabolic cages to determine the type of fuel consumption during different phases of the day in Syn1Cre mice. An RER value close to 0.7 indicates that fat is the predominant fuel source, while an RER of 1.0 indicates that carbohydrates are the predominant fuel source, and a value in between suggests a mix of both. Consistent with our locomotor activity and energy expenditure findings, we did not detect any significant difference of RER in male (Fig. 36c) or female (Fig. 36d) Syn1Cre mice.

All together we find no significant effect of neuronal Cre recombinase expression on peripheral metabolism, providing the field with a new tool to study neuronal control of metabolism.

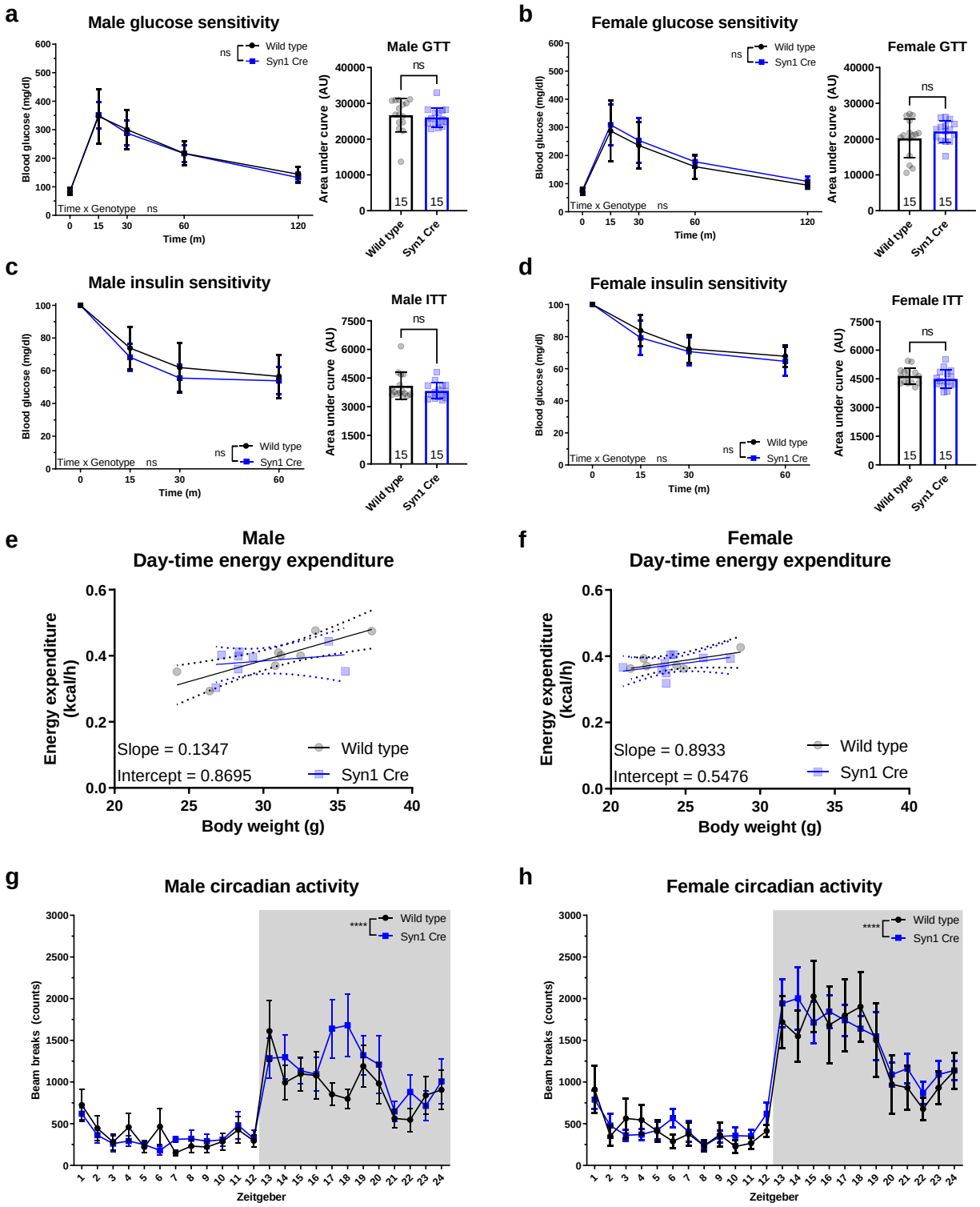

Figure 35: Effect of Syn1Cre expression on peripheral metabolic health outcomes

Glucose tolerance test (GTT) on male Syn1Cre mice **(A)** and female Syn1Cre mice **(B)** did not detect any significant difference relative to their respective wild type littermates. Insulin sensitivity test (ITT) on male Syn1Cre mice **(C)** and female Syn1Cre mice **(D)** did not detect any significant difference relative to their wild type littermates. ANCOVA on day-time energy expenditure of Syn1Cre mice showed no significant difference between male **(E)** or female **(F)** Syn1Cre and their respective wild type littermates (male wild type and Syn1Cre n=8, female wild type n=7 and Syn1Cre n=9). Locomotor activity of single-housed male **(G)** and female **(H)** Syn1Cre mice plotted against zeitgeber revealed no significant difference between Syn1Cre mice and wild type littermates.

Number of animals reported at the bottom of the bars. All error bars correspond to standard deviation of the mean. For ANCOVA analysis the 95% confidence interval is plotted. Detailed statistical values found in Table 4.

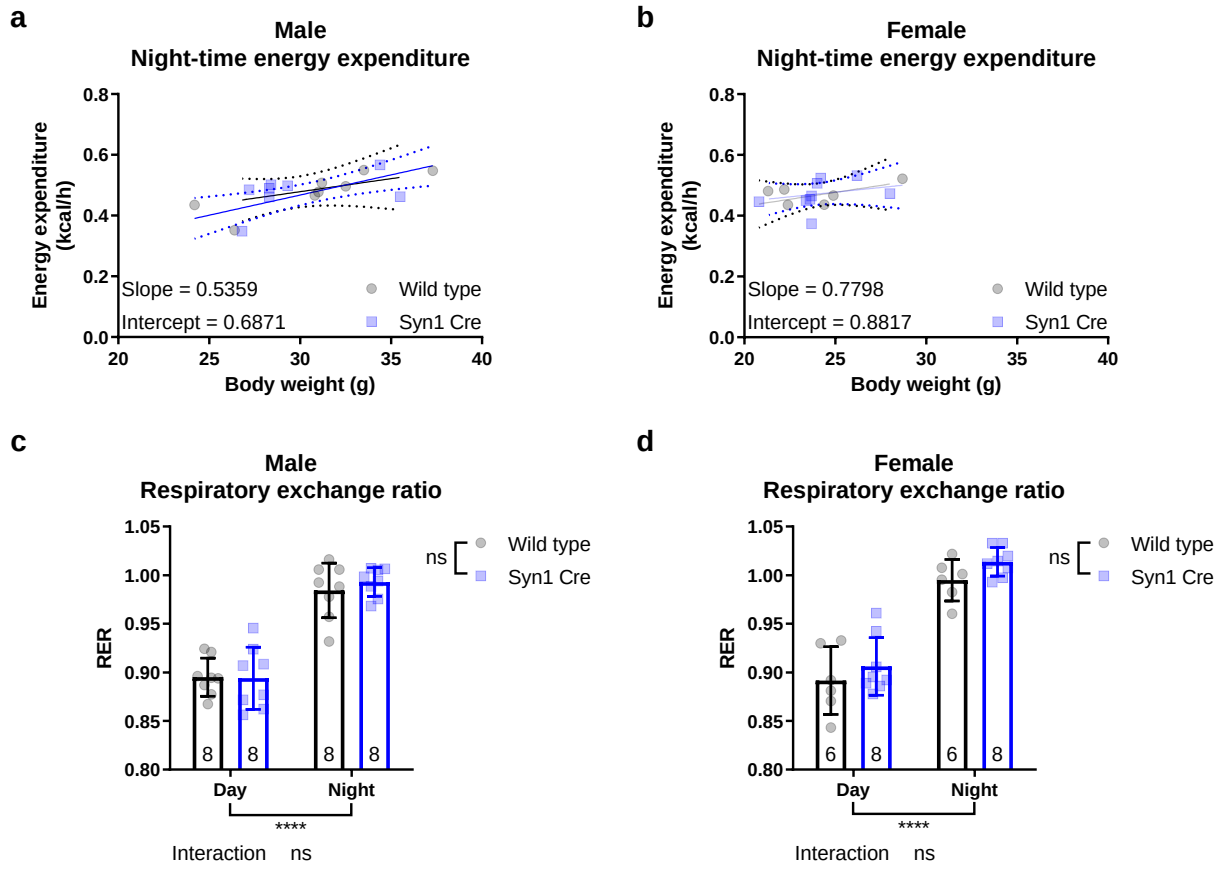

Figure 36: Additional metabolic measures of Syn1Cre mice

ANCOVA on night-time energy expenditure of Syn1Cre mice showed no significant difference between male **(A)** or female **(B)** Syn1Cre and their respective wild type littermates (male wild type and Syn1Cre n=8, female wild type n=7 and Syn1Cre n=9). Respiratory exchange ratio of male **(C)** and female **(D)** Syn1Cre mice did show any significant difference due to genotype compared to wild type littermates. Number of animals reported at the bottom of the bars. All error bars correspond to standard deviation of the mean. For ANCOVA analysis the 95% confidence interval is plotted. Detailed statistical values found in Table 4.

5.3 Discussion

In this study we report behavioural and metabolic phenotyping of Syn1Cre mice. We focused on phenotypes relevant for metabolic and neuropsychiatric disorders, as those were the primary applications for pan-neuronal genetic tools. Sex is increasingly recognised as an important influence on the brain in health [163] and disease [164], and we therefore characterised both male and female Syn1Cre mice[165].

Many of the previous reports on the neuronal control of metabolism have used Nestin-Cre mice. However, given the recent evidence of the metabolic pitfalls [56], an alternative pan neuronal gene driver, such as Cre expressed under the rat Synapsin- promoter, is desirable. According to the mouse genome database, more than 170 studies have used Syn1Cre mice [166], but a study of the effect of Cre expression on basic phenotypes in males and females is missing. Therefore, we asked what the effect of Syn1Cre on the behavioural and metabolic parameters of young male and female mice.

We did not observe any significant effects on motor learning, neuromuscular strength, or locomotor activity in male or female Syn1Cre mice. However, when mice were placed in the anxiogenic open field context, both male and female Syn1Cre mice exhibited reduced exploratory drive. In addition, we detected a male-specific increase in anxiety-like behaviour in the open field, a trait that was previously shown to be modified by sex [165]. Centre occupancy in a non-aversive arena further confirmed that the observed phenotype is being mediated by the anxiogenic illumination of the open field. Interestingly, previous reports in Nestin-Cre mice also found an increase in anxiety-like phenotype in male mice [167], suggesting a shared cause in these two genetic drivers.

When we assessed the learning capability of Syn1Cre mice, again we detected a significant deficit in the ability of male Syn1Cre mice to use distal spatial cues to locate the hidden platform, unlike wild type males and both female groups. The probe trial further confirmed the deficit in memory formation in male Syn1Cre mice. Surprisingly, both female groups also did not perform in the probe trial. However, given that wild type females did not show enriched target quadrant occupancy, we could not conclude if female Syn1Cre mice exhibited deficits in memory formation or simply the number of training trials was insufficient. We also administered cued trials in the water maze to test the motivation and visual acuity in male and female Syn1Cre mice. We detected a deficit in male Syn1Cre mice as they were the only group to have a significantly increased latency to the platform when a proximal cue was added. This data suggests that male Syn1Cre mice are not appropriate for use in assays that require visual acuity. Previous reports have found microphthalmia and anophthalmia are found in C57BL/6 mice (~20% of all females and ~2% of male mice) [168]. However, our data from male Syn1Cre mice suggests the presence of an interaction between the strain and the intervention leading to increased visual defects in male mice. Data from the Y-maze suggests that short-term memory formation is still functional in male and female Syn1Cre mice.

Similar to results from Nestin-Cre mice [159], we observed a significant reduction in the body weight of Syn1Cre positive mice without a difference in body composition or feeding. Consistent with the Nestin-Cre study, we detected an overexpression of a Cre-hGH mRNA transcript due to the construct design used to generate this genetic tool [8]. Although we found high hGH transcripts in the hypothalamus of Syn1Cre mice, we could not detect STAT5 activation in the liver unlike the Nestin-Cre model[159]. However, we also found evidence of an activation of a negative feedback loop leading to reduced growth in a sex-specific manner in male Syn1Cre mice. Finally, we could not detect any significant effect on peripheral metabolism, namely body composition, glucose tolerance, and insulin sensitivity in male or female Syn1Cre mice, suggesting the potential application of this genetic model in neuronal control of metabolism studies. Moreover, no effect on peripheral metabolism was observed in old male or female Syn1Cre mice (Chapter 3).

In summary, our study describes for the first time a comprehensive characterization of a heavily used Cre mouse line in neurobiology. Importantly, our data indicate that indirect effects from the techniques used to generate the model can confound certain behavioural tests in a sex-specific manner, but not on general metabolic assays. Moreover, our study highlights the need of including both male and female mice in future studies as well as the use of appropriate experimental control groups to delineate the effects of the Cre transgene.

6. List of figures

Figure 1 Increased lifespan and improved health parameters in Irs1KO mice

Figure 2 Characterisation of young Irs1KO

Figure 3 Additional parameters of old Irs1KO

Figure 4 Validation of mouse models used in the study

Figure 5 Tissue-specific deletion of IRS1 is not sufficient for lifespan extension

Figure 6 Body weight and composition of tissue-specific Irs1KO mice

Figure 7 Energy expenditure of tissue-specific Irs1KO mice

Figure 8 Locomotor activity of tissue-specific Irs1KO mice

Figure 9 Insulin tolerance test of tissue-specific Irs1KO mice

Figure 10 Glucose tolerance test of tissue-specific Irs1KO mice

Figure 11 Neuron-specific Irs1 knockout (nKO) mice show male-specific improvement in metabolic health

Figure 12 Characterisation of young nKO

Figure 13 Additional parameters of old nKO

Figure 14 Neuronal Syn1Cre expression does not affect peripheral metabolism

Figure 15 Investigation of mitochondrial function implicated the integrated stress response

Figure 16 No activation of ISR in brains of young Irs1KO and nKO mice

Figure 17 Syn1Cre expression does not lead to brain ISR activation

Figure 18 IRS1 deletion in peripheral tissues is insufficient to induce local ISR signature in old mice

Figure 19 Sex-specific brain ISR signal did not lead to systemic FGF21 signal

Figure 20 Energy expenditure is acting through an FGF21 independent manner

Figure 21 No deficit in locomotor coordination or capacity in young Irs1KO mice

Figure 22 No deficit in locomotor coordination or capacity of old Irs1KO mice

Figure 23 Reduced exploratory behaviour in young Irs1KO mice

Figure 24 Reduced exploration and anxiety-like behaviour in old Irs1KO mice

Figure 25 No deficit in learning or long-term memory in old Irs1KO mice

Figure 26 No deficiency in motivation or visual acuity of old Irs1KO mice

Figure 27 No significant difference in working memory of young Irs1KO mice

Figure 28 Reduced age-associated decline in working memory of old Irs1KO mice

Figure 29 Characterisation of neuromuscular function in Syn1Cre mice

Figure 30 Exploratory and anxiety-like behaviour in Syn1Cre mice

Figure 31 Spatial reference memory and working memory of Syn1Cre mice

Figure 32 Additional outcome measures from memory tasks

Figure 33 Cre transgene triggers increased hGH expression leading to a sex-specific reduction in body size of male Syn1Cre mice

Figure 34 Daily food consumption and Cre expression in Syn1Cre mice

Figure 35 Effect of Syn1Cre expression on peripheral metabolic health outcomes

Figure 36 Additional metabolic measures of Syn1Cre mice

7. List of tables

Table 1 Supplementary statistics of Chapter 3

Table 2 detailed quantitative and qualitative transitions and electronic settings for the analysed metabolites, as well as raw metabolites detected

Table 3 Supplementary statistics of Chapter 4

Table 4 Supplementary statistics of Chapter 5

Table 5 Supplementary information about genotyping primers, Q-RT-PCR oligonucleotides, and antibodies used in the study

8. Bibliography

1. Selman, C. *et al.* Evidence for lifespan extension and delayed age-related biomarkers in insulin receptor substrate 1 null mice. *FASEB J.* **22**, (2008).
2. Fontaine, D. A. & Davis, D. B. Attention to Background Strain Is Essential for Metabolic Research: C57BL/6 and the International Knockout Mouse Consortium. *Diabetes* **65**, 25–33 (2016).
3. Essers, P. *et al.* Reduced insulin/insulin-like growth factor signaling decreases translation in Drosophila and mice. *Sci. Rep.* **6**, 30290 (2016).
4. Kellendonk, C., Opherk, C., Anlag, K., Schütz, G. & Tronche, F. Hepatocyte-specific expression of Cre recombinase. *Genesis* **26**, (2000).
5. Brüning, J. C. *et al.* A muscle-specific insulin receptor knockout exhibits features of the metabolic syndrome of NIDDM without altering glucose tolerance. *Mol. Cell* **2**, (1998).
6. Eguchi, J. *et al.* Transcriptional control of adipose lipid handling by IRF4. *Cell Metab.* **13**, 249 (2011).
7. Madison, B. B. *et al.* Cis elements of the villin gene control expression in restricted domains of the vertical (crypt) and horizontal (duodenum, cecum) axes of the intestine. *J. Biol. Chem.* **277**, (2002).
8. Zhu, Y. *et al.* Ablation of NF1 function in neurons induces abnormal development of cerebral cortex and reactive gliosis in the brain. *Genes Dev.* **15**, 859 (2001).
9. Rempe, D. *et al.* Synapsin I Cre transgene expression in male mice produces germline recombination in progeny. *Genesis* **44**, (2006).
10. Mähler, C. M. *et al.* FELASA recommendations for the health monitoring of mouse, rat, hamster, guinea pig and rabbit colonies in breeding and experimental units. *Lab. Anim.* **48**, (2014).
11. Müller, T. D., Klingenspor, M. & Tschöp, M. H. Revisiting energy expenditure: how to correct mouse metabolic rate for body mass. *Nature Metabolism* **3**, 1134–1136 (2021).
12. Tschöp, M. H. *et al.* A guide to analysis of mouse energy metabolism. *Nat. Methods* **9**,

(2011).

13. Moore, S. J., Deshpande, K., Stinnett, G. S., Seasholtz, A. F. & Murphy, G. G. Conversion of short-term to long-term memory in the novel object recognition paradigm. *Neurobiol. Learn. Mem.* **105**, (2013).
14. Tran, L. T. *et al.* Hypothalamic control of energy expenditure and thermogenesis. *Exp. Mol. Med.* **54**, 358–369 (2022).
15. van Woerden, G. M. *et al.* Rescue of neurological deficits in a mouse model for Angelman syndrome by reduction of alphaCaMKII inhibitory phosphorylation. *Nat. Neurosci.* **10**, (2007).
16. Benani, A. *et al.* Method for functional study of mitochondria in rat hypothalamus. *J. Neurosci. Methods* **178**, 301–307 (2009).
17. Wong, J. M. *et al.* Benzoyl chloride derivatization with liquid chromatography-mass spectrometry for targeted metabolomics of neurochemicals in biological samples. *J. Chromatogr. A* **1446**, (2016).
18. Schwaiger, M. *et al.* Anion-Exchange Chromatography Coupled to High-Resolution Mass Spectrometry: A Powerful Tool for Merging Targeted and Non-targeted Metabolomics. *Anal. Chem.* **89**, (2017).
19. Partridge, L., Deelen, J. & Slagboom, P. E. Facing up to the global challenges of ageing. *Nature* **561**, 45–56 (2018).
20. Austad, S. N. & Fischer, K. E. Sex Differences in Lifespan. *Cell Metab.* **23**, (2016).
21. Fontana, L. & Partridge, L. Promoting health and longevity through diet: from model organisms to humans. *Cell* **161**, (2015).
22. Kenyon, C. J. The genetics of ageing. *Nature* **464**, 504–512 (2010).
23. Piper, M. D. W. & Partridge, L. Drosophila as a model for ageing. *Biochim. Biophys. Acta Mol. Basis Dis.* **1864**, (2018).
24. Yuyang Lu, J., Seluanov, A. & Gorbunova, V. Long-lived fish in a big pond. *Science* vol. 374 824–825.
25. Selman, C., Partridge, L. & Withers, D. J. Replication of extended lifespan phenotype in mice with deletion of insulin receptor substrate 1. *PLoS One* **6**, (2011).

26. Nojima, A. *et al.* Haploinsufficiency of akt1 prolongs the lifespan of mice. *PLoS One* **8**, (2013).
27. Selman, C. *et al.* Ribosomal protein S6 kinase 1 signaling regulates mammalian life span. *Science* **326**, (2009).
28. Wu, J. J. *et al.* Increased mammalian lifespan and a segmental and tissue-specific slowing of aging after genetic reduction of mTOR expression. *Cell Rep.* **4**, (2013).
29. Deelen, J. *et al.* A meta-analysis of genome-wide association studies identifies multiple longevity genes. *Nat. Commun.* **10**, 1–14 (2019).
30. Lin, J.-R. *et al.* Rare genetic coding variants associated with human longevity and protection against age-related diseases. *Nature Aging* **1**, 783–794 (2021).
31. Tazearslan, C., Huang, J., Barzilai, N. & Suh, Y. Impaired IGF1R signaling in cells expressing longevity-associated human IGF1R alleles. *Aging Cell* **10**, (2011).
32. Björnholm, M. *et al.* Absence of functional insulin receptor substrate-3 (IRS-3) gene in humans. *Diabetologia* **45**, (2002).
33. Cheng, Z. *et al.* Foxo1 integrates insulin signaling with mitochondrial function in the liver. *Nat. Med.* **15**, (2009).
34. Nunnari, J. & Suomalainen, A. Mitochondria: in sickness and in health. *Cell* **148**, (2012).
35. Lin, M. T. & Flint Beal, M. Mitochondrial dysfunction and oxidative stress in neurodegenerative diseases. *Nature* vol. 443 787–795 (2006).
36. Quirós, P. M. *et al.* Multi-omics analysis identifies ATF4 as a key regulator of the mitochondrial stress response in mammals. *J. Cell Biol.* **216**, (2017).
37. Li, W., Li, X. & Miller, R. A. ATF4 activity: a common feature shared by many kinds of slow-aging mice. *Aging Cell* **13**, (2014).
38. Zhang, Y. *et al.* The starvation hormone, fibroblast growth factor-21, extends lifespan in mice. *Elife* **1**, (2012).
39. Zhou, D. *et al.* Phosphorylation of eIF2 directs ATF5 translational control in response to diverse stress conditions. *J. Biol. Chem.* **283**, (2008).
40. Fiorese, C. J. *et al.* The Transcription Factor ATF5 Mediates a Mammalian Mitochondrial

UPR. *Curr. Biol.* **26**, (2016).

41. Bellantuono, I. *et al.* A toolbox for the longitudinal assessment of healthspan in ageing mice. *Nat. Protoc.* **15**, 540 (2020).
42. Speakman, J. R. Body size, energy metabolism and lifespan. *J. Exp. Biol.* **208**, (2005).
43. Yanai, S. & Endo, S. Functional Aging in Male C57BL/6J Mice Across the Life-Span: A Systematic Behavioral Analysis of Motor, Emotional, and Memory Function to Define an Aging Phenotype. *Front. Aging Neurosci.* **13**, 697621 (2021).
44. White, M. F. & Kahn, C. R. Insulin action at a molecular level - 100 years of progress. *Molecular metabolism* **52**, (2021).
45. Blüher, M., Kahn, B. B. & Ronald Kahn, C. Extended Longevity in Mice Lacking the Insulin Receptor in Adipose Tissue. *Science* (2003) doi:10.1126/science.1078223.
46. Della Torre, S. *et al.* Short-Term Fasting Reveals Amino Acid Metabolism as a Major Sex-Discriminating Factor in the Liver. *Cell Metab.* **28**, 256 (2018).
47. Previs, S. F., Withers, D. J., Ren, J. M., White, M. F. & Shulman, G. I. Contrasting effects of IRS-1 versus IRS-2 gene disruption on carbohydrate and lipid metabolism in vivo. *J. Biol. Chem.* **275**, (2000).
48. Long, Y. C., Cheng, Z., Copps, K. D. & White, M. F. Insulin receptor substrates Irs1 and Irs2 coordinate skeletal muscle growth and metabolism via the Akt and AMPK pathways. *Mol. Cell. Biol.* **31**, (2011).
49. Blüher, M. *et al.* Adipose tissue selective insulin receptor knockout protects against obesity and obesity-related glucose intolerance. *Dev. Cell* **3**, (2002).
50. A Muscle-Specific Insulin Receptor Knockout Exhibits Features of the Metabolic Syndrome of NIDDM without Altering Glucose Tolerance. *Mol. Cell* **2**, 559–569 (1998).
51. Boucher, J. *et al.* Differential Roles of Insulin and IGF-1 Receptors in Adipose Tissue Development and Function. *Diabetes* **65**, (2016).
52. O'Neill, B. T. *et al.* Differential Role of Insulin/IGF-1 Receptor Signaling in Muscle Growth and Glucose Homeostasis. *Cell Rep.* **11**, (2015).
53. Dong, X. C. *et al.* Inactivation of hepatic Foxo1 by insulin signaling is required for adaptive

nutrient homeostasis and endocrine growth regulation. *Cell Metab.* **8**, (2008).

54. Ruud, J., Steculorum, S. M. & Brüning, J. C. Neuronal control of peripheral insulin sensitivity and glucose metabolism. *Nat. Commun.* **8**, 1–12 (2017).
55. Hill, C. M. *et al.* FGF21 Signals Protein Status to the Brain and Adaptively Regulates Food Choice and Metabolism. *Cell Rep.* **27**, 2934–2947.e3 (2019).
56. Harno, E., Cottrell, E. C. & White, A. Metabolic pitfalls of CNS Cre-based technology. *Cell Metab.* **18**, (2013).
57. Könner, A. C. *et al.* Role for insulin signaling in catecholaminergic neurons in control of energy homeostasis. *Cell Metab.* **13**, (2011).
58. Zhang, Y. *et al.* Leptin-receptor-expressing neurons in the dorsomedial hypothalamus and median preoptic area regulate sympathetic brown adipose tissue circuits. *J. Neurosci.* **31**, (2011).
59. Rezai-Zadeh, K. *et al.* Leptin receptor neurons in the dorsomedial hypothalamus are key regulators of energy expenditure and body weight, but not food intake. *Molecular metabolism* **3**, (2014).
60. Hausen, A. C. *et al.* Insulin-Dependent Activation of MCH Neurons Impairs Locomotor Activity and Insulin Sensitivity in Obesity. *Cell Rep.* **17**, (2016).
61. Yadava, N. & Nicholls, D. G. Spare respiratory capacity rather than oxidative stress regulates glutamate excitotoxicity after partial respiratory inhibition of mitochondrial complex I with rotenone. *J. Neurosci.* **27**, (2007).
62. Johnson-Cadwell, L. I., Jekabsons, M. B., Wang, A., Polster, B. M. & Nicholls, D. G. 'Mild Uncoupling' does not decrease mitochondrial superoxide levels in cultured cerebellar granule neurons but decreases spare respiratory capacity and increases toxicity to glutamate and oxidative stress. *J. Neurochem.* **101**, (2007).
63. Choi, S. W., Gerencser, A. A. & Nicholls, D. G. Bioenergetic analysis of isolated cerebrocortical nerve terminals on a microgram scale: spare respiratory capacity and stochastic mitochondrial failure. *J. Neurochem.* **109**, (2009).
64. Harding, H. P. *et al.* An integrated stress response regulates amino acid metabolism and

resistance to oxidative stress. *Mol. Cell* **11**, (2003).

65. Young, S. K. & Wek, R. C. Upstream Open Reading Frames Differentially Regulate Gene-specific Translation in the Integrated Stress Response. *J. Biol. Chem.* **291**, (2016).
66. Amar, F. *et al.* Rapid ATF4 Depletion Resets Synaptic Responsiveness after cLTP. *eNeuro* **8**, (2021).
67. Kühl, I. *et al.* Transcriptomic and proteomic landscape of mitochondrial dysfunction reveals secondary coenzyme Q deficiency in mammals. (2017) doi:10.7554/eLife.30952.
68. Khan, N. A. *et al.* mTORC1 Regulates Mitochondrial Integrated Stress Response and Mitochondrial Myopathy Progression. *Cell Metab.* **26**, (2017).
69. Nikkanen, J. *et al.* Mitochondrial DNA Replication Defects Disturb Cellular dNTP Pools and Remodel One-Carbon Metabolism. *Cell Metab.* **23**, 635–648 (2016).
70. Ben-Sahra, I., Hoxhaj, G., Ricoult, S. J. H., Asara, J. M. & Manning, B. D. mTORC1 induces purine synthesis through control of the mitochondrial tetrahydrofolate cycle. *Science* **351**, (2016).
71. Byles, V. *et al.* Hepatic mTORC1 signaling activates ATF4 as part of its metabolic response to feeding and insulin. *Molecular metabolism* **53**, (2021).
72. Motori, E. *et al.* Neuronal metabolic rewiring promotes resilience to neurodegeneration caused by mitochondrial dysfunction. *Science advances* **6**, (2020).
73. Timper, K. *et al.* GLP-1 Receptor Signaling in Astrocytes Regulates Fatty Acid Oxidation, Mitochondrial Integrity, and Function. *Cell Metab.* **31**, (2020).
74. Restelli, L. M. *et al.* Neuronal Mitochondrial Dysfunction Activates the Integrated Stress Response to Induce Fibroblast Growth Factor 21. *Cell Rep.* **24**, (2018).
75. Hill, C. M. *et al.* FGF21 is required for protein restriction to extend lifespan and improve metabolic health in male mice. *Nat. Commun.* **13**, 1–14 (2022).
76. Gong, Q. *et al.* Fibroblast growth factor 21 improves hepatic insulin sensitivity by inhibiting mammalian target of rapamycin complex 1 in mice. *Hepatology* **64**, (2016).
77. Becker, C. *et al.* CLPP deficiency protects against metabolic syndrome but hinders adaptive thermogenesis. *EMBO Rep.* **19**, (2018).

78. Markan, K. R. *et al.* Circulating FGF21 is liver derived and enhances glucose uptake during refeeding and overfeeding. *Diabetes* **63**, (2014).
79. Richardson, N. E. *et al.* Lifelong restriction of dietary branched-chain amino acids has sex-specific benefits for frailty and life span in mice. *Nature Aging* **1**, 73–86 (2021).
80. Yu, D. *et al.* Short-term methionine deprivation improves metabolic health via sexually dimorphic, mTORC1-independent mechanisms. *The FASEB Journal* **32**, 3471 (2018).
81. De Sousa-Coelho, A. L., Marrero, P. F. & Haro, D. Activating transcription factor 4-dependent induction of FGF21 during amino acid deprivation. *Biochem. J.* **443**, (2012).
82. Pereira, R. O. *et al.* OPA1 deletion in brown adipose tissue improves thermoregulation and systemic metabolism via FGF21. *Elife* **10**, (2021).
83. Stöhr, O., Tao, R., Miao, J., Copps, K. D. & White, M. F. FoxO1 suppresses Fgf21 during hepatic insulin resistance to impair peripheral glucose utilization and acute cold tolerance. *Cell Rep.* **34**, (2021).
84. Douris, N. *et al.* Central Fibroblast Growth Factor 21 Browns White Fat via Sympathetic Action in Male Mice. *Endocrinology* **156**, (2015).
85. Owen, B. M. *et al.* FGF21 acts centrally to induce sympathetic nerve activity, energy expenditure, and weight loss. *Cell Metab.* **20**, (2014).
86. Tain, L. S. *et al.* A proteomic atlas of insulin signalling reveals tissue-specific mechanisms of longevity assurance. *Mol. Syst. Biol.* **13**, 939 (2017).
87. Mulvey, L., Sinclair, A. & Selman, C. Lifespan modulation in mice and the confounding effects of genetic background. *J. Genet. Genomics* **41**, 497–503 (2014).
88. Bokov, A. F. *et al.* Does Reduced IGF-1R Signaling in Igf1r +/− Mice Alter Aging? *PLoS One* **6**, (2011).
89. Holzenberger, M. *et al.* IGF-1 receptor regulates lifespan and resistance to oxidative stress in mice. *Nature* **421**, 182–187 (2002).
90. Bansal, A., Zhu, L. J., Yen, K. & Tissenbaum, H. A. Uncoupling lifespan and healthspan in Caenorhabditis elegans longevity mutants. *Proc. Natl. Acad. Sci. U. S. A.* **112**, (2015).
91. Metaxakis, A. *et al.* Lowered Insulin Signalling Ameliorates Age-Related Sleep

Fragmentation in Drosophila. *PLoS Biol.* **12**, e1001824 (2014).

92. Podshivalova, K., Kerr, R. A. & Kenyon, C. How a mutation that slows aging can also disproportionately extend end-of-life decrepitude. *Cell Rep.* **19**, 441 (2017).
93. Steculorum, S. M., Solas, M. & Brüning, J. C. The paradox of neuronal insulin action and resistance in the development of aging-associated diseases. *Alzheimers. Dement.* **10**, S3–11 (2014).
94. Merry, T. L. *et al.* Impairment of insulin signalling in peripheral tissue fails to extend murine lifespan. *Aging Cell* **16**, (2017).
95. Wolkow, C. A., Kimura, K. D., Lee, M. S. & Ruvkun, G. Regulation of C. elegans life-span by insulinlike signaling in the nervous system. *Science* **290**, (2000).
96. Zhang, Y. *et al.* Neuronal TORC1 modulates longevity via AMPK and cell nonautonomous regulation of mitochondrial dynamics in C. elegans. (2019) doi:10.7554/eLife.49158.
97. Cohen, E. *et al.* Reduced IGF-1 signaling delays age-associated proteotoxicity in mice. *Cell* **139**, (2009).
98. Ismail, M. Z. B. *et al.* The Drosophila Insulin Receptor Independently Modulates Lifespan and Locomotor Senescence. *PLoS One* **10**, e0125312 (2015).
99. Augustin, H. *et al.* Reduced insulin signaling maintains electrical transmission in a neural circuit in aging flies. *PLoS Biol.* **15**, e2001655 (2017).
100. Baar, E. L., Carbajal, K. A., Ong, I. M. & Lamming, D. W. Sex- and tissue-specific changes in mTOR signaling with age in C57BL/6J mice. *Aging Cell* **15**, 155 (2016).
101. Durieux, J., Wolff, S. & Dillin, A. The cell-non-autonomous nature of electron transport chain-mediated longevity. *Cell* **144**, (2011).
102. Copeland, J. M. *et al.* Extension of Drosophila life span by RNAi of the mitochondrial respiratory chain. *Curr. Biol.* **19**, (2009).
103. Tyynismaa, H. *et al.* Mitochondrial myopathy induces a starvation-like response. *Hum. Mol. Genet.* **19**, 3948–3958 (2010).
104. Castillo-Armengol, J., Fajas, L. & Lopez-Mejia, I. C. Inter-organ communication: a gatekeeper for metabolic health. *EMBO Rep.* **20**, (2019).

105. Croon, M. *et al.* FGF21 modulates mitochondrial stress response in cardiomyocytes only under mild mitochondrial dysfunction. *Sci Adv* **8**, eabn7105 (2022).

106. Irwin, R. W. *et al.* Progesterone and Estrogen Regulate Oxidative Metabolism in Brain Mitochondria. *Endocrinology* **149**, 3167 (2008).

107. Felicio, L. S., Nelson, J. F. & Finch, C. E. Longitudinal studies of estrous cyclicity in aging C57BL/6J mice: II. Cessation of cyclicity and the duration of persistent vaginal cornification. *Biol. Reprod.* **31**, (1984).

108. Guilbert, J. J. The World Health Report 2006: working together for health. *Educ. Health* **19**, (2006).

109. Ferri, C. P. *et al.* Global prevalence of dementia: a Delphi consensus study. *Lancet* **366**, (2005).

110. Ballard, C. *et al.* Alzheimer's disease. *Lancet* **377**, (2011).

111. Millán-Calenti, J. C. *et al.* Cognitive impairment as predictor of functional dependence in an elderly sample. *Arch. Gerontol. Geriatr.* **54**, (2012).

112. Park, H. L., O'Connell, J. E. & Thomson, R. G. A systematic review of cognitive decline in the general elderly population. *Int. J. Geriatr. Psychiatry* **18**, (2003).

113. Prince, M. *et al.* Recent global trends in the prevalence and incidence of dementia, and survival with dementia. *Alzheimers. Res. Ther.* **8**, (2016).

114. Brayne, C. The elephant in the room - healthy brains in later life, epidemiology and public health. *Nat. Rev. Neurosci.* **8**, (2007).

115. Fontana, L., Meyer, T. E., Klein, S. & Holloszy, J. O. Long-term calorie restriction is highly effective in reducing the risk for atherosclerosis in humans. *Proc. Natl. Acad. Sci. U. S. A.* **101**, (2004).

116. Fontana, L., Partridge, L. & Longo, V. D. Extending healthy life span--from yeast to humans. *Science* **328**, (2010).

117. Colman, R. J. *et al.* Caloric restriction reduces age-related and all-cause mortality in rhesus monkeys. *Nat. Commun.* **5**, 1–5 (2014).

118. Piper, M. D. W., Selman, C., McElwee, J. J. & Partridge, L. Models of insulin signalling and

longevity. *Drug Discovery Today: Disease Models* vol. 2 249–256 (2005).

119. Clancy, D. J. *et al.* Extension of life-span by loss of CHICO, a Drosophila insulin receptor substrate protein. *Science* **292**, (2001).

120. McElwee, J. J., Schuster, E., Blanc, E., Thomas, J. H. & Gems, D. Shared transcriptional signature in Caenorhabditis elegans Dauer larvae and long-lived daf-2 mutants implicates detoxification system in longevity assurance. *J. Biol. Chem.* **279**, (2004).

121. Brüning, J. C., Winnay, J., Cheatham, B. & Kahn, C. R. Differential signaling by insulin receptor substrate 1 (IRS-1) and IRS-2 in IRS-1-deficient cells. *Mol. Cell. Biol.* **17**, (1997).

122. van Heemst, D. Insulin, IGF-1 and longevity. *Aging Dis.* **1**, (2010).

123. Fernandez, A. M. & Torres-Alemán, I. The many faces of insulin-like peptide signalling in the brain. *Nat. Rev. Neurosci.* **13**, (2012).

124. Soreq, L. *et al.* Major Shifts in Glial Regional Identity Are a Transcriptional Hallmark of Human Brain Aging. *Cell Rep.* **18**, 557–570 (2017).

125. Grillo, C. A. *et al.* Hippocampal Insulin Resistance Impairs Spatial Learning and Synaptic Plasticity. *Diabetes* **64**, 3927–3936 (2015).

126. Acarin, L., González, B. & Castellano, B. Neuronal, astroglial and microglial cytokine expression after an excitotoxic lesion in the immature rat brain. *Eur. J. Neurosci.* **12**, 3505–3520 (2000).

127. Chu, C.-H. *et al.* Neurons and astroglia govern microglial endotoxin tolerance through macrophage colony-stimulating factor receptor-mediated ERK1/2 signals. *Brain Behav. Immun.* **55**, 260–272 (2016).

128. Stark, A.-K., Sriskantharajah, S., Hessel, E. M. & Okkenhaug, K. PI3K inhibitors in inflammation, autoimmunity and cancer. *Curr. Opin. Pharmacol.* **23**, 82–91 (2015).

129. Rosenzweig, E. S. & Barnes, C. A. Impact of aging on hippocampal function: plasticity, network dynamics, and cognition. *Prog. Neurobiol.* **69**, (2003).

130. Murphy, G. G. et al. Increased Neuronal Excitability, Synaptic Plasticity, and Learning in Aged Kvβ1.1 Knockout Mice. Current Biology vol. 14 1907–1915 (2004).

131. Sheth, K. A. et al. Muscle strength and size are associated with motor unit connectivity in

aged mice. Neurobiol. Aging 67, 128 (2018).

132. Karp, N. A., Segonds-Pichon, A., Gerdin, A.-K. B., Ramírez-Solis, R. & White, J. K. The fallacy of Ratio Correction to address confounding factors. Lab. Anim. 46, 245 (2012).

133. Miller, G. A. & Chapman, J. P. Misunderstanding analysis of covariance. J. Abnorm. Psychol. 110, (2001).

134. Age-related cognitive decline in spatial learning and memory of C57BL/6J mice. Behav. Brain Res. 418, 113649 (2022).

135. Benice, T. S., Rizk, A., Kohama, S., Pfankuch, T. & Raber, J. Sex-differences in age-related cognitive decline in C57BL/6J mice associated with increased brain microtubule-associated protein 2 and synaptophysin immunoreactivity. Neuroscience 137, (2006).

136. Antunes, M. & Biala, G. The novel object recognition memory: neurobiology, test procedure, and its modifications. Cogn. Process. 13, 93 (2012).

137. Shoji, H., Takao, K., Hattori, S. & Miyakawa, T. Age-related changes in behavior in C57BL/6J mice from young adulthood to middle age. Mol. Brain 9, (2016).

138. Bailey, K. R. & Crawley, J. N. Anxiety-Related Behaviors in Mice. (2009).

139. Pietropaolo, S., Feldon, J. & Yee, B. K. Environmental enrichment eliminates the anxiety phenotypes in a triple transgenic mouse model of Alzheimer's disease. Cogn. Affect. Behav. Neurosci. 14, (2014).

140. Murphy, G. G., Rahnama, N. P. & Silva, A. J. Investigation of age-related cognitive decline using mice as a model system: behavioral correlates. Am. J. Geriatr. Psychiatry 14, (2006).

141. Antion, M. D. et al. Removal of S6K1 and S6K2 leads to divergent alterations in learning, memory, and synaptic plasticity. Learn. Mem. 15, 29 (2008).

142. Xu, J. et al. Insulin enhances growth hormone induction of the MEK/ERK signaling pathway. J. Biol. Chem. 281, (2006).

143. Kushner, S. A. et al. Modulation of presynaptic plasticity and learning by the H-ras/extracellular signal-regulated kinase/synapsin I signaling pathway. J. Neurosci. 25, (2005).

144. Magnuson, B., Ekim, B. & Fingar, D. C. Regulation and function of ribosomal protein S6

kinase (S6K) within mTOR signalling networks. Biochem. J. 441, (2012).

145. Nader, K., Schafe, G. E. & Le Doux, J. E. Fear memories require protein synthesis in the amygdala for reconsolidation after retrieval. Nature 406, (2000).

146. Klemm, D. J. et al. Insulin stimulates cAMP-response element binding protein activity in HepG2 and 3T3-L1 cell lines. J. Biol. Chem. 273, (1998).

147. Zhou, Y. et al. CREB regulates excitability and the allocation of memory to subsets of neurons in the amygdala. Nat. Neurosci. 12, (2009).

148. Wimmer, M. E., Hernandez, P. J., Blackwell, J. & Abel, T. Aging impairs hippocampus-dependent long-term memory for object location in mice. Neurobiol. Aging 33, (2012).

149. Halloran, J. et al. Corrigendum to ‘Chronic inhibition of mTOR by rapamycin modulates cognitive and non-cognitive components of behavior throughout lifespan in mice’ [Neuroscience 223 (2012) 102–113]. Neuroscience vol. 306 151 (2015).

150. Harris, J. A. et al. Anatomical characterization of Cre driver mice for neural circuit mapping and manipulation. Front. Neural Circuits 8, (2014).

151. Brüning, J. C. et al. Role of brain insulin receptor in control of body weight and reproduction. Science 289, (2000).

152. Bernal, A. & Arranz, L. Nestin-expressing progenitor cells: function, identity and therapeutic implications. Cell. Mol. Life Sci. 75, (2018).

153. Forni, P. E. et al. High levels of Cre expression in neuronal progenitors cause defects in brain development leading to microencephaly and hydrocephaly. J. Neurosci. 26, (2006).

154. Hoesche, C., Sauerwald, A., Veh, R. W., Krippl, B. & Kilimann, M. W. The 5’-flanking region of the rat synapsin I gene directs neuron-specific and developmentally regulated reporter gene expression in transgenic mice. J. Biol. Chem. 268, (1993).

155. Nóbrega, C. et al. Overexpression of Mutant Ataxin-3 in Mouse Cerebellum Induces Ataxia and Cerebellar Neuropathology. Cerebellum 12, 441–455 (2012).

156. Michael L. Seibenhener, M. C. W. Use of the Open Field Maze to Measure Locomotor and Anxiety-like Behavior in Mice. J. Vis. Exp. (2015) doi:10.3791/52434.

157. Charles V Vorhees, M. T. W. Morris water maze: procedures for assessing spatial and

related forms of learning and memory. Nat. Protoc. 1, 848 (2006).

158. Elmquist, J. K., Elias, C. F. & Saper, C. B. From lesions to leptin: hypothalamic control of food intake and body weight. Neuron 22, (1999).

159. Declercq, J. et al. Metabolic and Behavioural Phenotypes in Nestin-Cre Mice Are Caused by Hypothalamic Expression of Human Growth Hormone. PLoS One 10, (2015).

160. Tronche, F. et al. Disruption of the glucocorticoid receptor gene in the nervous system results in reduced anxiety. Nat. Genet. 23, (1999).

161. Barclay, J. L. et al. GH-dependent STAT5 signaling plays an important role in hepatic lipid metabolism. Endocrinology 152, (2011).

162. Szabo, M., Butz, M. R., Banerjee, S. A., Chikaraishi, D. M. & Frohman, L. A. Autofeedback suppression of growth hormone (GH) secretion in transgenic mice expressing a human GH reporter targeted by tyrosine hydroxylase 5’-flanking sequences to the hypothalamus. Endocrinology 136, (1995).

163. Luders, E., Gaser, C., Narr, K. L. & Toga, A. W. Why sex matters: brain size independent differences in gray matter distributions between men and women. J. Neurosci. 29, 14265–14270 (2009).

164. Young, L. J. & Pfaff, D. W. Sex differences in neurological and psychiatric disorders. Frontiers in Neuroendocrinology vol. 35 253–254 (2014).

165. Karp, N. A. et al. Prevalence of sexual dimorphism in mammalian phenotypic traits. Nat. Commun. 8, 15475 (2017).

166. Bult, C. J., Blake, J. A., Smith, C. L., Kadin, J. A. & Richardson, J. E. Mouse Genome Database (MGD) 2019. Nucleic Acids Res. 47, (2019).

167. Giusti, S. A. et al. Behavioral phenotyping of Nestin-Cre mice: implications for genetic mouse models of psychiatric disorders. J. Psychiatr. Res. 55, (2014).

168. Pierro, L. J. & Spiggle, J. Congenital eye defects in the mouse. I. Corneal opacity in C57black mice. J. Exp. Zool. 166, (1967).

9. Signed thesis declaration

Erklärung zur Dissertation
gemäß der Promotionsordnung vom 12. März 2020

Diese Erklärung muss in der Dissertation enthalten sein.
(This version must be included in the doctoral thesis)

„Hiermit versichere ich an Eides statt, dass ich die vorliegende Dissertation selbstständig und ohne die Benutzung anderer als der angegebenen Hilfsmittel und Literatur angefertigt habe. Alle Stellen, die wörtlich oder sinngemäß aus veröffentlichten und nicht veröffentlichten Werken dem Wortlaut oder dem Sinn nach entnommen wurden, sind als solche kenntlich gemacht. Ich versichere an Eides statt, dass diese Dissertation noch keiner anderen Fakultät oder Universität zur Prüfung vorgelegen hat; dass sie - abgesehen von unten angegebenen Teilpublikationen und eingebundenen Artikeln und Manuskripten - noch nicht veröffentlicht worden ist sowie, dass ich eine Veröffentlichung der Dissertation vor Abschluss der Promotion nicht ohne Genehmigung des Promotionsausschusses vornehmen werde. Die Bestimmungen dieser Ordnung sind mir bekannt. Darüber hinaus erkläre ich hiermit, dass ich die Ordnung zur Sicherung guter wissenschaftlicher Praxis und zum Umgang mit wissenschaftlichem Fehlverhalten der Universität zu Köln gelesen und sie bei der Durchführung der Dissertation zugrundeliegenden Arbeiten und der schriftlich verfassten Dissertation beachtet habe und verpflichte mich hiermit, die dort genannten Vorgaben bei allen wissenschaftlichen Tätigkeiten zu beachten und umzusetzen. Ich versichere, dass die eingereichte elektronische Fassung der eingereichten Druckfassung vollständig entspricht."

Teilpublikationen:

Baghdadi, et al. Reduced insulin signaling in neurons induces sex-specific health benefits. In preparation.
Baghdadi, et al. Sex-specific effects of Cre expression in SynCre mouse model.

Datum, Name und Unterschrift

11.05.2022 Maarouf Baghdadi

10. Publications

Baghdadi, M., Nespital, T., Mesaros, A., Buschbaum, S., Grönke, S., Partridge, L. Reduced insulin signaling in neurons induces sex-specific health benefits. Biorxiv. (in preparation)

Baghdadi, M., Mesaros, A., Partridge, L. Sex-specific effects of Cre expression in Syn1Cre mouse model. Biorxiv. (in preparation)